Disulfide-based dynamic combinatorial libraries of macrocyclic pseudopeptides as bio-inspired complex chemical systems

Joan Atcher Ubiergo

ADVERTIMENT. La consulta d'aquesta tesi queda condicionada a l'acceptació de les següents condicions d'ús: La difusió d'aquesta tesi per mitjà del servei TDX (**www.tdx.cat**) i a través del Dipòsit Digital de la UB (**diposit.ub.edu**) ha estat autoritzada pels titulars dels drets de propietat intel·lectual únicament per a usos privats emmarcats en activitats d'investigació i docència. No s'autoritza la seva reproducció amb finalitats de lucre ni la seva difusió i posada a disposició des d'un lloc aliè al servei TDX ni al Dipòsit Digital de la UB. No s'autoritza la presentació del seu contingut en una finestra o marc aliè a TDX o al Dipòsit Digital de la UB (framing). Aquesta reserva de drets afecta tant al resum de presentació de la tesi com als seus continguts. En la utilització o cita de parts de la tesi és obligat indicar el nom de la persona autora.

ADVERTENCIA. La consulta de esta tesis queda condicionada a la aceptación de las siguientes condiciones de uso: La difusión de esta tesis por medio del servicio TDR (**www.tdx.cat**) y a través del Repositorio Digital de la UB (**diposit.ub.edu**) ha sido autorizada por los titulares de los derechos de propiedad intelectual únicamente para usos privados enmarcados en actividades de investigación y docencia. No se autoriza su reproducción con finalidades de lucro ni su difusión y puesta a disposición desde un sitio ajeno al servicio TDR o al Repositorio Digital de la UB. No se autoriza la presentación de su contenido en una ventana o marco ajeno a TDR o al Repositorio Digital de la UB (framing). Esta reserva de derechos afecta tanto al resumen de presentación de la tesis como a sus contenidos. En la utilización o cita de partes de la tesis es obligado indicar el nombre de la persona autora.

WARNING. On having consulted this thesis you're accepting the following use conditions: Spreading this thesis by the TDX (**www.tdx.cat**) service and by the UB Digital Repository (**diposit.ub.edu**) has been authorized by the titular of the intellectual property rights only for private uses placed in investigation and teaching activities. Reproduction with lucrative aims is not authorized nor its spreading and availability from a site foreign to the TDX service or to the UB Digital Repository. Introducing its content in a window or frame foreign to the TDX service or to the UB Digital Repository is not authorized (framing). Those rights affect to the presentation summary of the thesis as well as to its contents. In the using or citation of parts of the thesis it's obliged to indicate the name of the author.

ANNEX

Disulfide-based dynamic combinatorial libraries of macrocyclic pseudopeptides as bio-inspired complex chemical systems

Doctoral thesis

Joan Atcher Ubiergo

TABLE OF CONTENTS

Characterization of building blocks 1a-m and (*RR*)-1i-d_4

Building block 1a

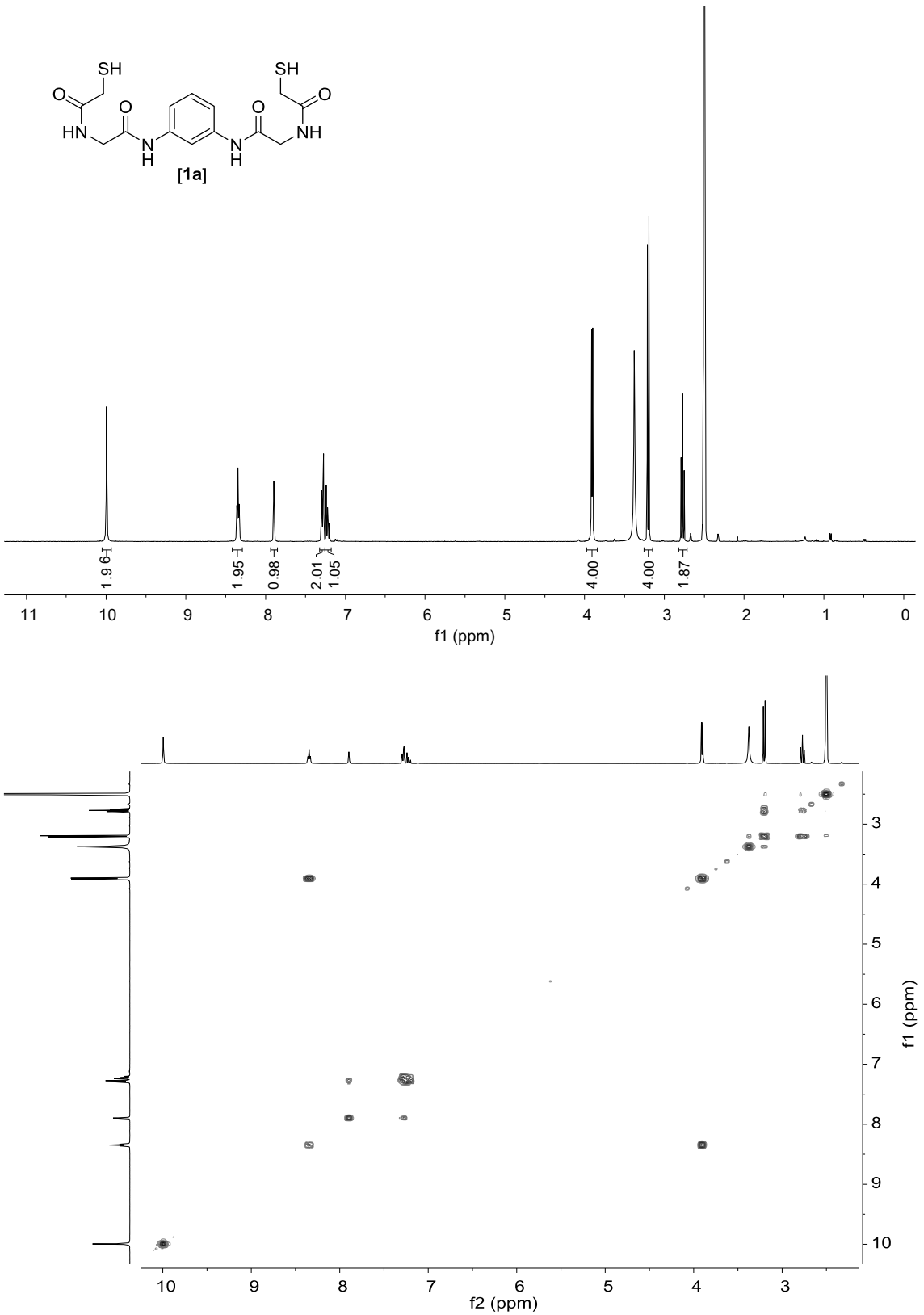

Figure A1. ^{1}H (400 MHz, 298 K in DMSO-d_6) and ^{1}H-^{1}H gCOSY (400 MHz, 298 K in DMSO-d_6) spectra of [**1a**].

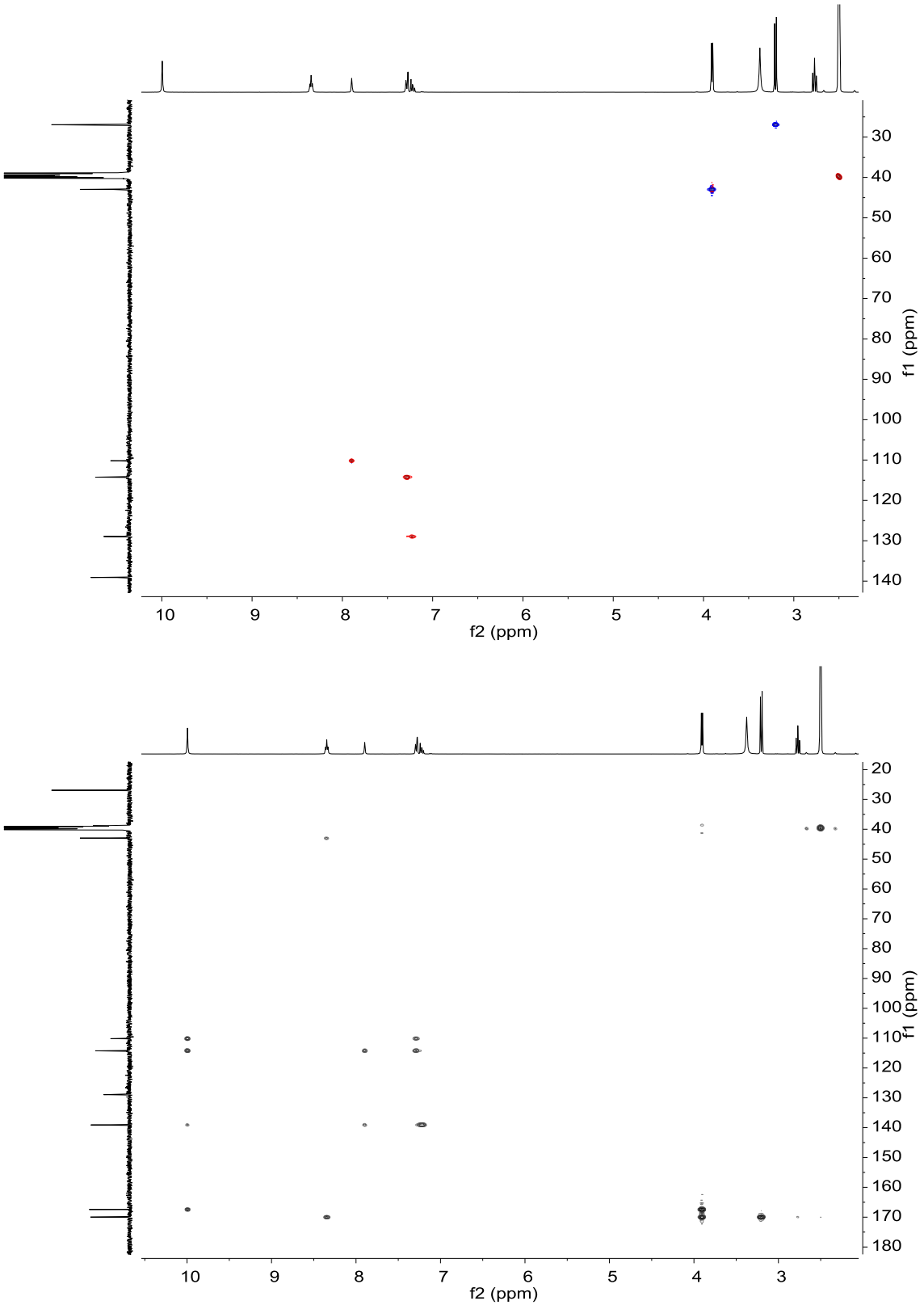

Figure A2. ^{1}H-^{13}C gHSQC (400 MHz, 298 K in DMSO-d_6) and ^{1}H-^{13}C gHMBC (400 MHz, 298 K in DMSO-d_6) spectra of [**1a**].

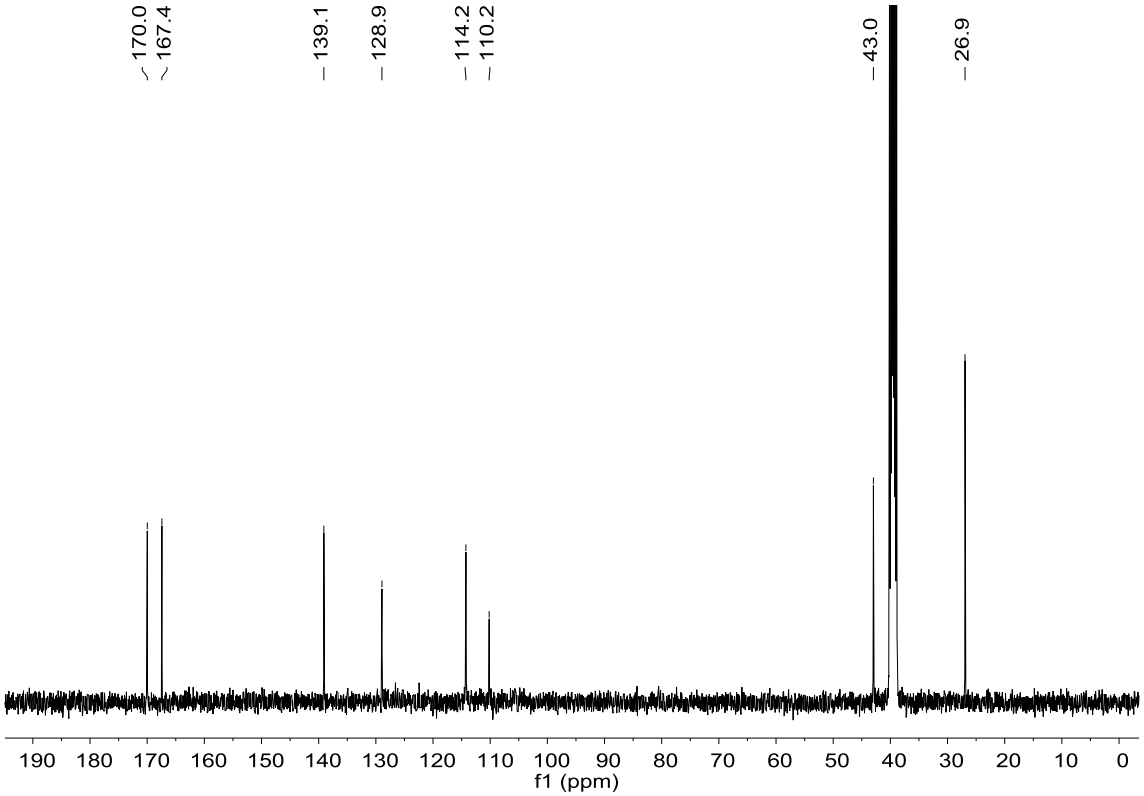

Figure A3. ^{13}C (101 MHz, 298 K in DMSO-d_6) spectrum of [**1a**].

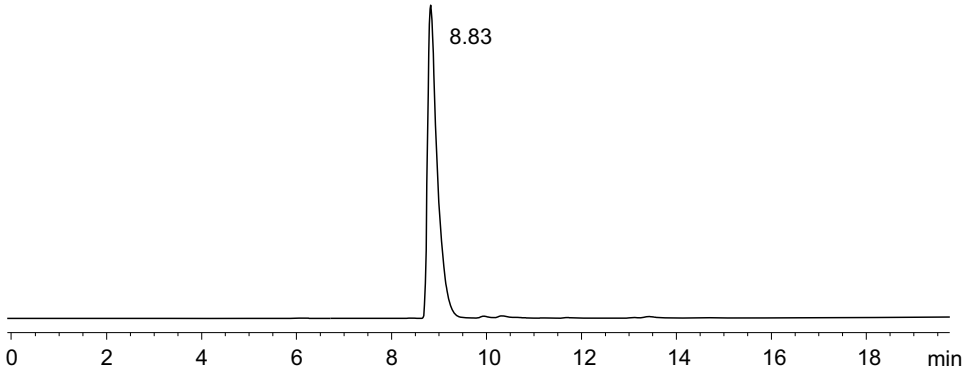

Figure A4. RP-HPLC analysis of [**1a**] (eluent: mixture of CH_3CN + 0.07% (v/v) TFA and H_2O + 0.1% (v/v) TFA; gradient: 2 min at 5% CH_3CN in H_2O, then linear gradient from 5% to 100% CH_3CN over 18 min).

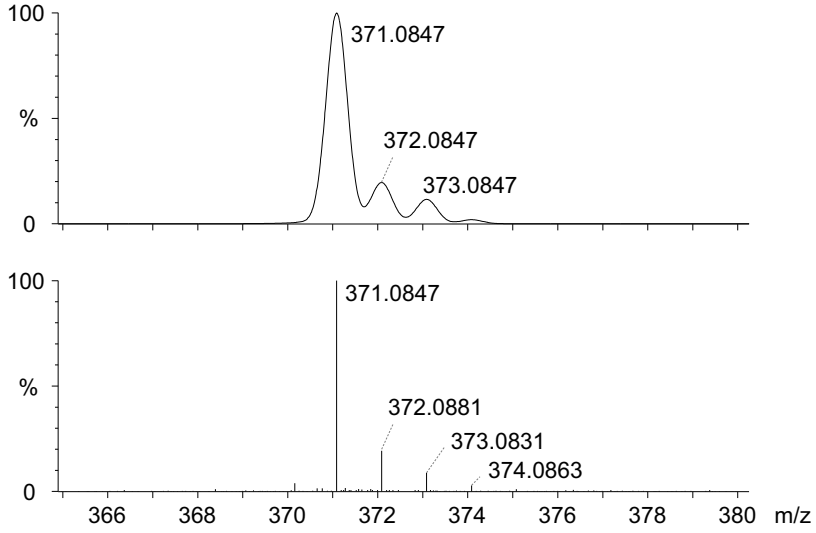

Figure A5. Experimental (lower trace) and simulated (upper trace) ESI-TOF mass spectra for $[M+H]^+$ of [**1a**].

Building block 1b

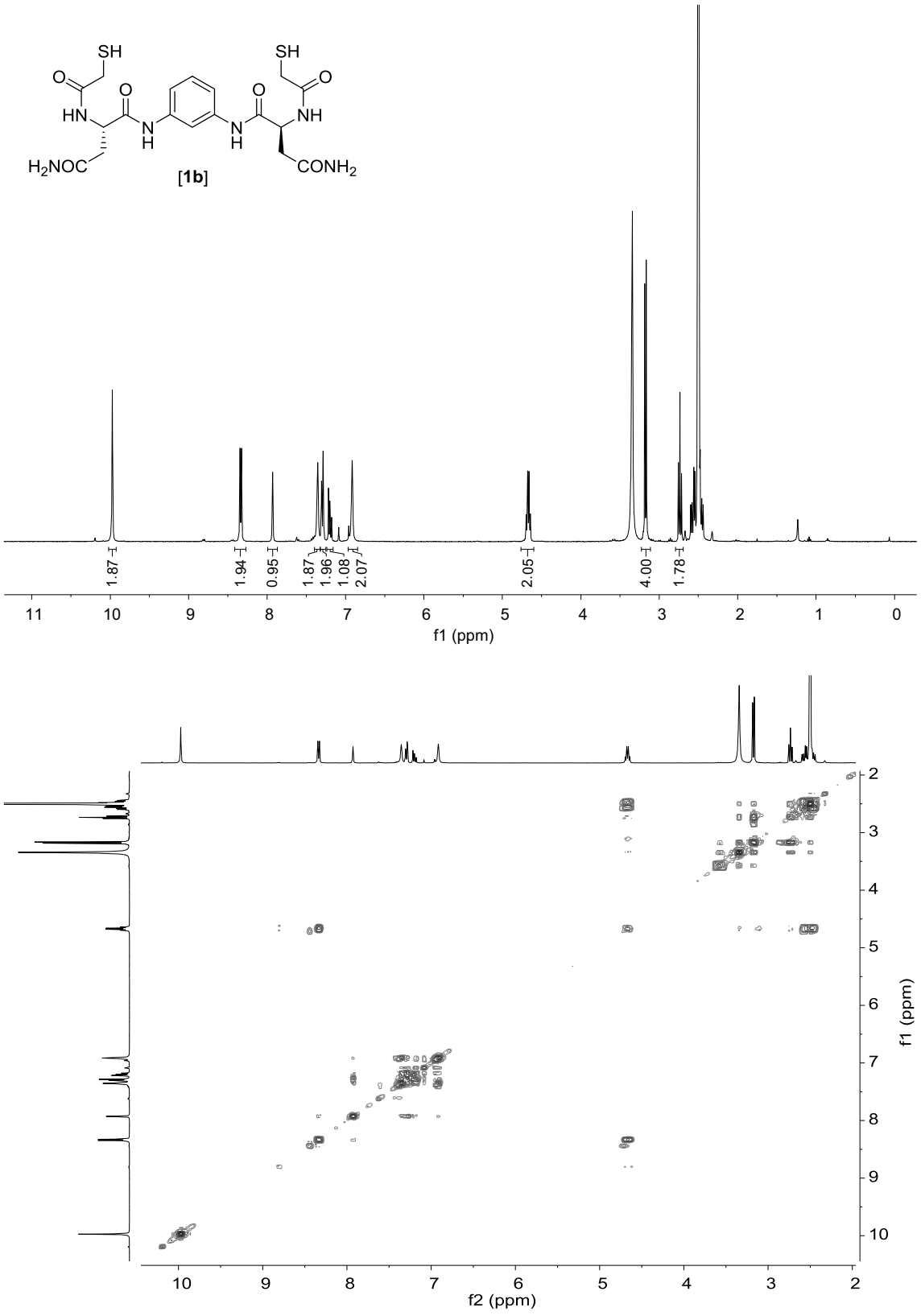

Figure A6. ^{1}H (400 MHz, 298 K in DMSO-d_6) and ^{1}H-^{1}H gCOSY (400 MHz, 298 K in DMSO-d_6) spectra of [**1b**].

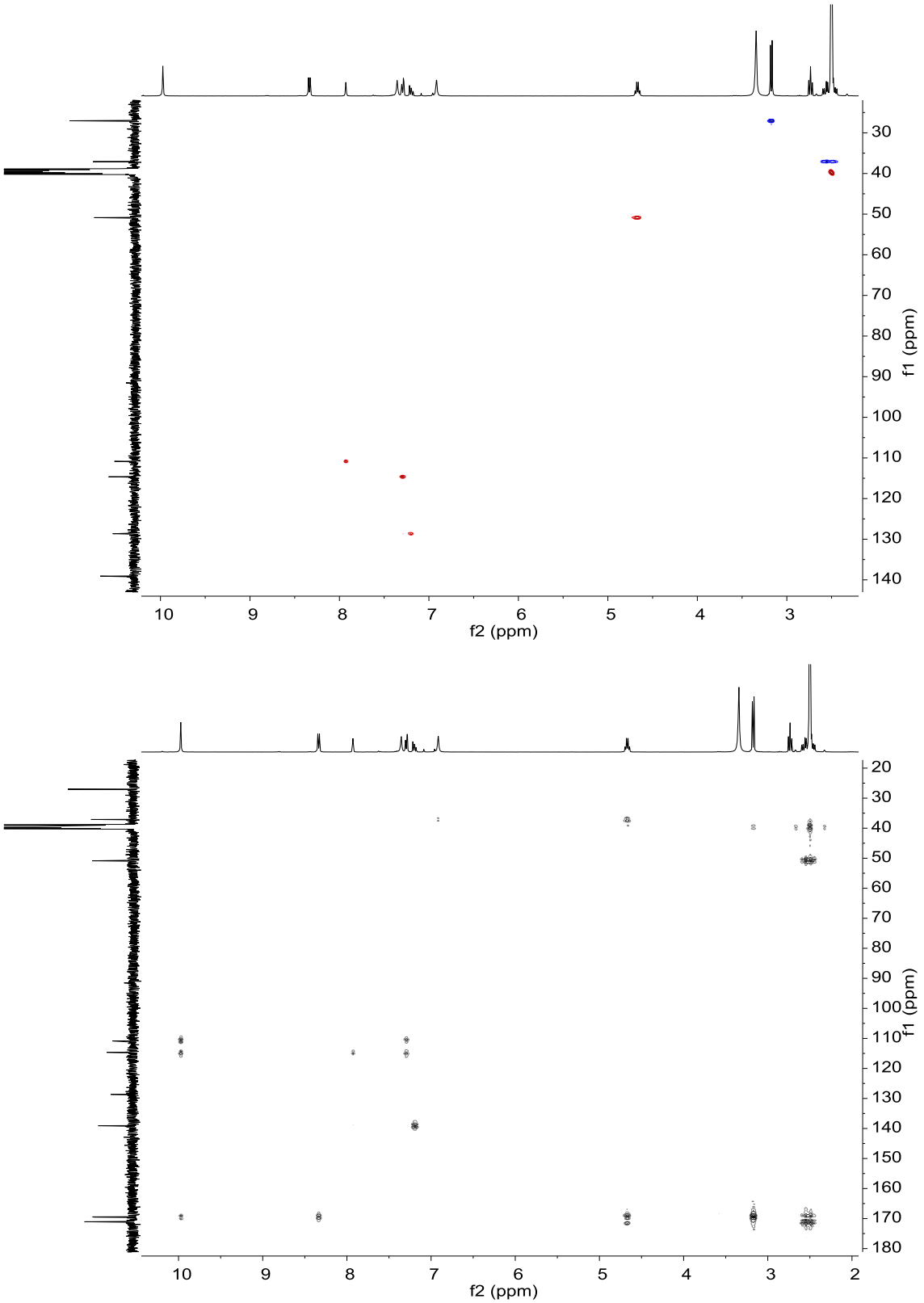

Figure A7. ^{1}H-^{13}C gHSQC (400 MHz, 298 K in DMSO-d_6) and ^{1}H-^{13}C gHMBC (400 MHz, 298 K in DMSO-d_6) spectra of [**1b**].

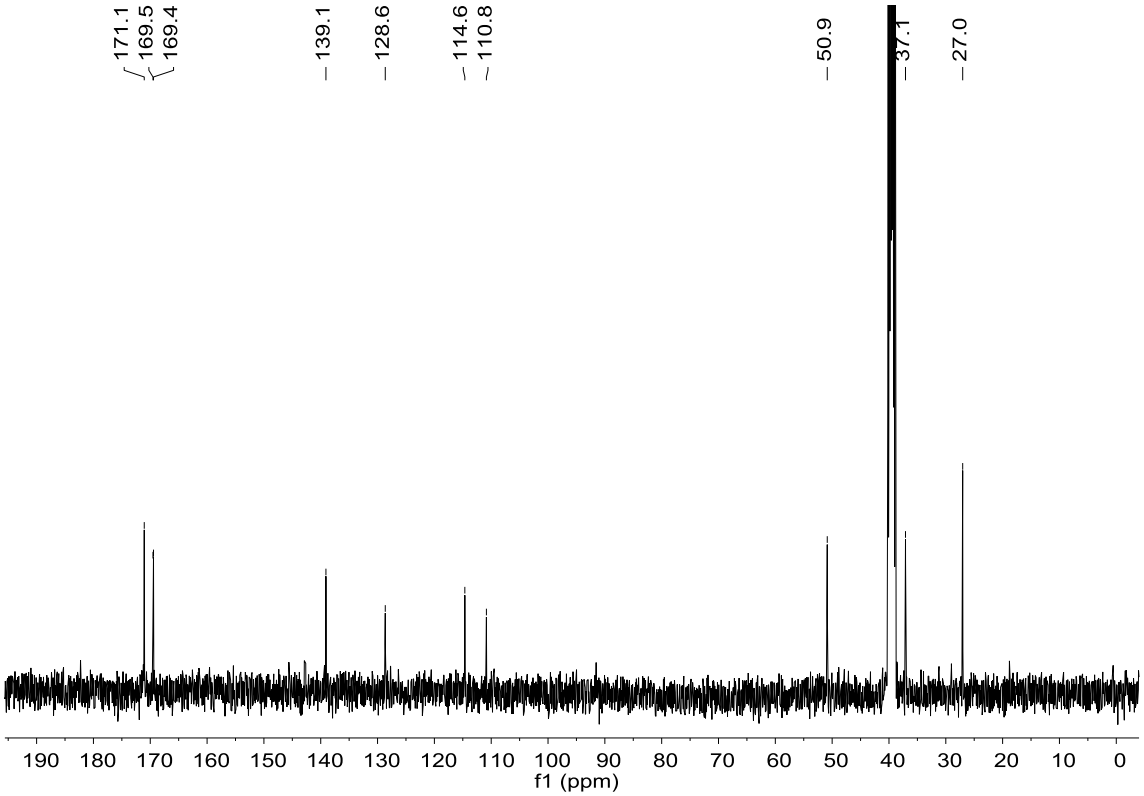

Figure A8. ^{13}C (101 MHz, 298 K in DMSO-d_6) spectrum of [**1b**].

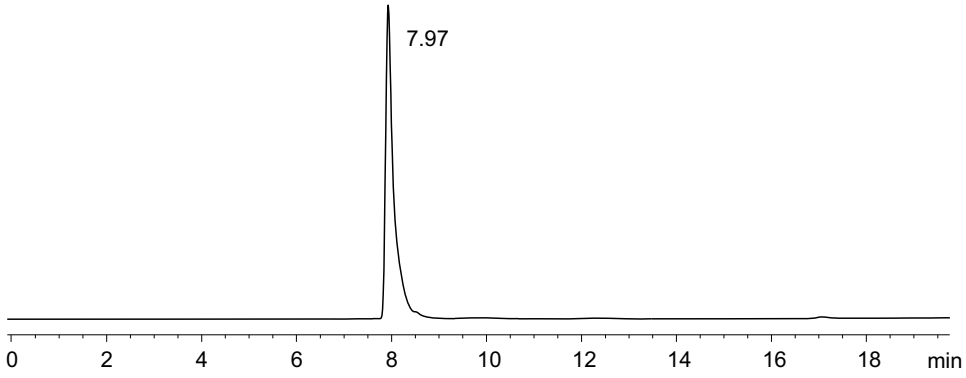

Figure A9. RP-HPLC analysis of [**1b**] (eluent: mixture of CH_3CN + 0.07% (v/v) TFA and H_2O + 0.1% (v/v) TFA; gradient: 2 min at 5% CH_3CN in H_2O, then linear gradient from 5% to 100% CH_3CN over 18 min).

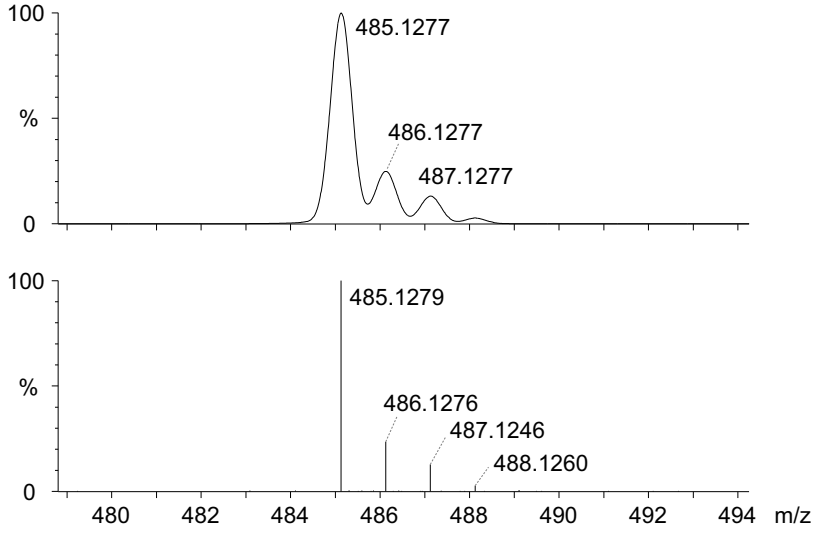

Figure A10. Experimental (lower trace) and simulated (upper trace) ESI-TOF mass spectra for $[M+H]^+$ of [**1b**].

Building block 1c

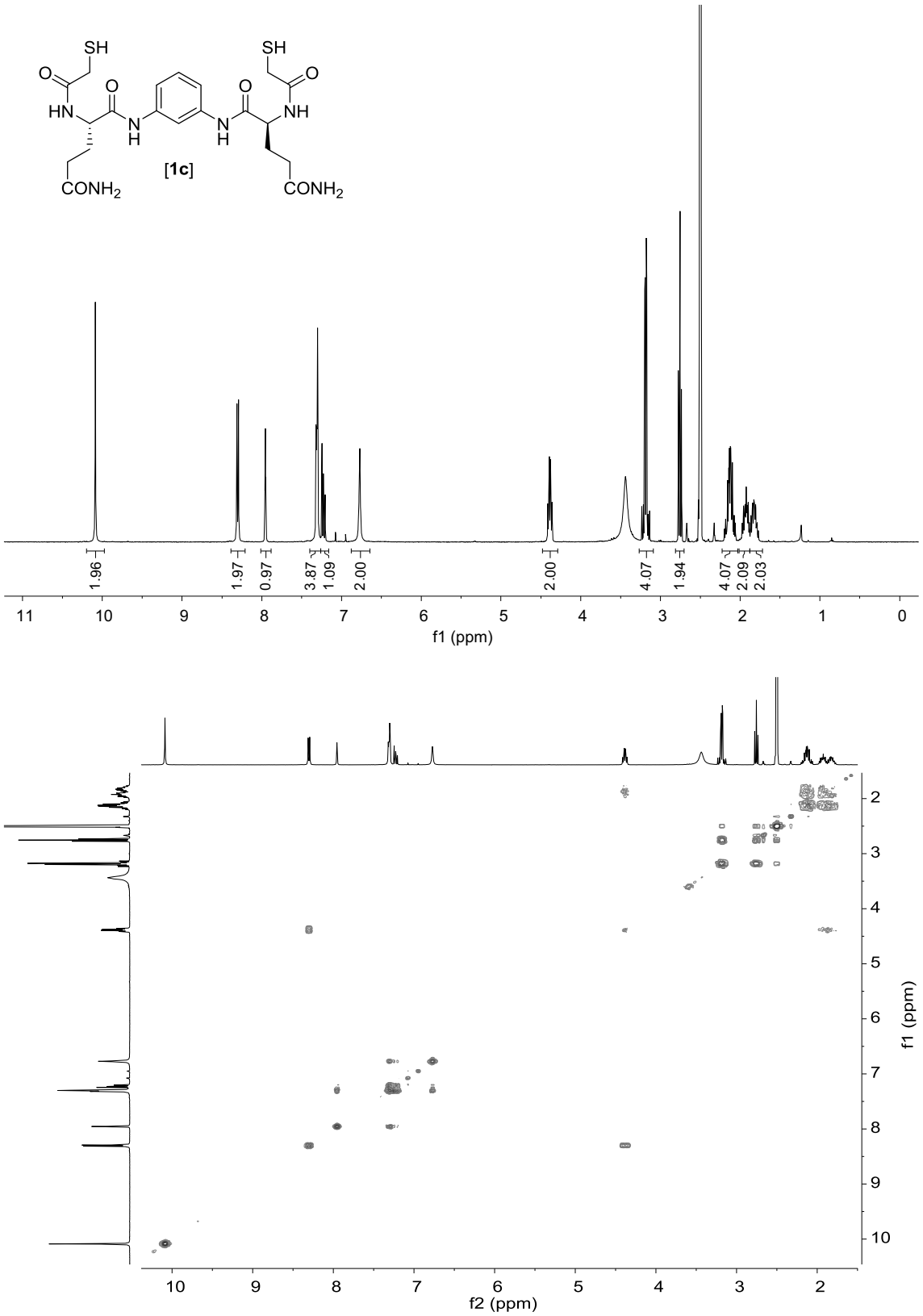

Figure A11. ^{1}H (400 MHz, 298 K in DMSO-d_6) and ^{1}H-^{1}H gCOSY (400 MHz, 298 K in DMSO-d_6) spectra of [**1c**].

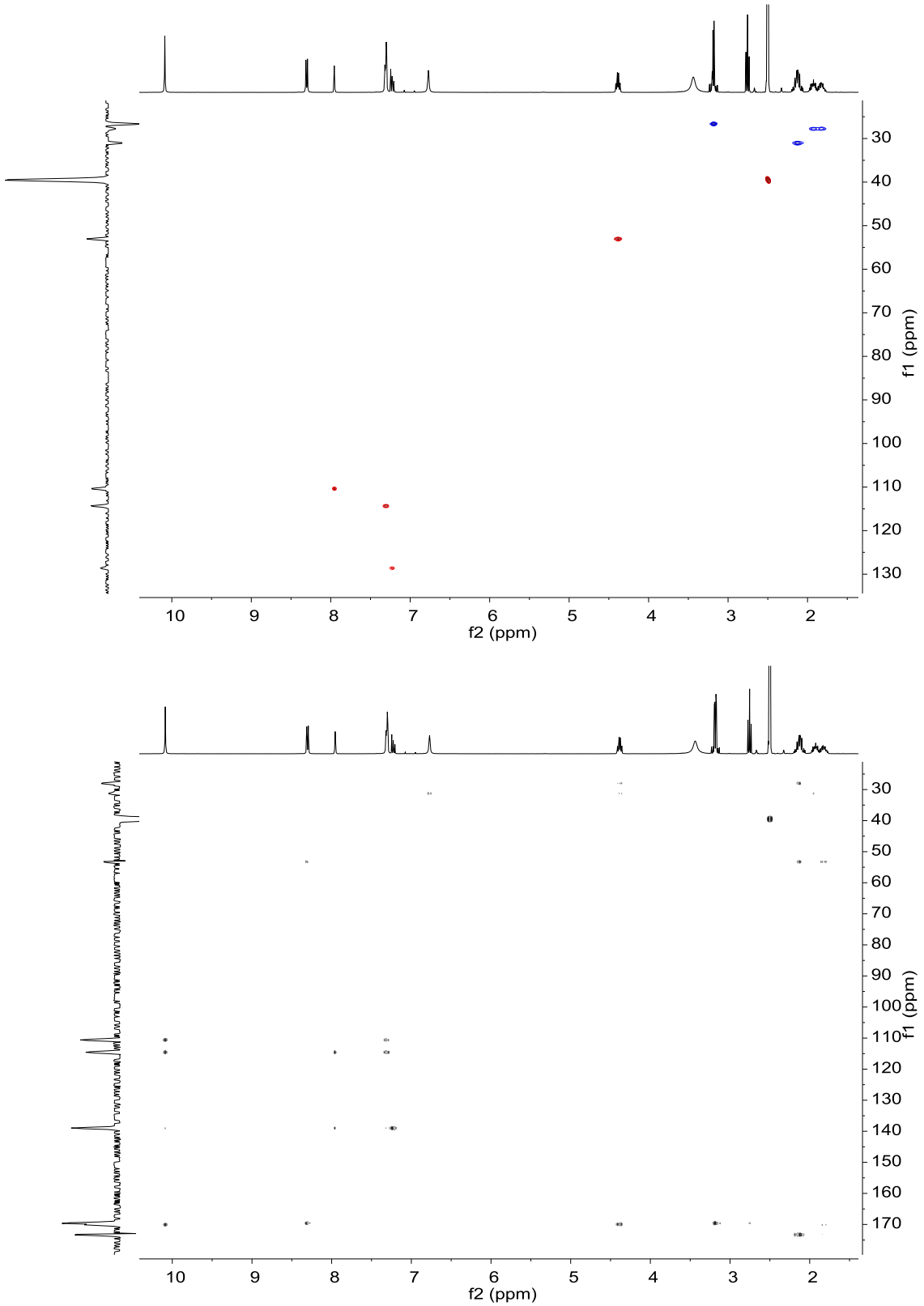

Figure A12. ^{1}H-^{13}C gHSQC (400 MHz, 298 K in DMSO-d_6) and ^{1}H-^{13}C gHMBC (400 MHz, 298 K in DMSO-d_6) spectra of [**1c**].

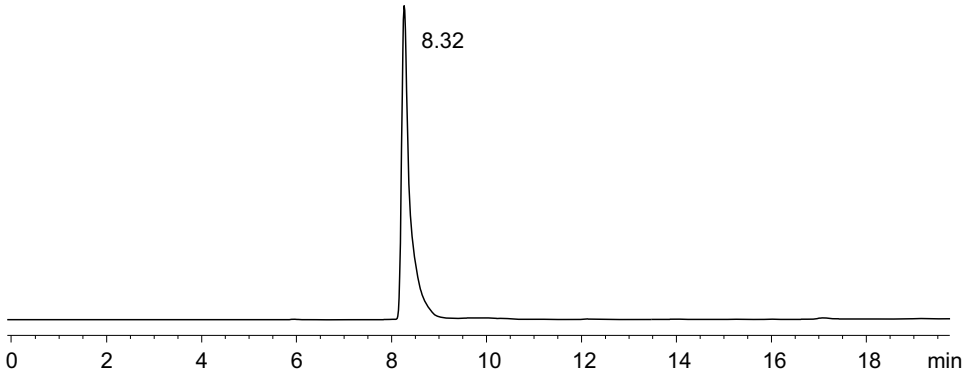

Figure A13. RP-HPLC analysis of [**1c**] (eluent: mixture of CH_3CN + 0.07% (v/v) TFA and H_2O + 0.1% (v/v) TFA; gradient: 2 min at 5% CH_3CN in H_2O, then linear gradient from 5% to 100% CH_3CN over 18 min).

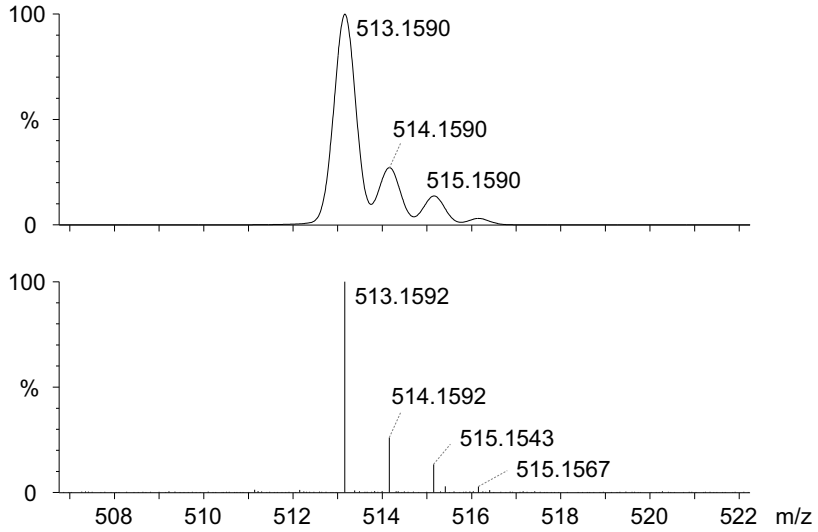

Figure A14. Experimental (lower trace) and simulated (upper trace) ESI-TOF mass spectra for $[M+H]^+$ of [**1c**].

Building block 1d

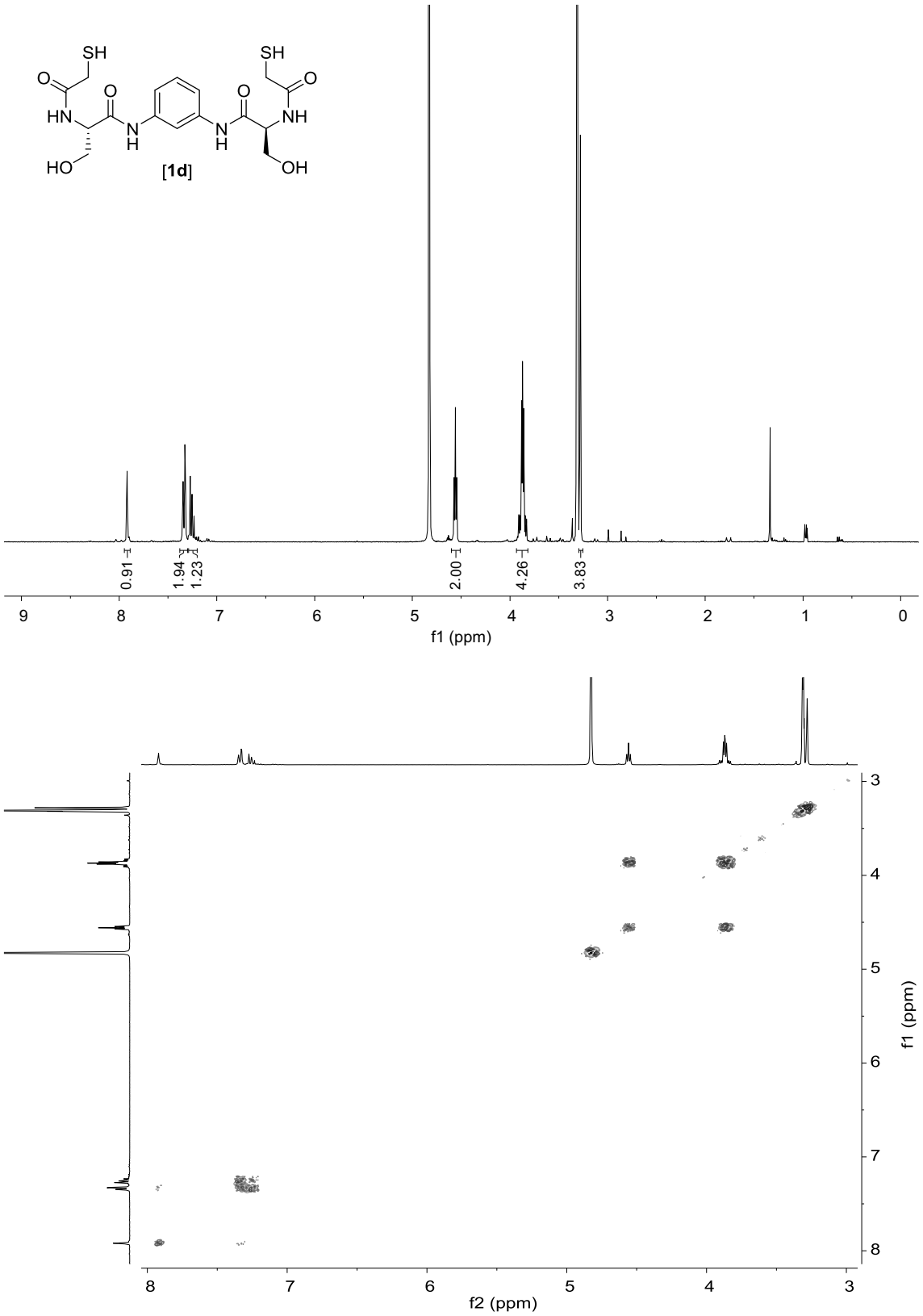

Figure A15. ^{1}H (400 MHz, 298 K in MeOD-d_4) and ^{1}H-^{1}H gCOSY (400 MHz, 298 K in MeOD-d_4) spectra of [**1d**].

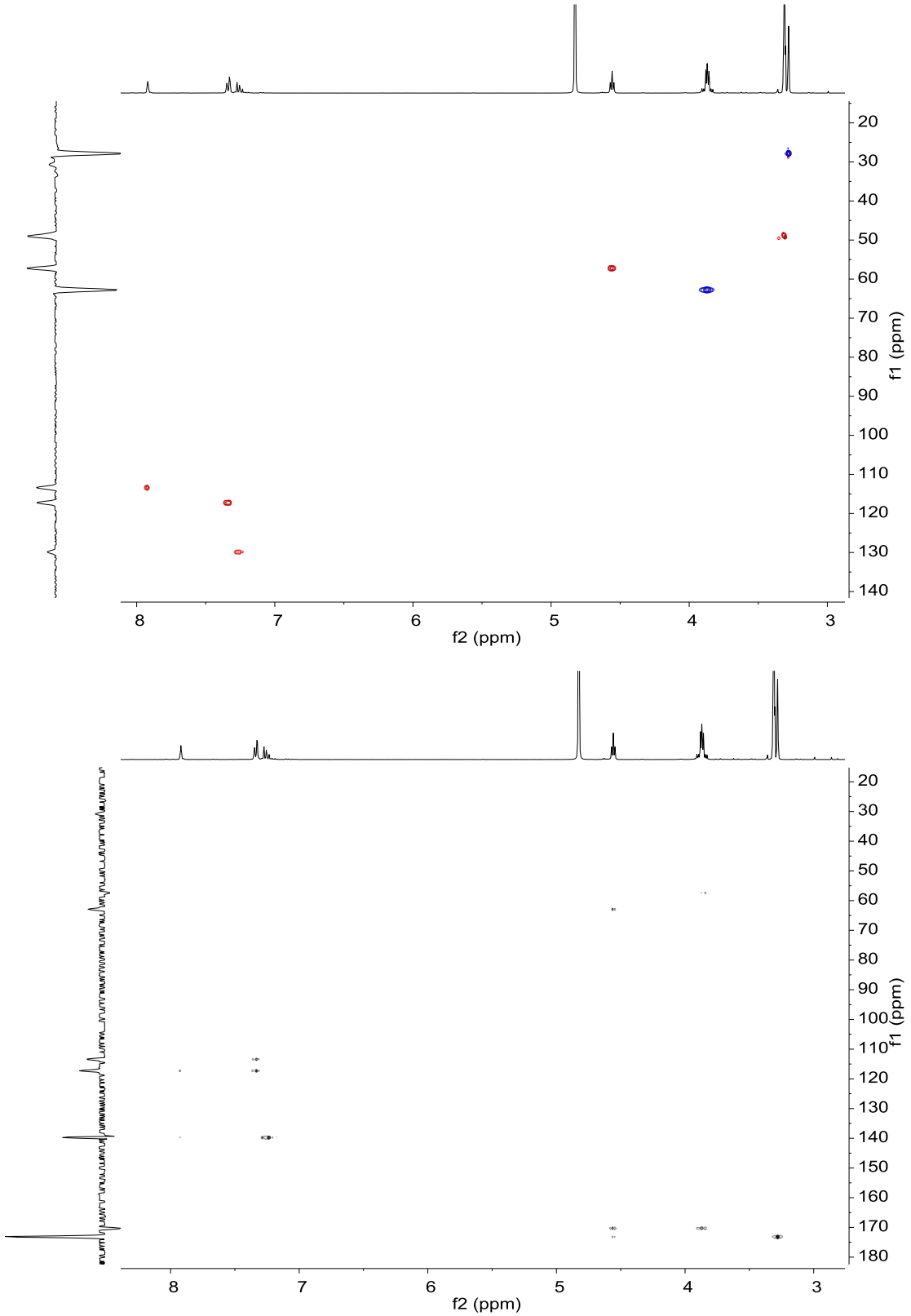

Figure A16. ^{1}H-^{13}C gHSQC (400 MHz, 298 K in MeOD-d_4) and ^{1}H-^{13}C gHMBC (400 MHz, 298 K in MeOD-d_4) spectra of [**1d**].

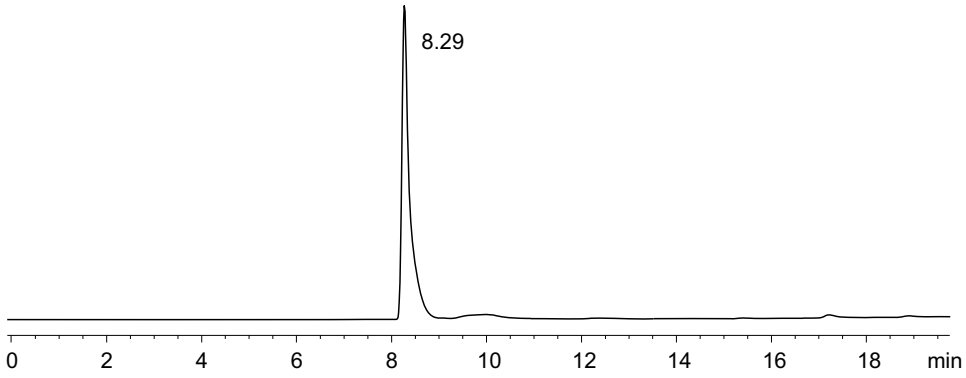

Figure A17. RP-HPLC analysis of [**1d**] (eluent: mixture of CH_3CN + 0.07% (v/v) TFA and H_2O + 0.1% (v/v) TFA; gradient: 2 min at 5% CH_3CN in H_2O, then linear gradient from 5% to 100% CH_3CN over 18 min).

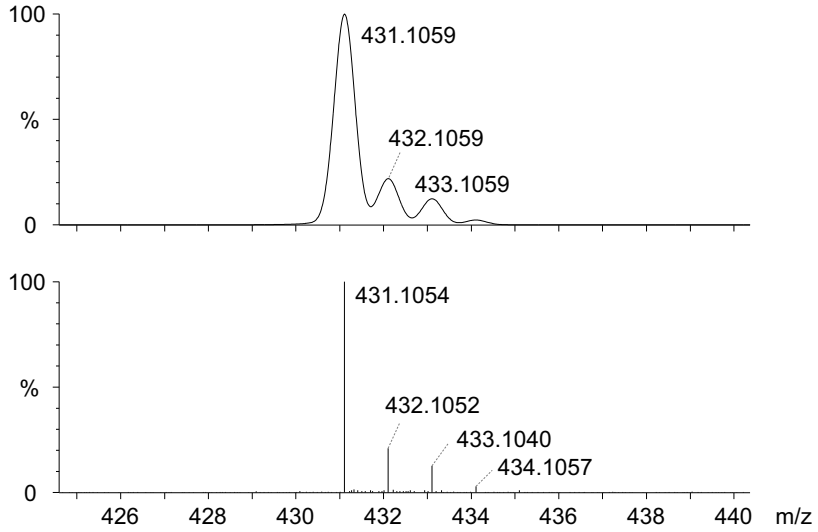

Figure A18. Experimental (lower trace) and simulated (upper trace) ESI-TOF mass spectra for $[M+H]^+$ of [**1d**].

Building block 1e

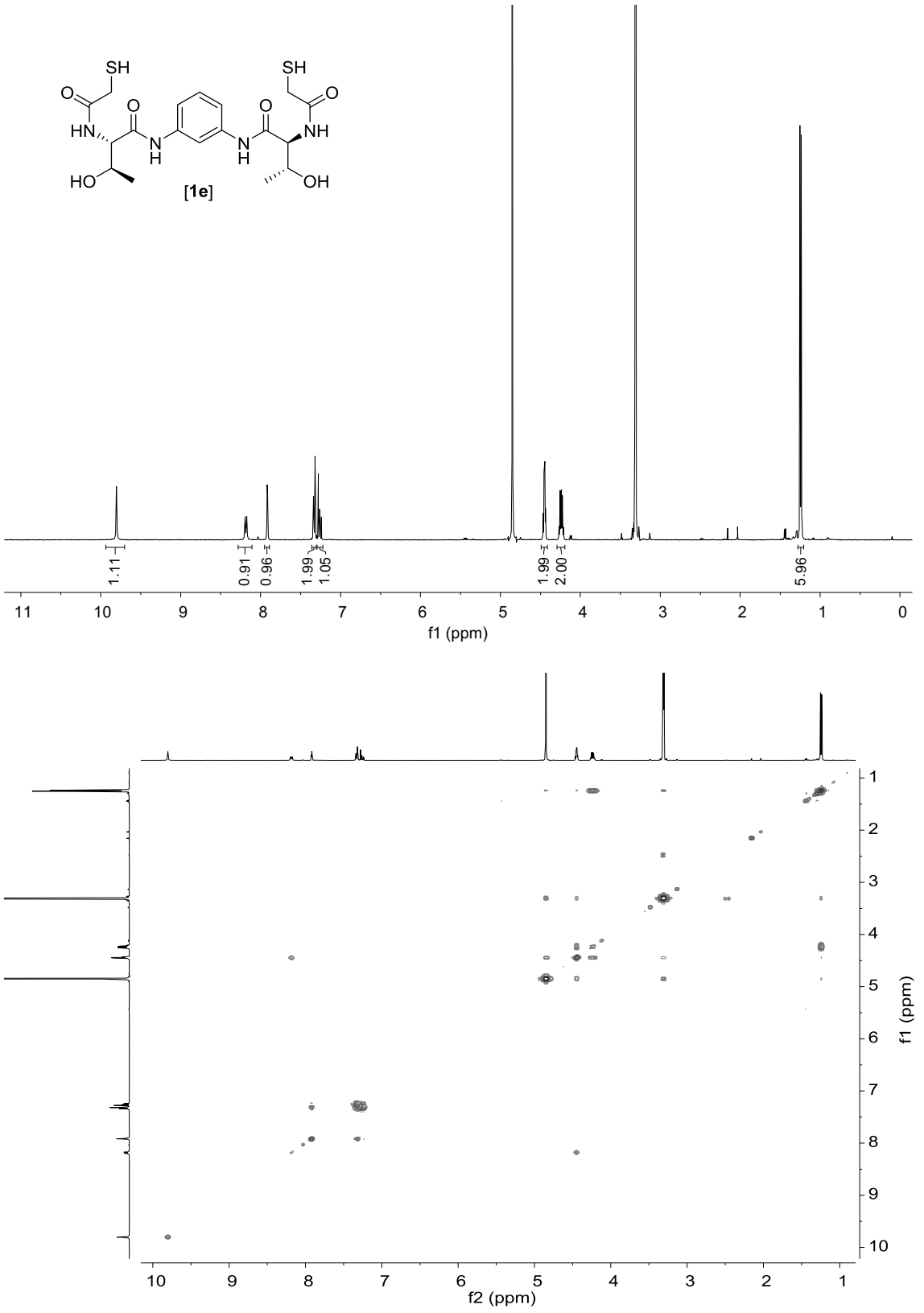

Figure A19. ^{1}H (400 MHz, 298 K in MeOD-d_4) and ^{1}H-^{1}H gCOSY (400 MHz, 298 K in MeOD-d_4) spectra of [**1e**].

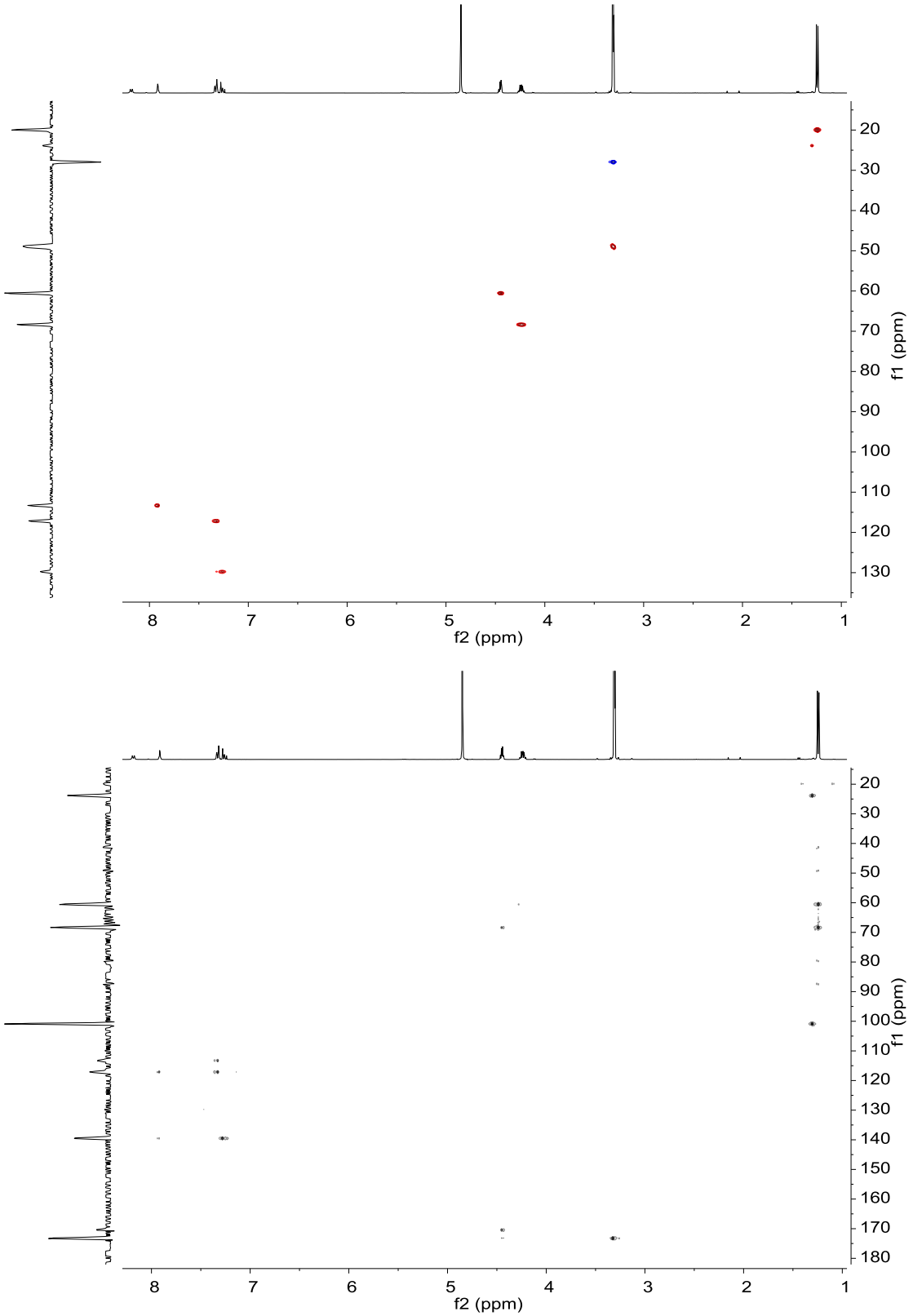

Figure A20. ^{1}H-^{13}C gHSQC (400 MHz, 298 K in MeOD-d_4) and ^{1}H-^{13}C gHMBC (400 MHz, 298 K in MeOD-d_4) spectra of [**1e**].

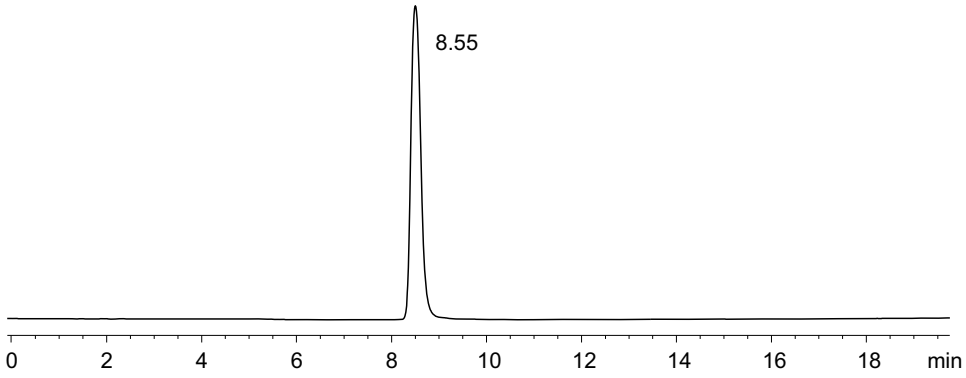

Figure A21. RP-HPLC analysis of [**1e**] (eluent: mixture of CH_3CN + 0.07% (v/v) TFA and H_2O + 0.1% (v/v) TFA; gradient: 2 min at 5% CH_3CN in H_2O, then linear gradient from 5% to 100% CH_3CN over 18 min).

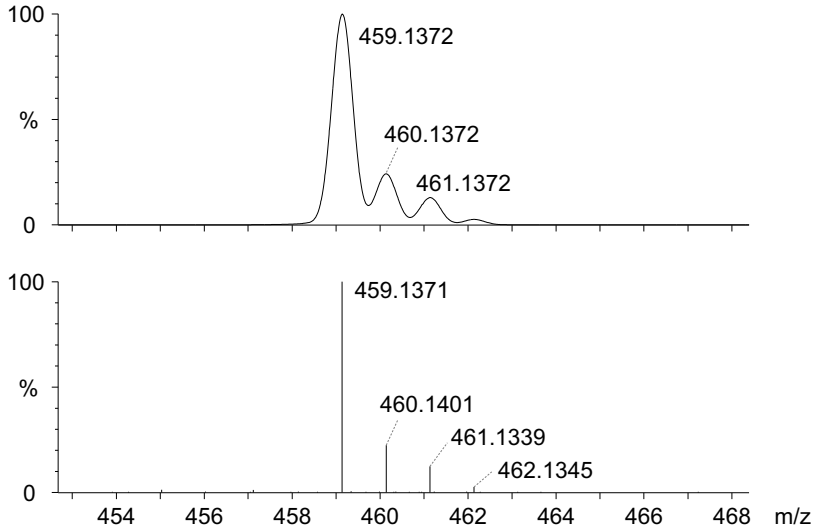

Figure A22. Experimental (lower trace) and simulated (upper trace) ESI-TOF mass spectra for $[M+H]^+$ of [**1e**].

Building block 1f

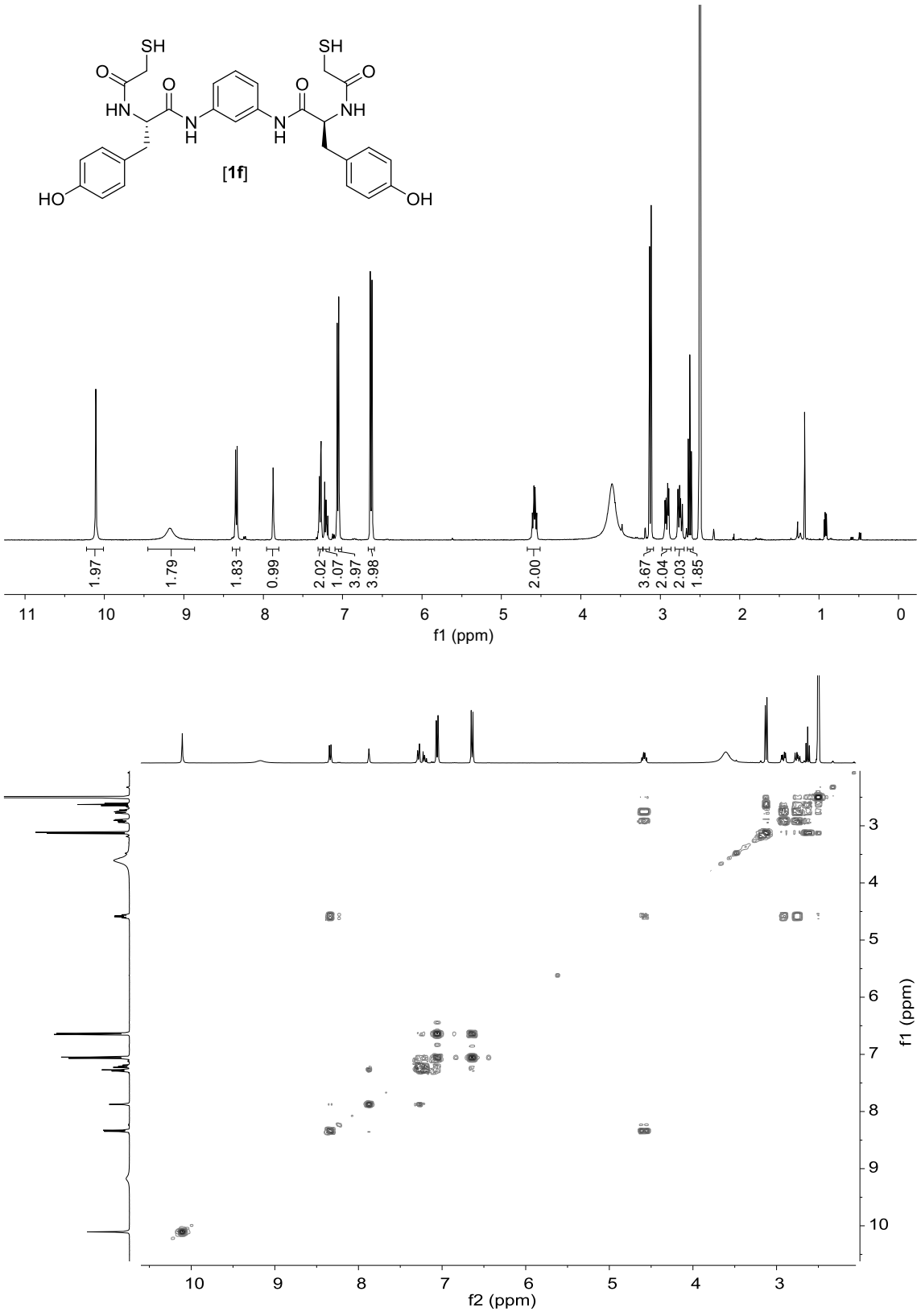

Figure A23. ^{1}H (400 MHz, 298 K in DMSO-d_6) and ^{1}H-^{1}H gCOSY (400 MHz, 298 K in DMSO-d_6) spectra of [**1f**].

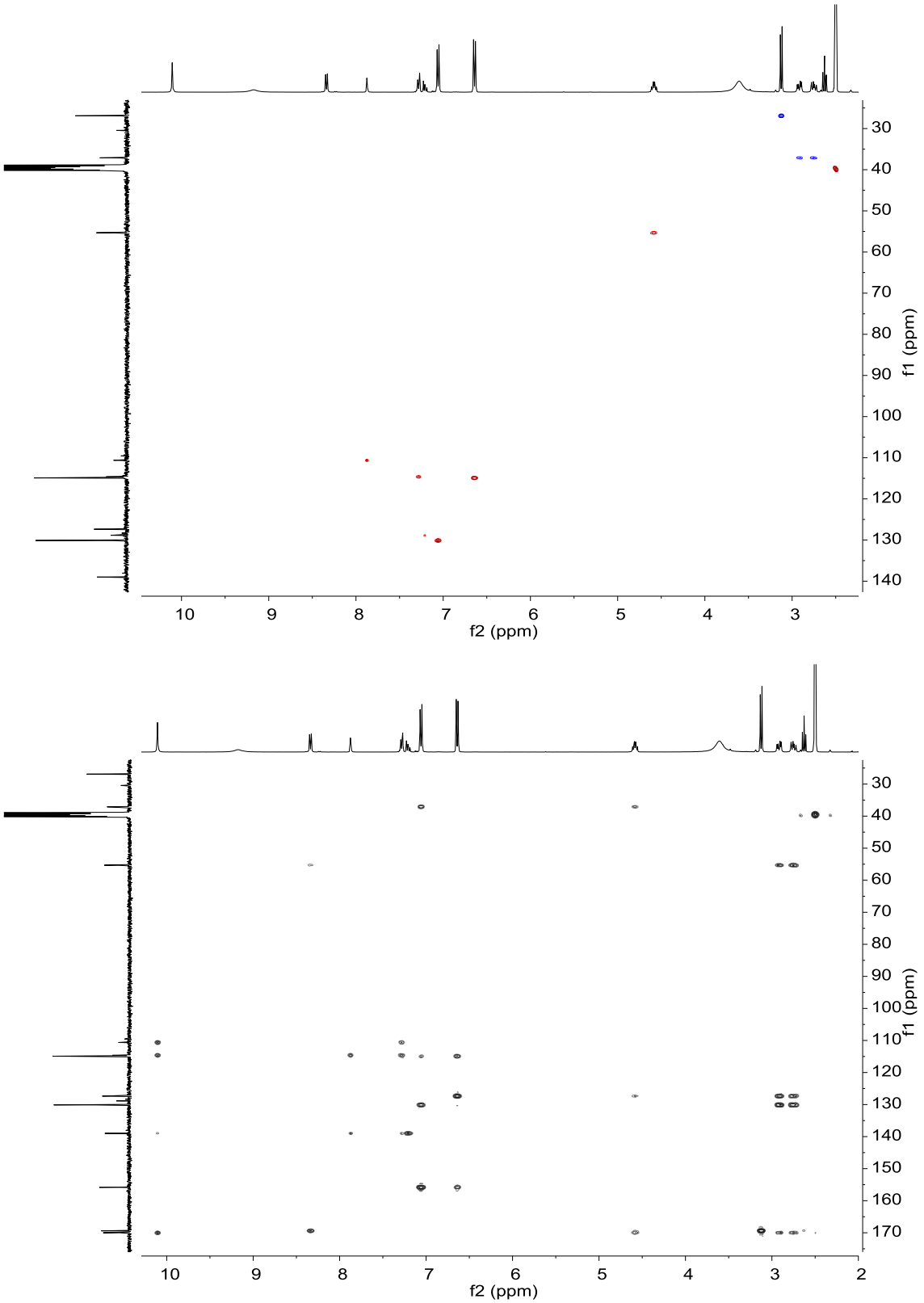

Figure A24. ^{1}H-^{13}C gHSQC (400 MHz, 298 K in DMSO-d_6) and ^{1}H-^{13}C gHMBC (400 MHz, 298 K in DMSO-d_6) spectra of [**1f**].

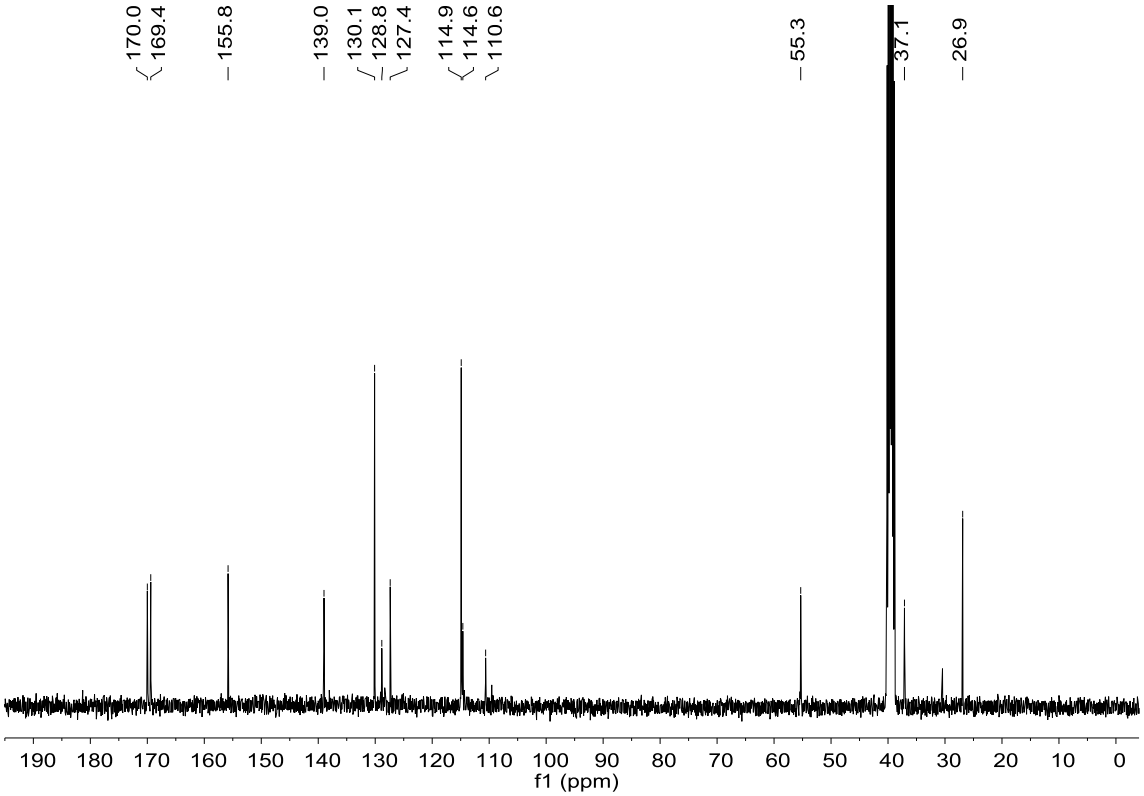

Figure A25. ^{13}C (101 MHz, 298 K in DMSO-d_6) spectrum of [**1f**].

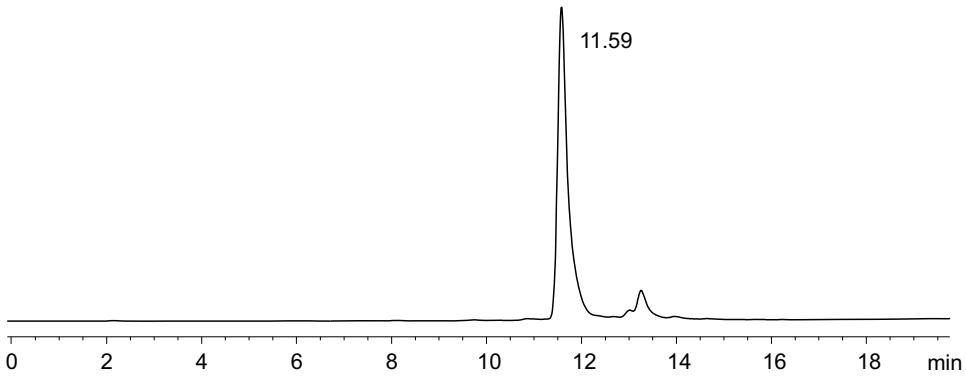

Figure A26. RP-HPLC analysis of [**1f**] (eluent: mixture of CH_3CN + 0.07% (v/v) TFA and H_2O + 0.1% (v/v) TFA; gradient: 2 min at 5% CH_3CN in H_2O, then linear gradient from 5% to 100% CH_3CN over 18 min).

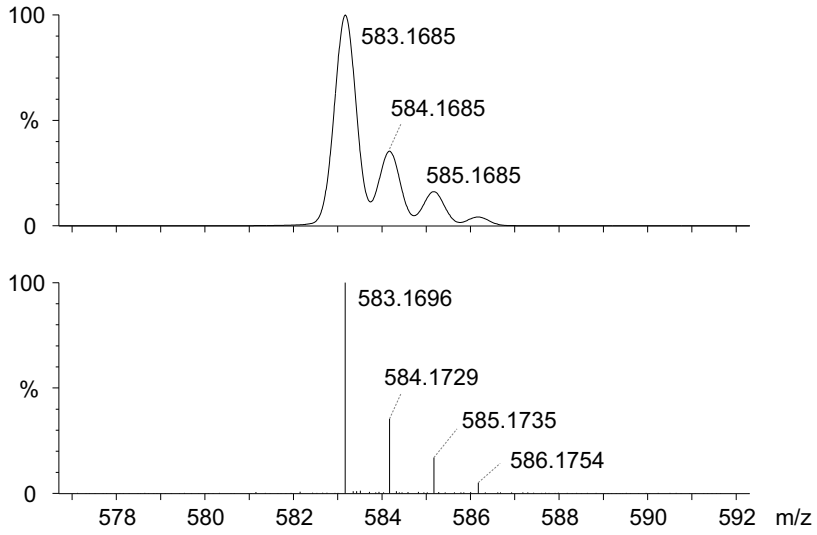

Figure A27. Experimental (lower trace) and simulated (upper trace) ESI-TOF mass spectra for $[M+H]^+$ of [**1f**].

Building block 1g

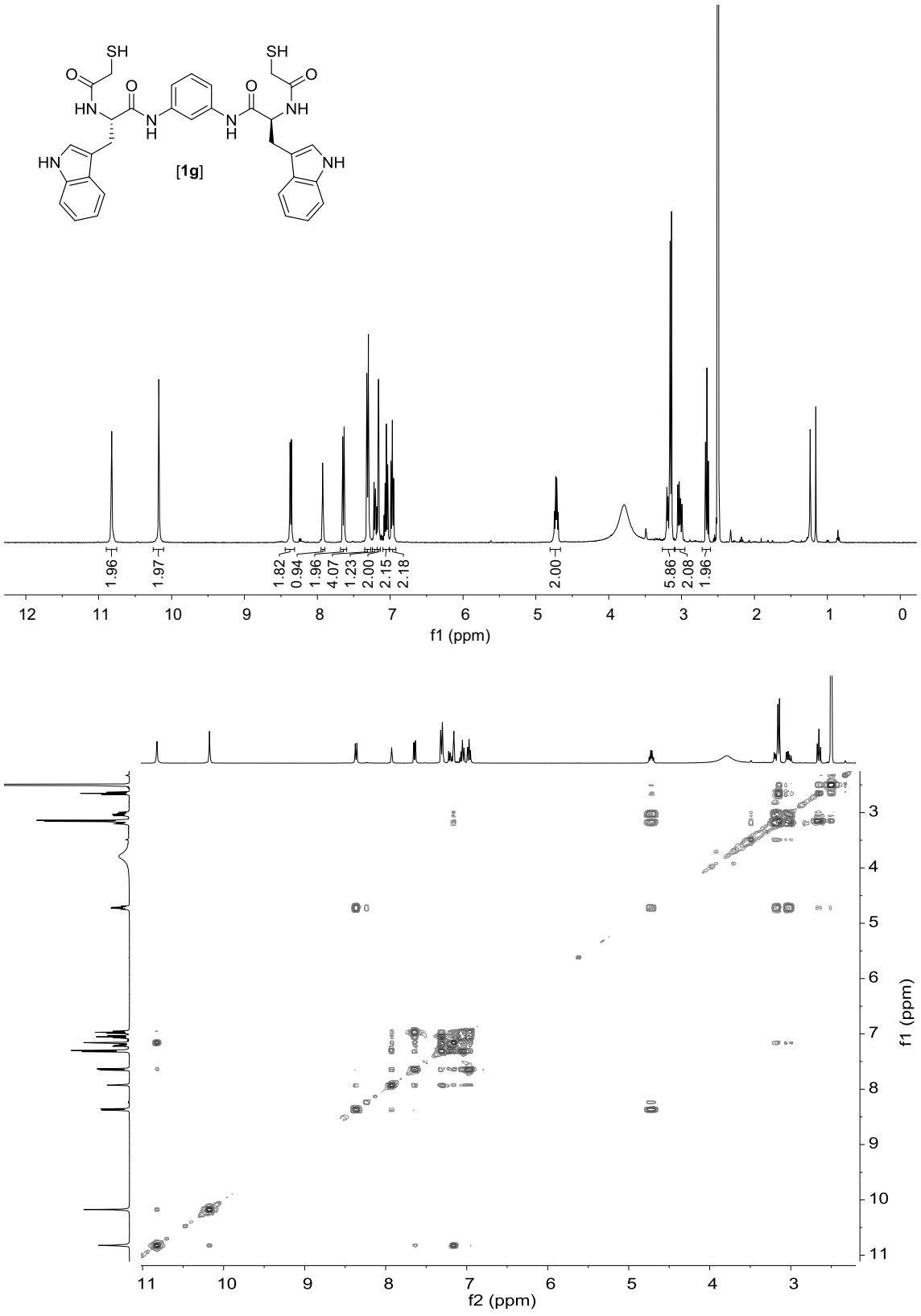

Figure A28. ^{1}H (400 MHz, 298 K in DMSO-d_6) and ^{1}H-^{1}H gCOSY (400 MHz, 298 K in DMSO-d_6) spectra of [**1g**].

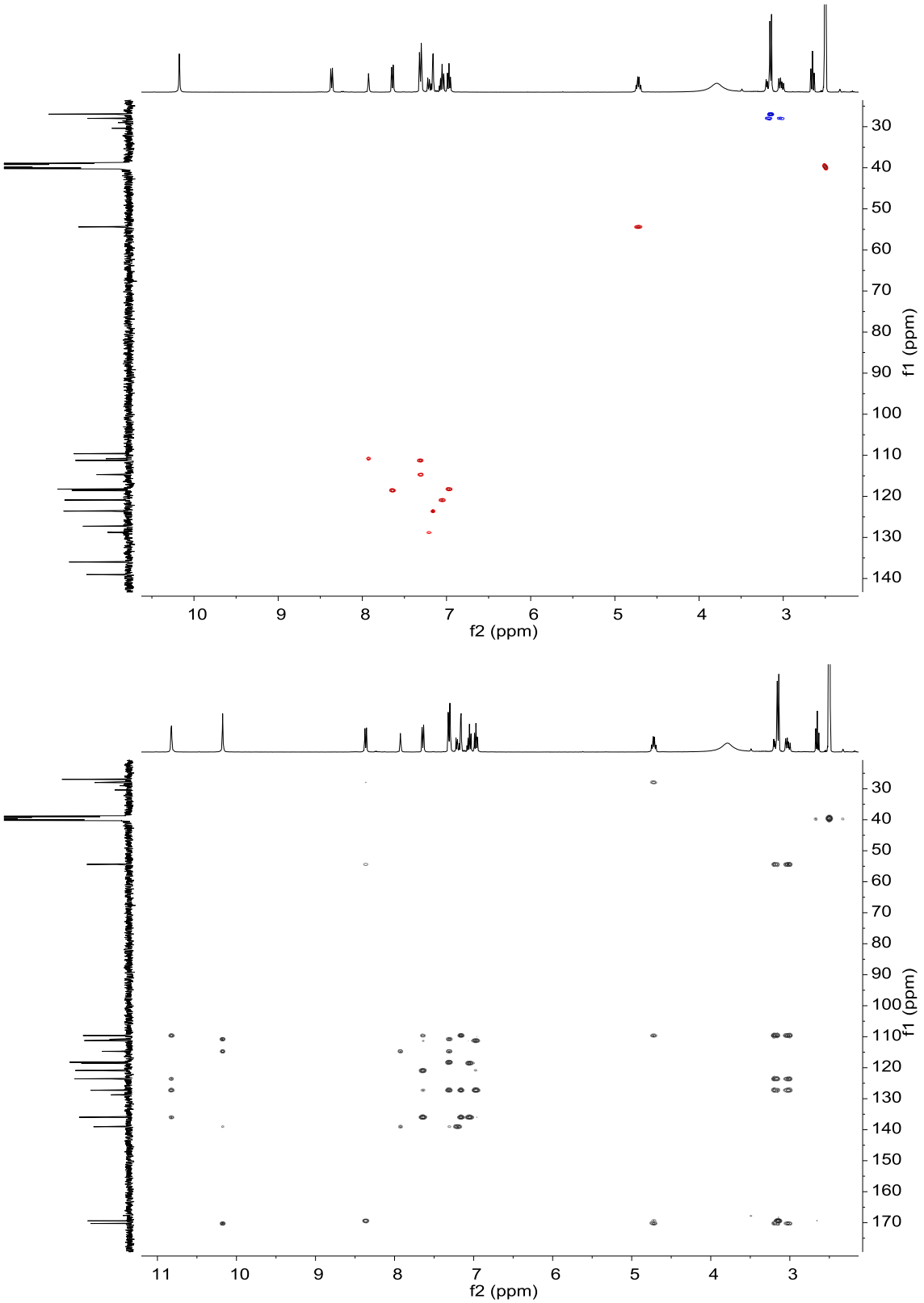

Figure A29. ^{1}H-^{13}C gHSQC (400 MHz, 298 K in DMSO-d_6) and ^{1}H-^{13}C gHMBC (400 MHz, 298 K in DMSO-d_6) spectra of [**1g**].

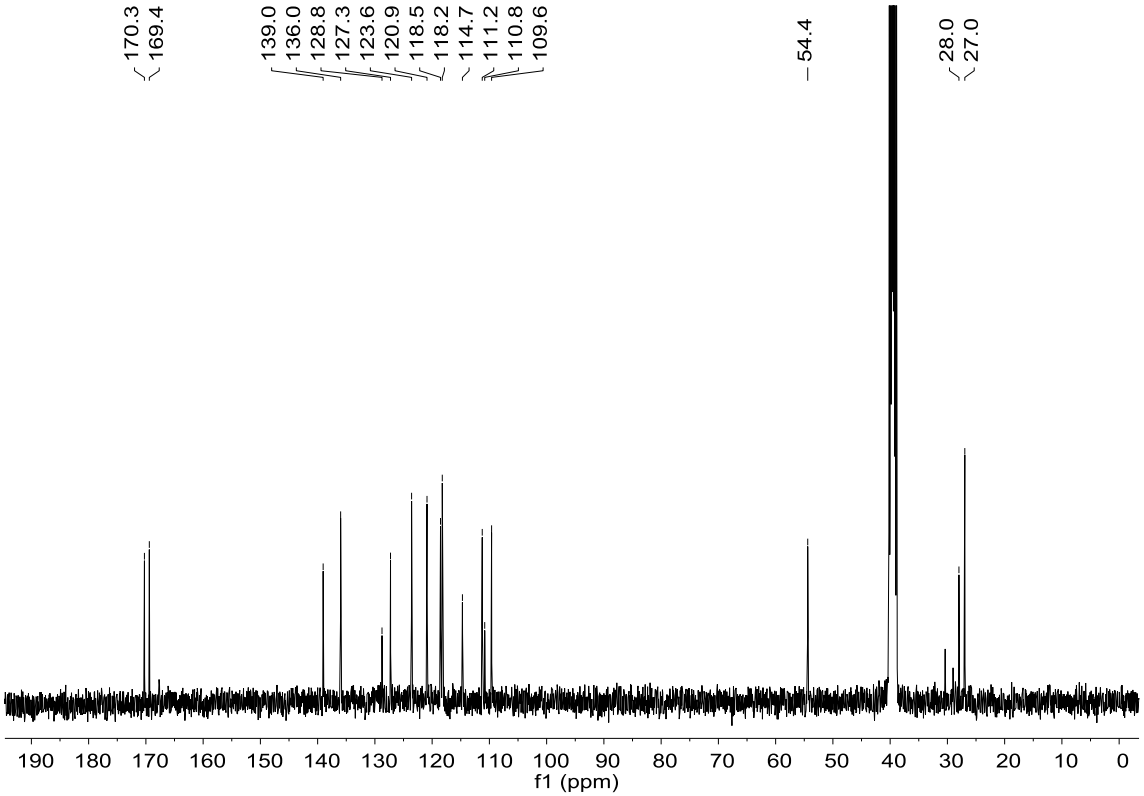

Figure A30. ^{13}C (101 MHz, 298 K in DMSO-d_6) spectrum of [**1g**].

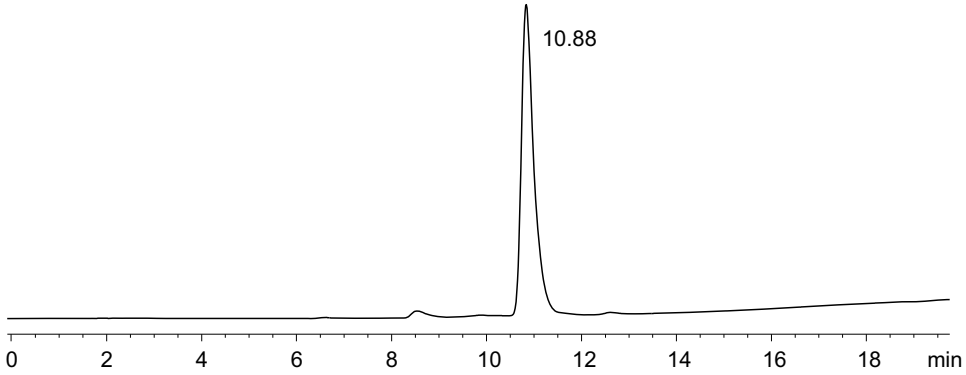

Figure A31. RP-HPLC analysis of [**1g**] (eluent: mixture of CH_3CN + 0.07% (v/v) TFA and H_2O + 0.1% (v/v) TFA; gradient: 2 min at 20% CH_3CN in H_2O, then linear gradient from 20% to 100% CH_3CN over 14 min).

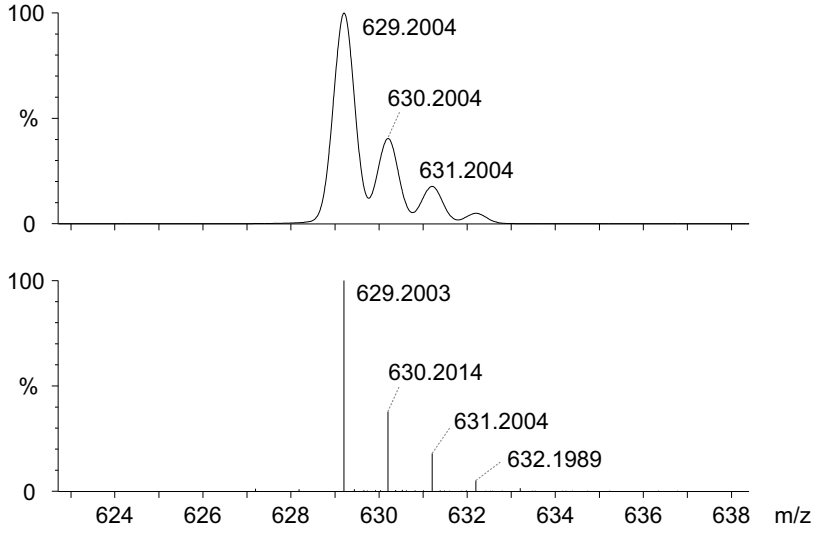

Figure A32. Experimental (lower trace) and simulated (upper trace) ESI-TOF mass spectra for $[M+H]^+$ of [**1g**].

Building block 1h

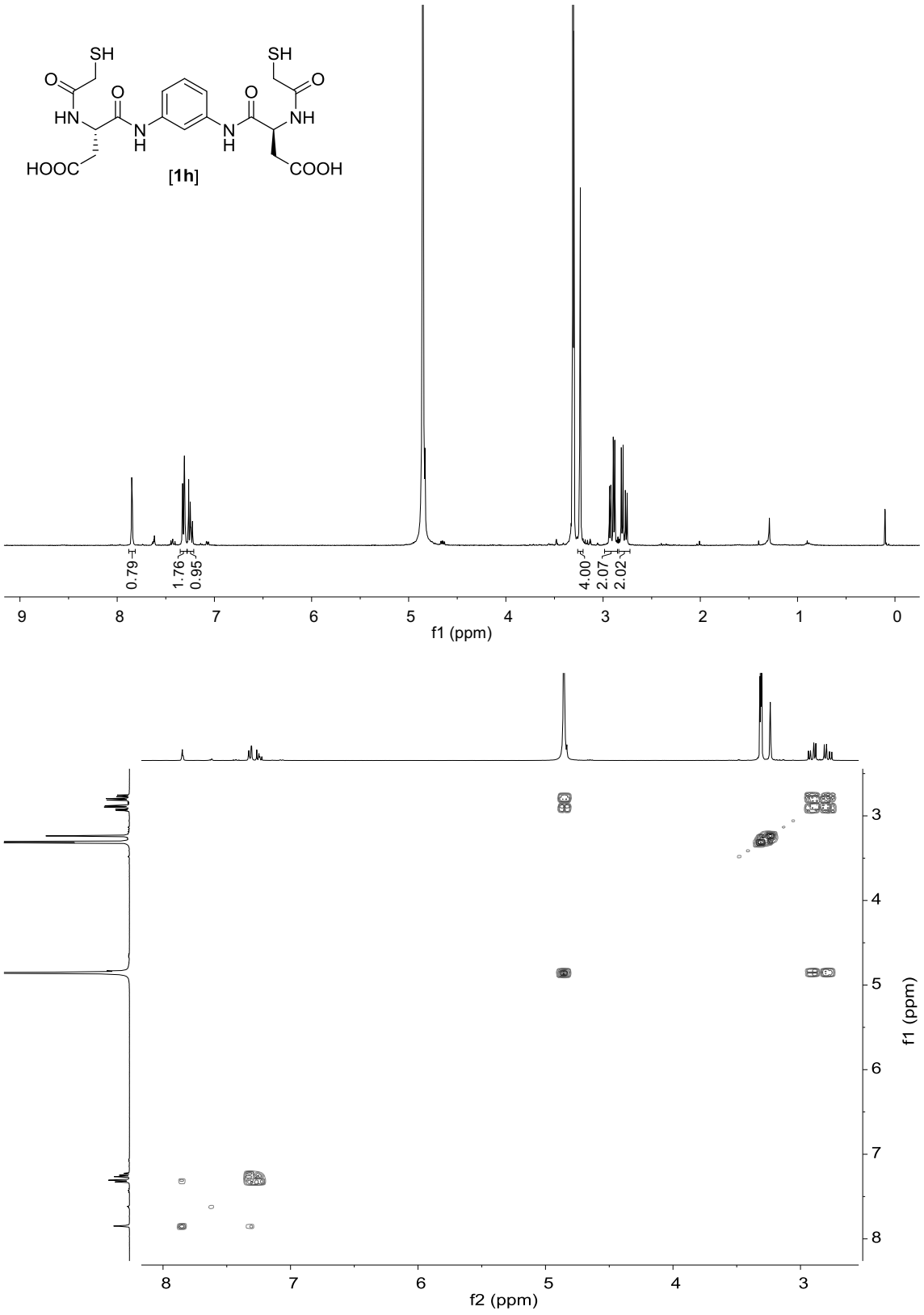

Figure A33. ^{1}H (400 MHz, 298 K in MeOD-d_4) and ^{1}H-^{1}H gCOSY (400 MHz, 298 K in MeOD-d_4) spectra of [**1h**].

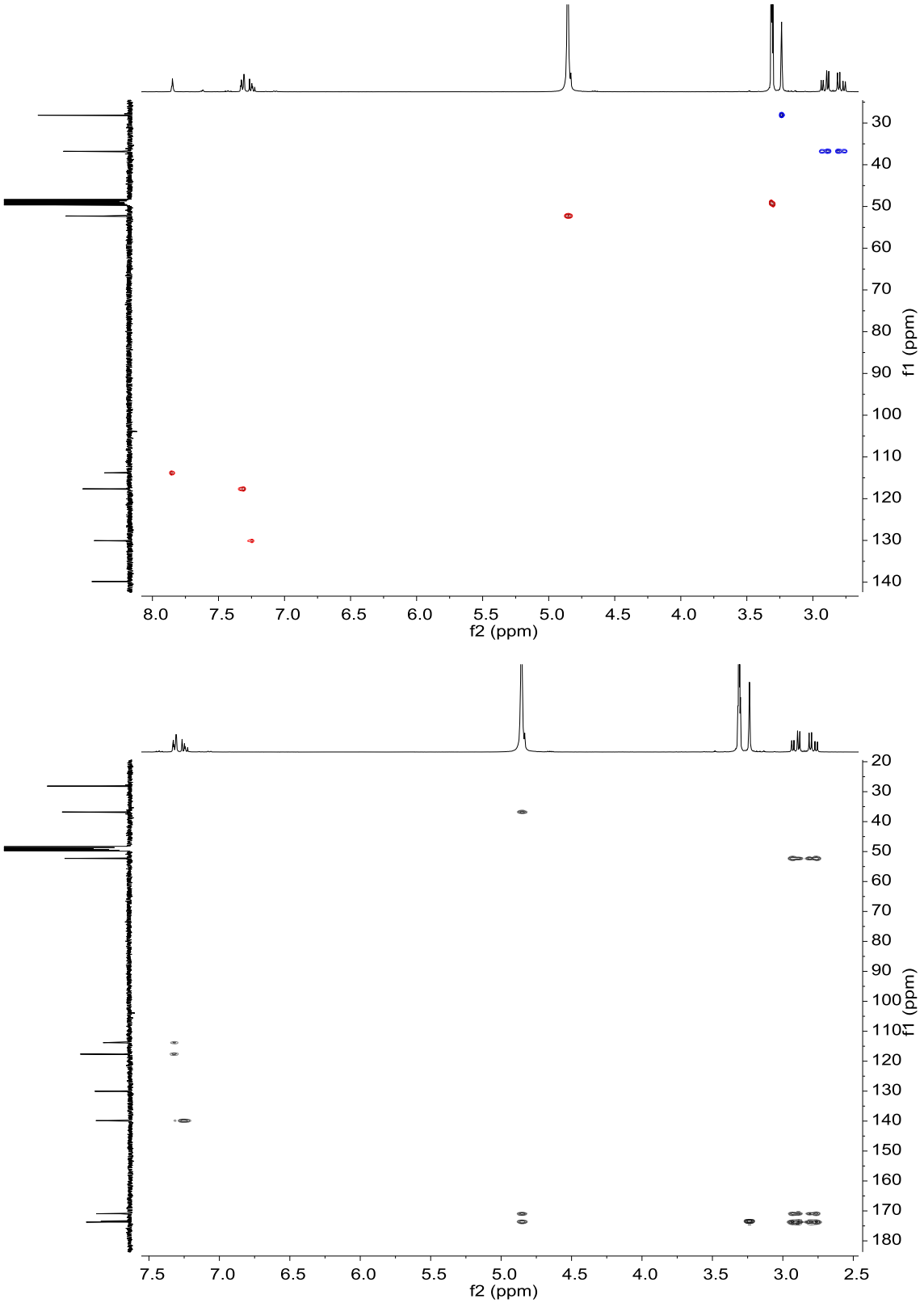

Figure A34. ^{1}H-^{13}C gHSQC (400 MHz, 298 K in MeOD-d_4) and ^{1}H-^{13}C gHMBC (400 MHz, 298 K in MeOD-d_4) spectra of [**1h**].

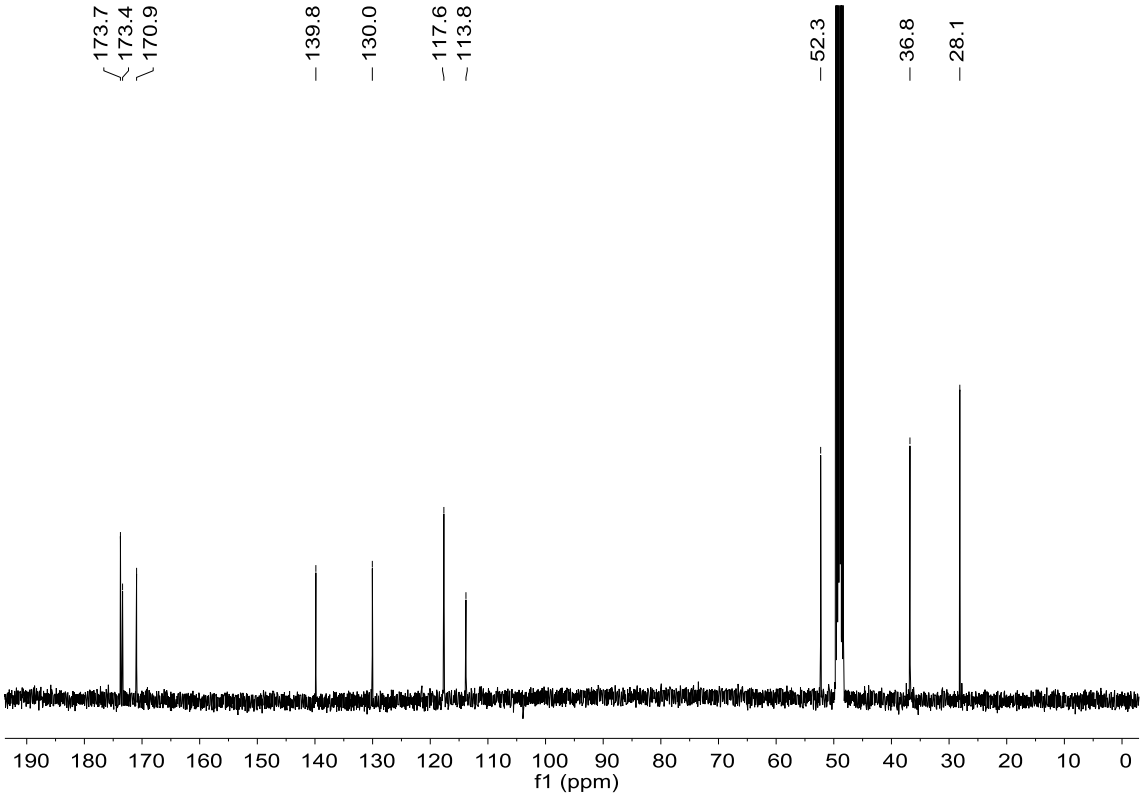

Figure A35. ^{13}C (101 MHz, 298 K in MeOD-d_4) spectrum of [**1h**].

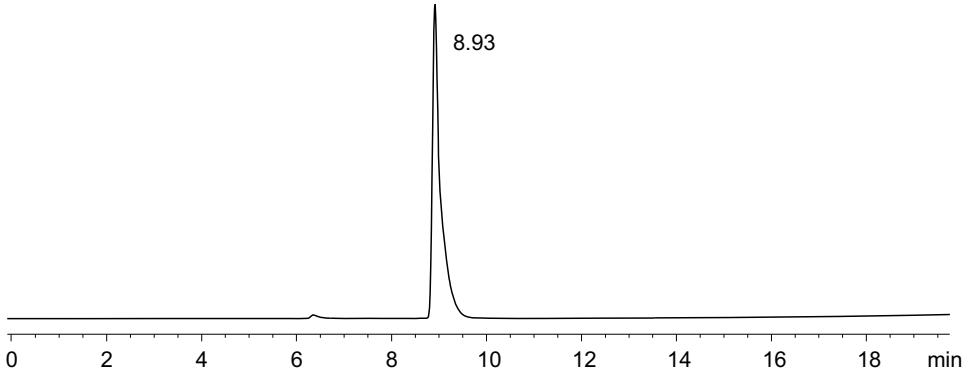

Figure A36. RP-HPLC analysis of [**1h**] (eluent: mixture of CH_3CN + 0.07% (v/v) TFA and H_2O + 0.1% (v/v) TFA; gradient: 2 min at 5% CH_3CN in H_2O, then linear gradient from 5% to 100% CH_3CN over 18 min).

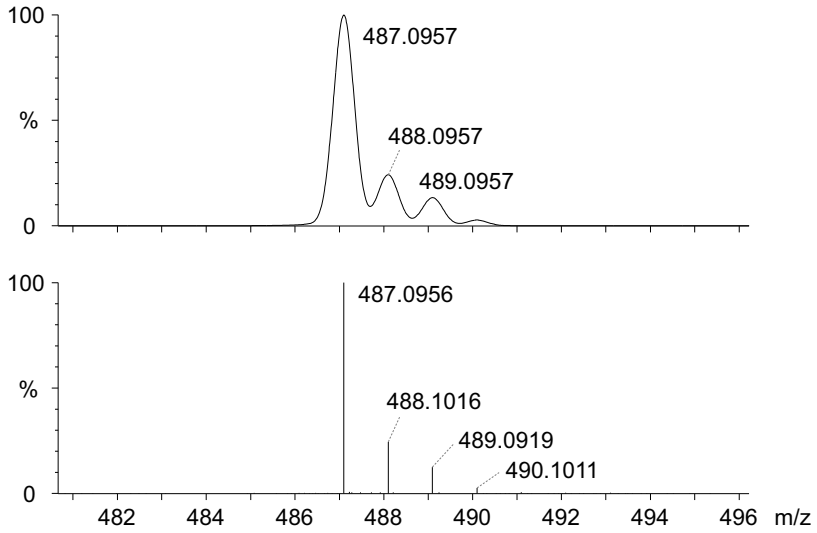

Figure A37. Experimental (lower trace) and simulated (upper trace) ESI-TOF mass spectra for $[M+H]^+$ of [**1h**].

Building block 1i

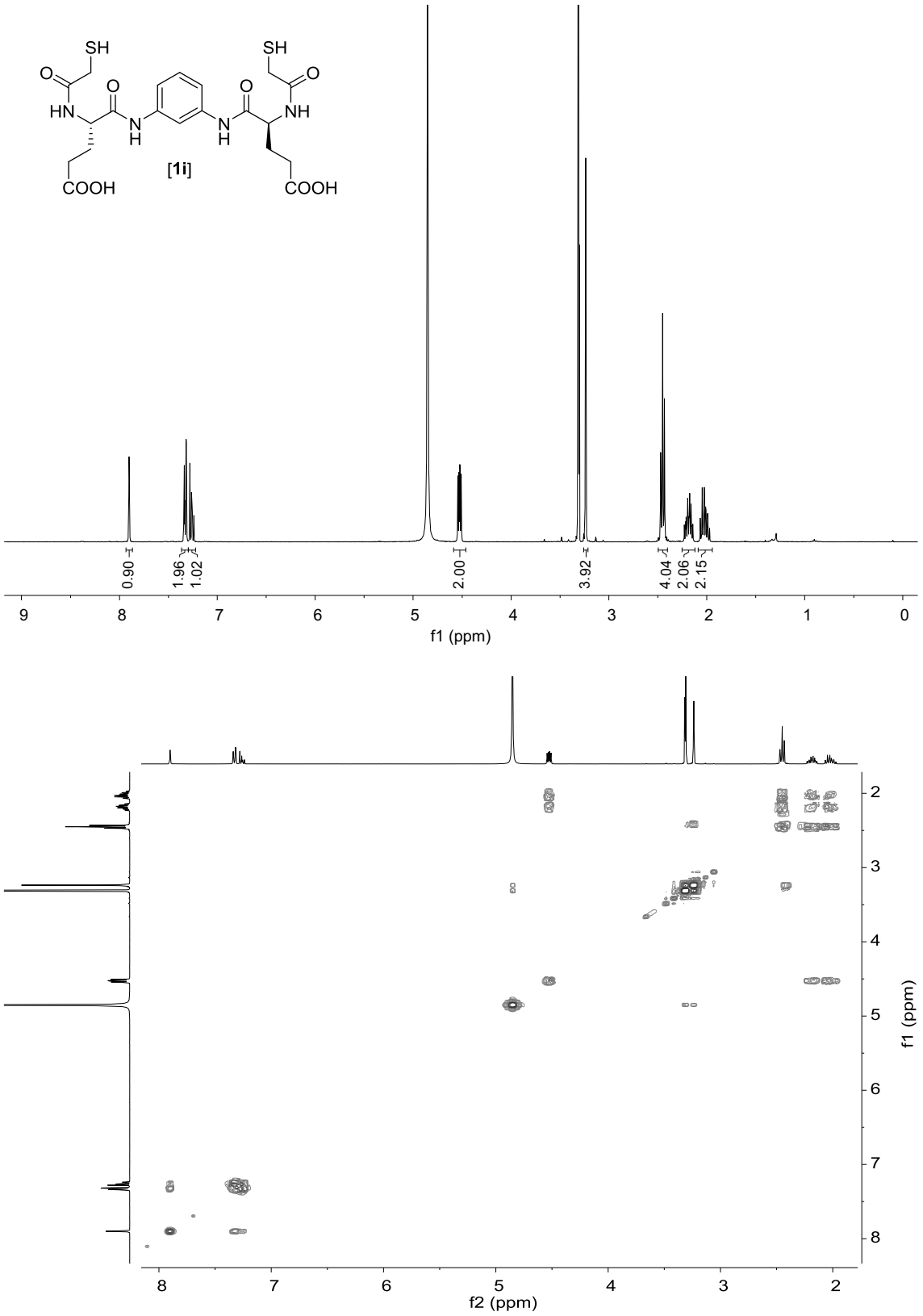

Figure A38. ^{1}H (400 MHz, 298 K in MeOD-d_4) and ^{1}H-^{1}H gCOSY (400 MHz, 298 K in MeOD-d_4) spectra of [**1i**].

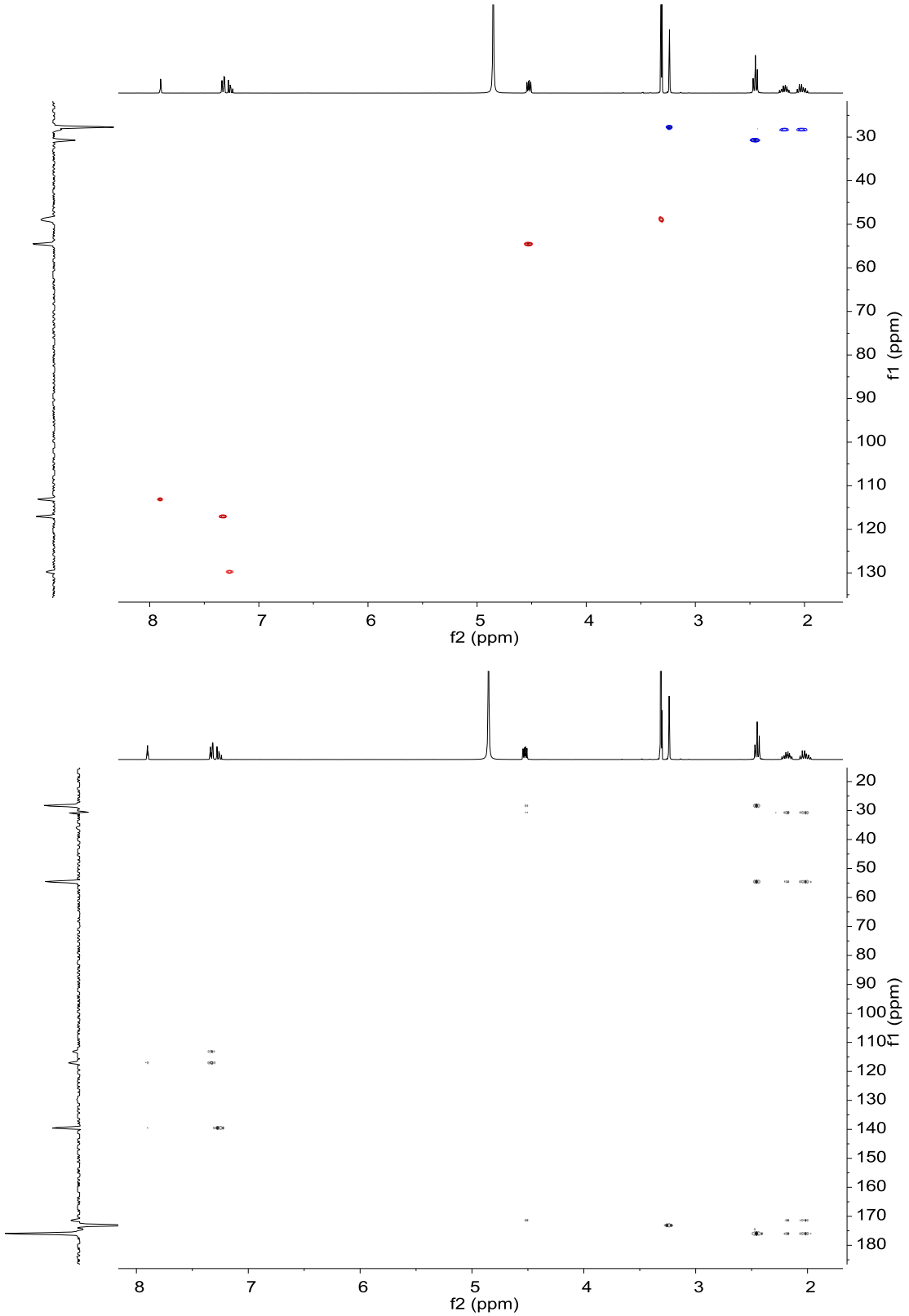

Figure A39. ^{1}H-^{13}C gHSQC (400 MHz, 298 K in MeOD-d_4) and ^{1}H-^{13}C gHMBC (400 MHz, 298 K in MeOD-d_4) spectra of [**1i**].

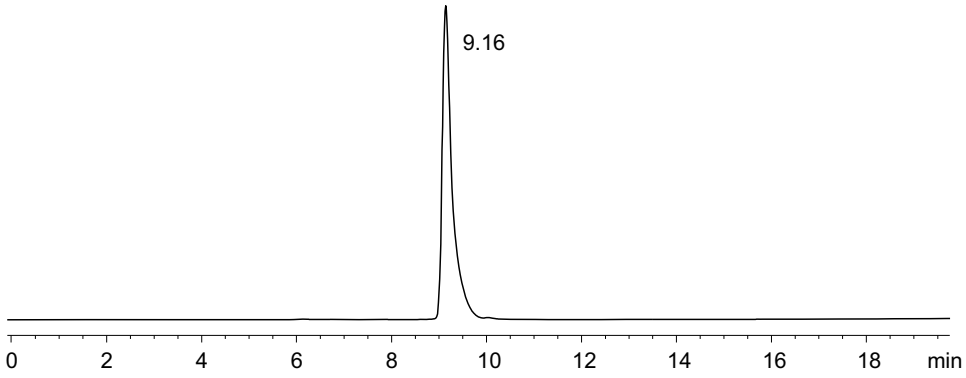

Figure A40. RP-HPLC analysis of [**1i**] (eluent: mixture of CH_3CN + 0.07% (v/v) TFA and H_2O + 0.1% (v/v) TFA; gradient: 2 min at 5% CH_3CN in H_2O, then linear gradient from 5% to 100% CH_3CN over 18 min).

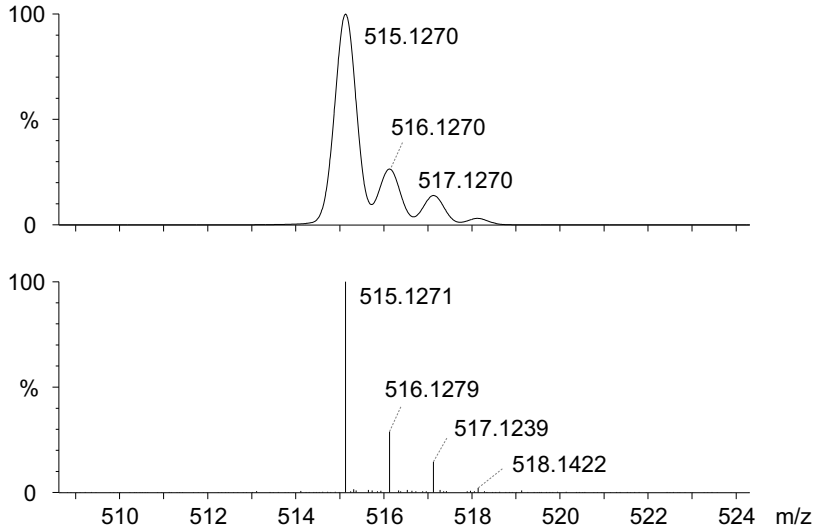

Figure A41. Experimental (lower trace) and simulated (upper trace) ESI-TOF mass spectra for $[M+H]^+$ of [**1i**].

Building block 1j

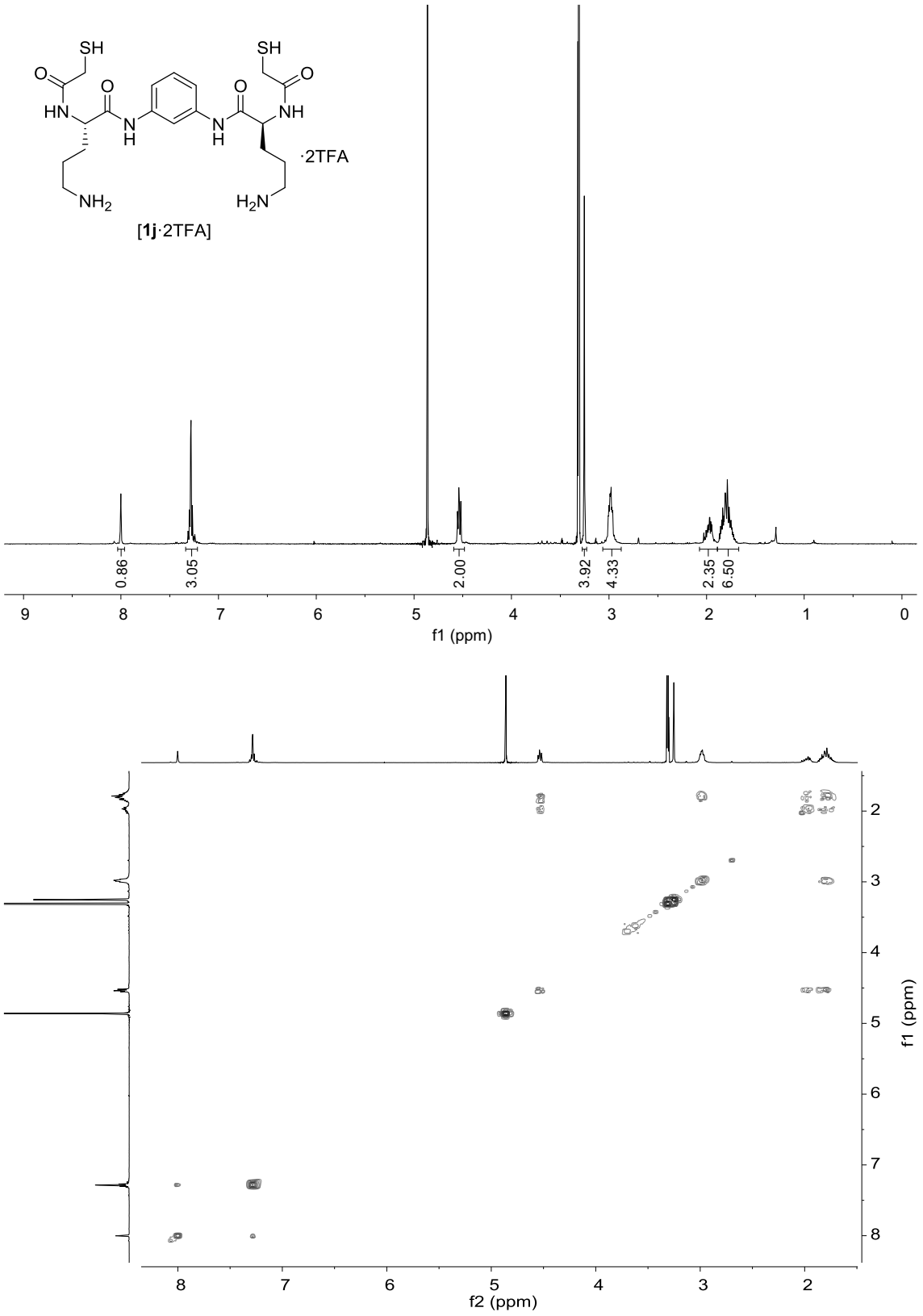

Figure A42. ^{1}H (400 MHz, 298 K in MeOD-d_4) and ^{1}H-^{1}H gCOSY (400 MHz, 298 K in MeOD-d_4) spectra of [**1j**·2TFA].

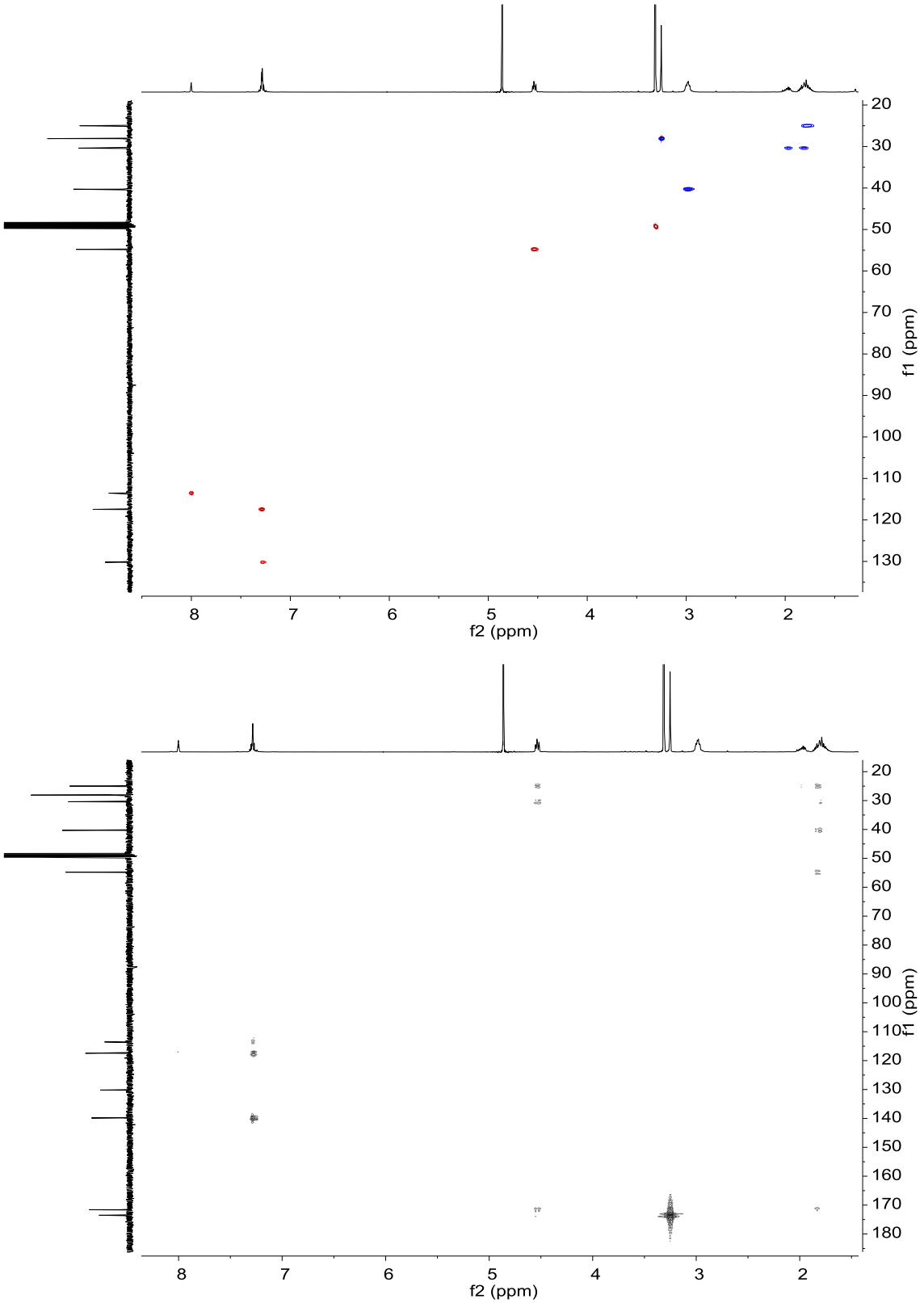

Figure A43. ^{1}H-^{13}C gHSQC (400 MHz, 298 K in MeOD-d_4) and ^{1}H-^{13}C gHMBC (400 MHz, 298 K in MeOD-d_4) spectra of [**1j**·2TFA].

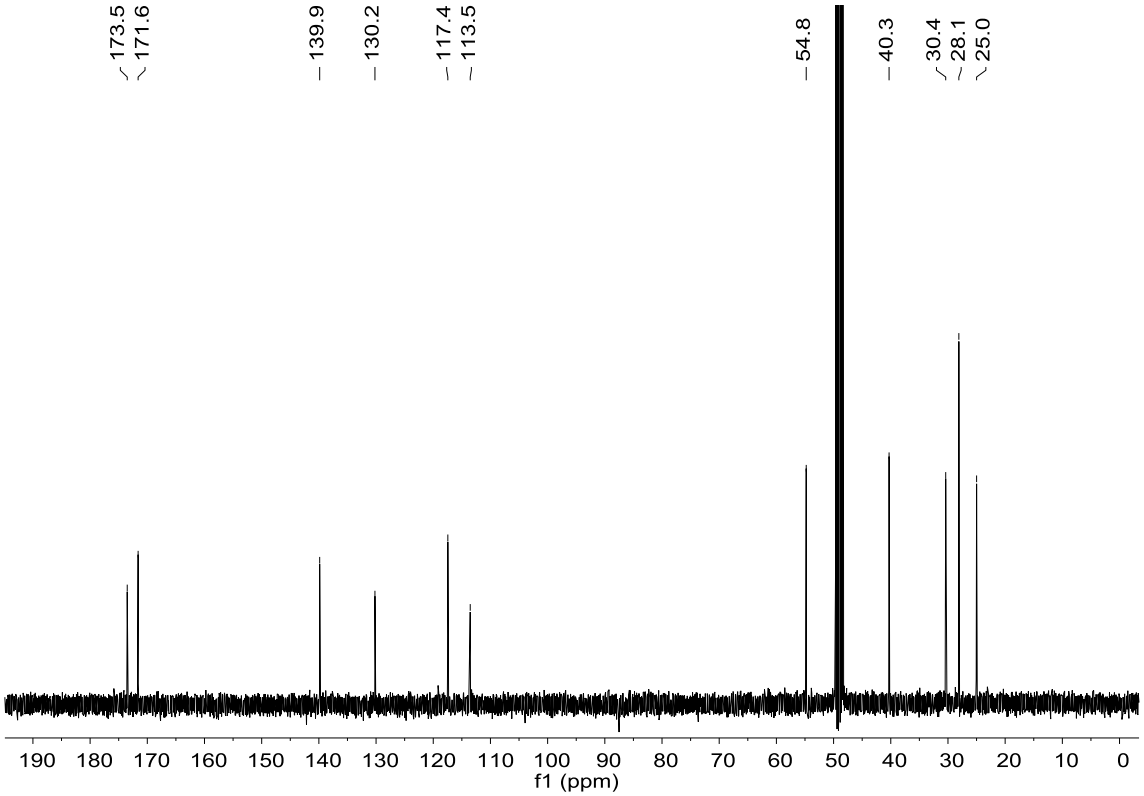

Figure A44. ^{13}C (101 MHz, 298 K in MeOD-d_4) spectrum of [**1j**·2TFA].

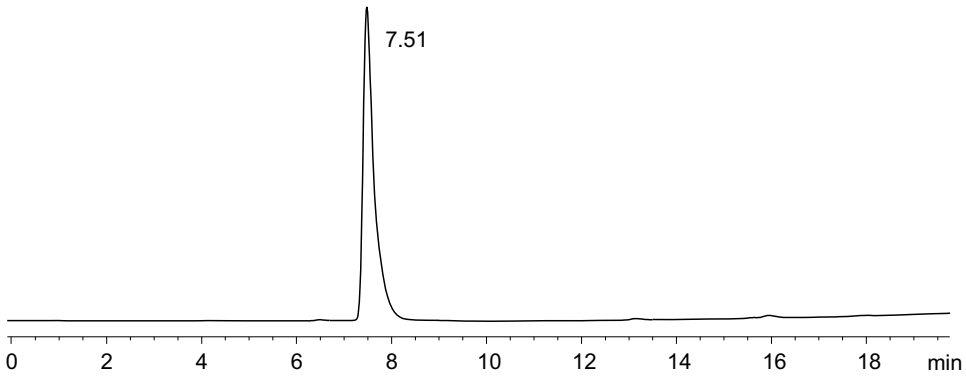

Figure A45. RP-HPLC analysis of [**1j**] (eluent: mixture of CH_3CN + 0.07% (v/v) TFA and H_2O + 0.1% (v/v) TFA; gradient: 2 min at 5% CH_3CN in H_2O, then linear gradient from 5% to 100% CH_3CN over 18 min).

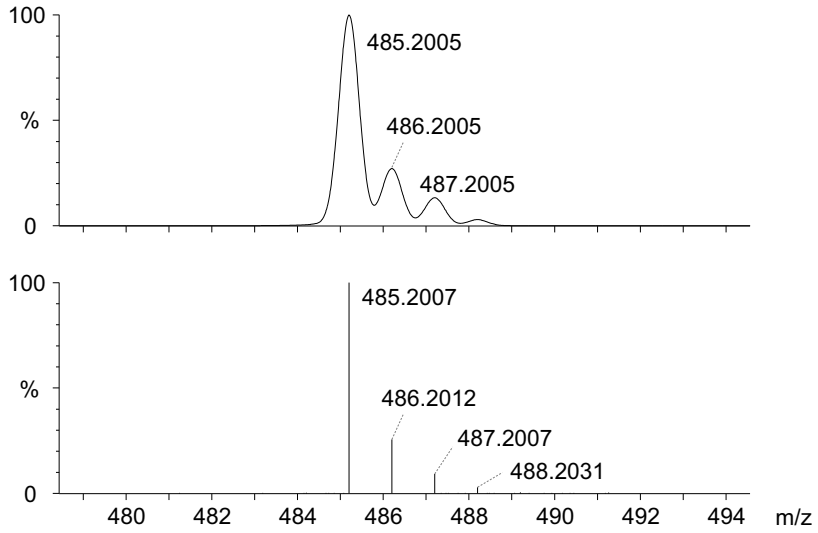

Figure A46. Experimental (lower trace) and simulated (upper trace) ESI-TOF mass spectra for $[M+H]^+$ of [**1j**].

Building block 1k

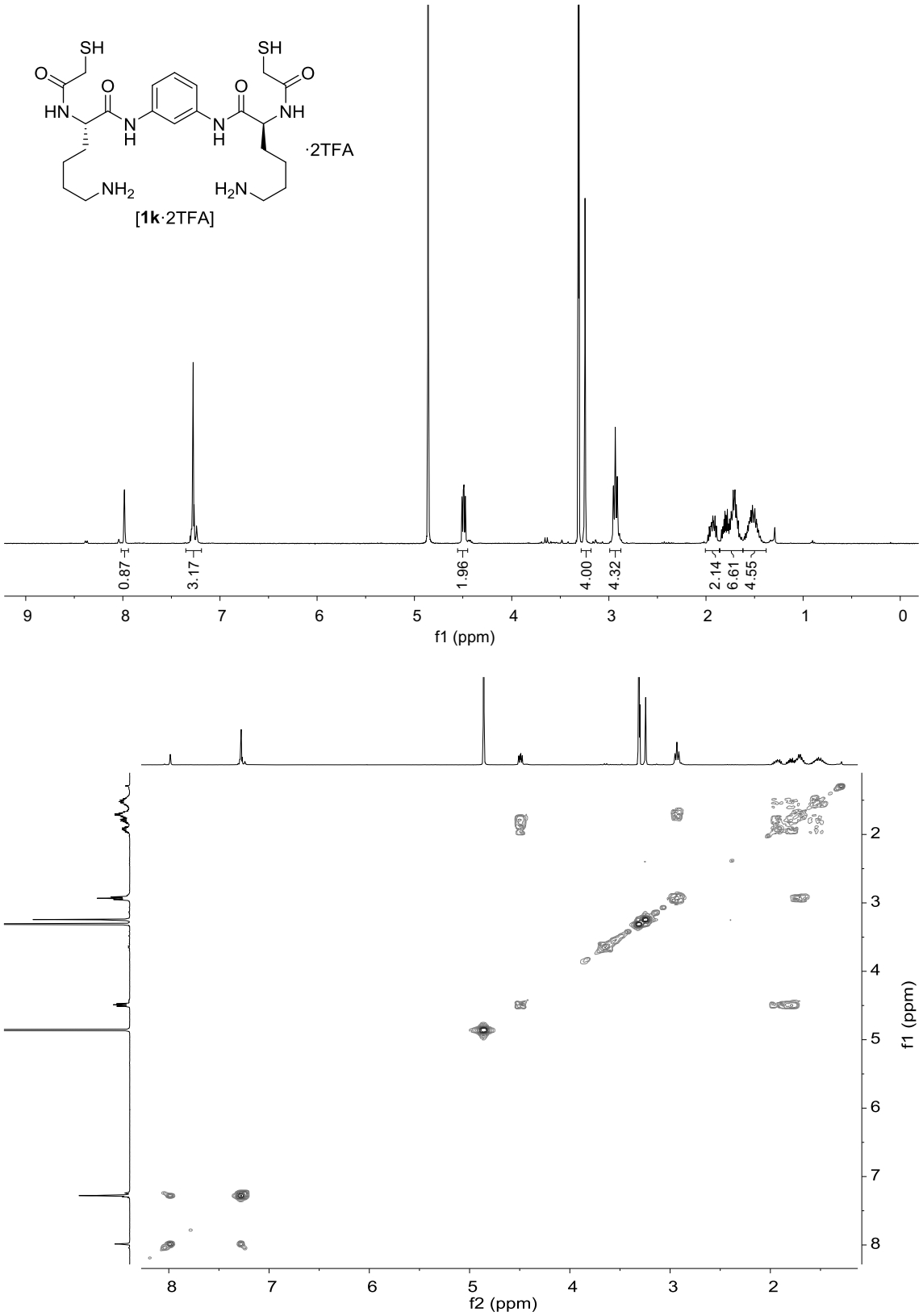

Figure A47. ^{1}H (400 MHz, 298 K in MeOD-d_4) and ^{1}H-^{1}H gCOSY (400 MHz, 298 K in MeOD-d_4) spectra of [**1k**·2TFA].

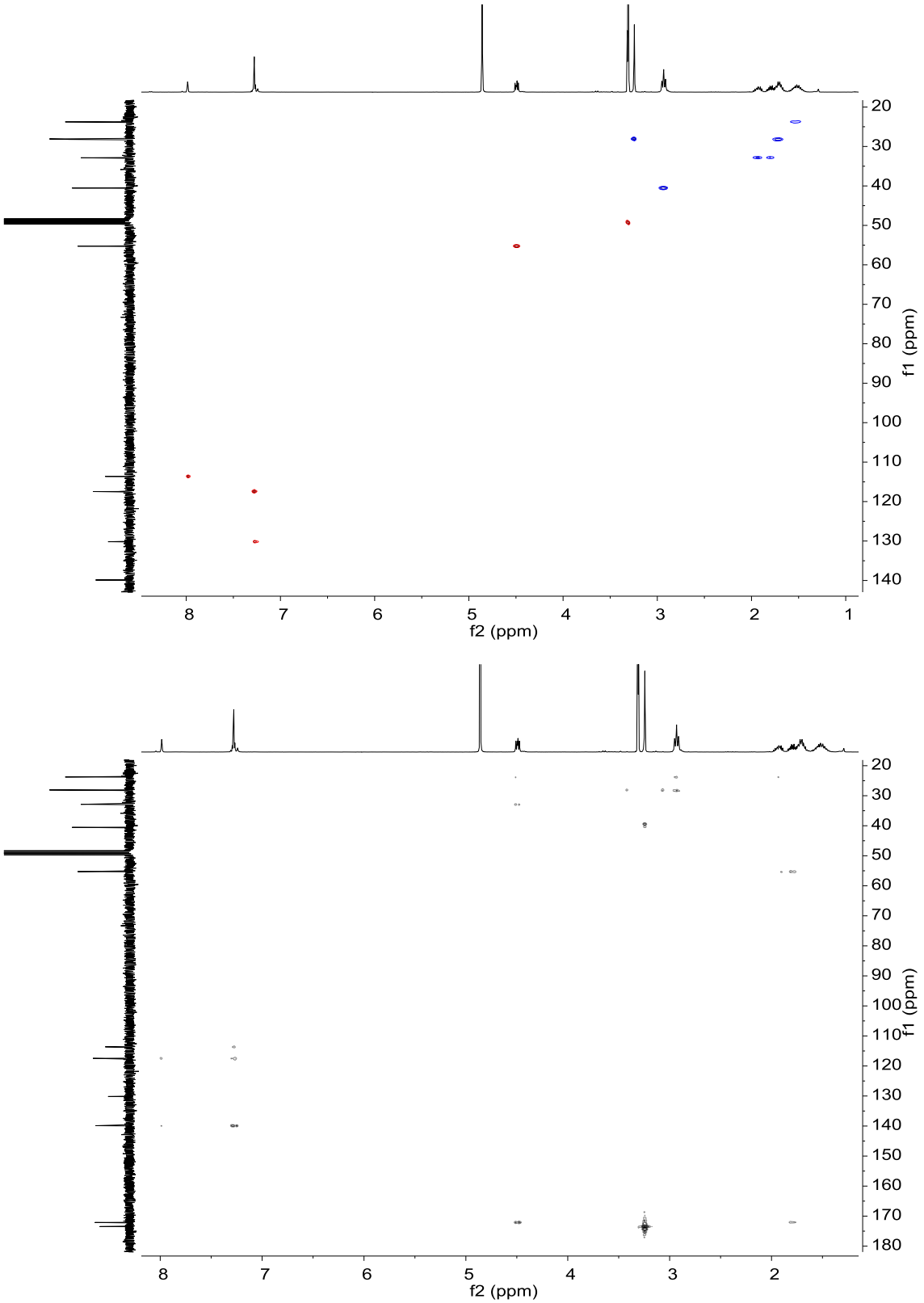

Figure A48. ^{1}H-^{13}C gHSQC (400 MHz, 298 K in MeOD-d_4) and ^{1}H-^{13}C gHMBC (400 MHz, 298 K in MeOD-d_4) spectra of [**1k**·2TFA].

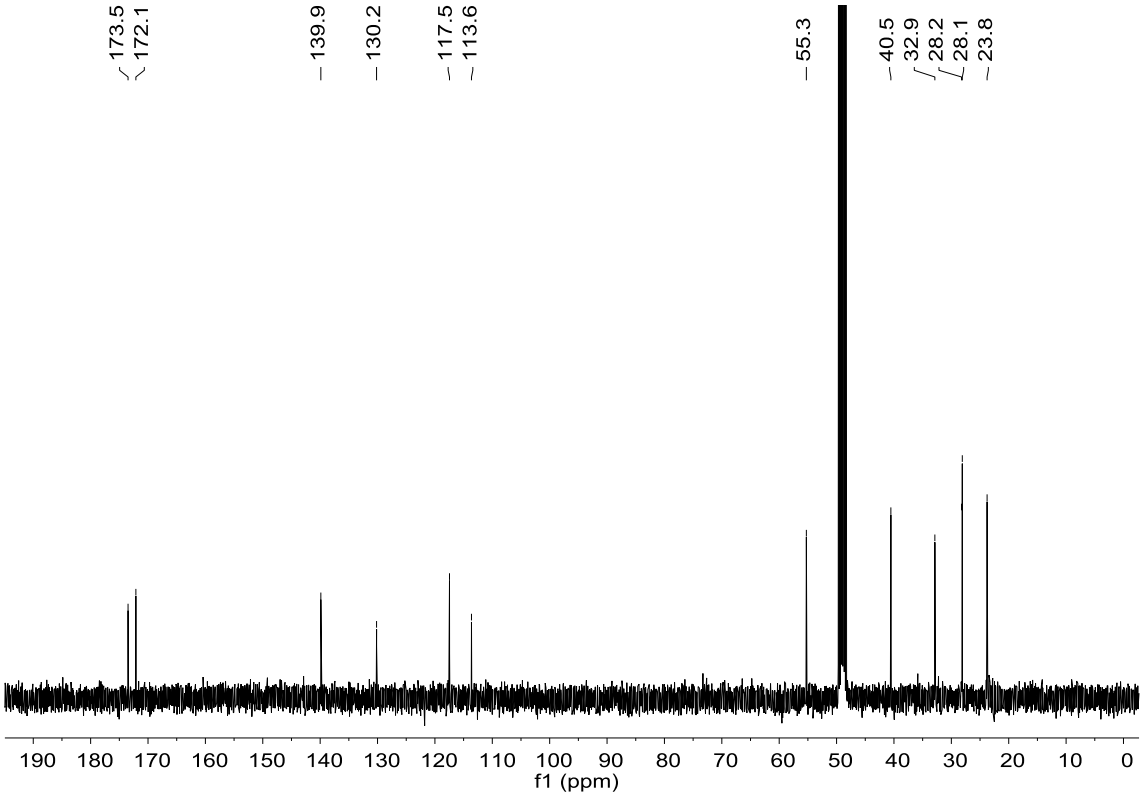

Figure A49. ^{13}C (101 MHz, 298 K in MeOD-d_4) spectrum of [**1k**·2TFA].

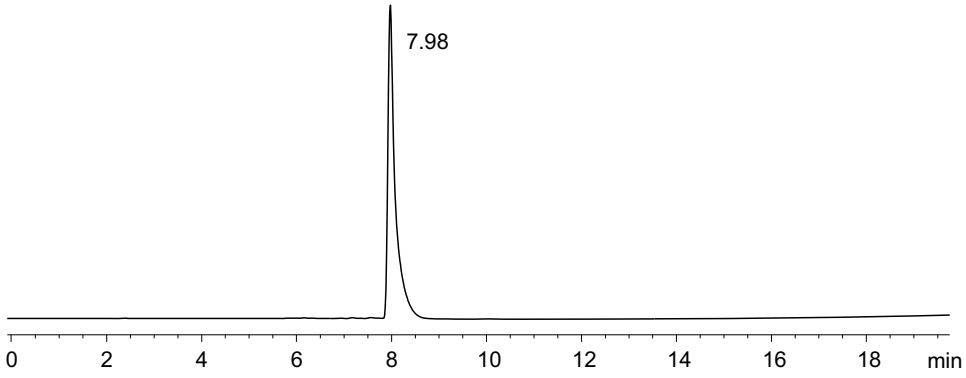

Figure A50. RP-HPLC analysis of [**1k**] (eluent: mixture of CH_3CN + 0.07% (v/v) TFA and H_2O + 0.1% (v/v) TFA; gradient: 2 min at 5% CH_3CN in H_2O, then linear gradient from 5% to 100% CH_3CN over 18 min).

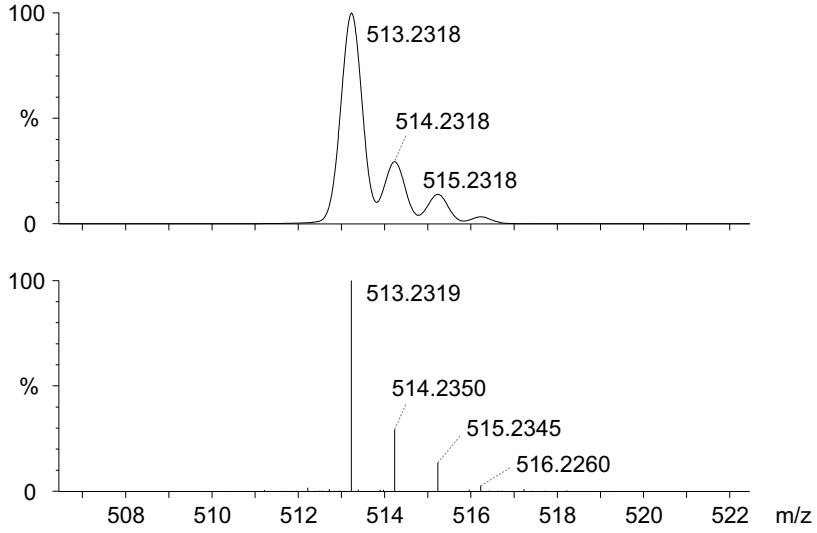

Figure A51. Experimental (lower trace) and simulated (upper trace) ESI-TOF mass spectra for $[M+H]^+$ of [**1k**].

Building block 1l

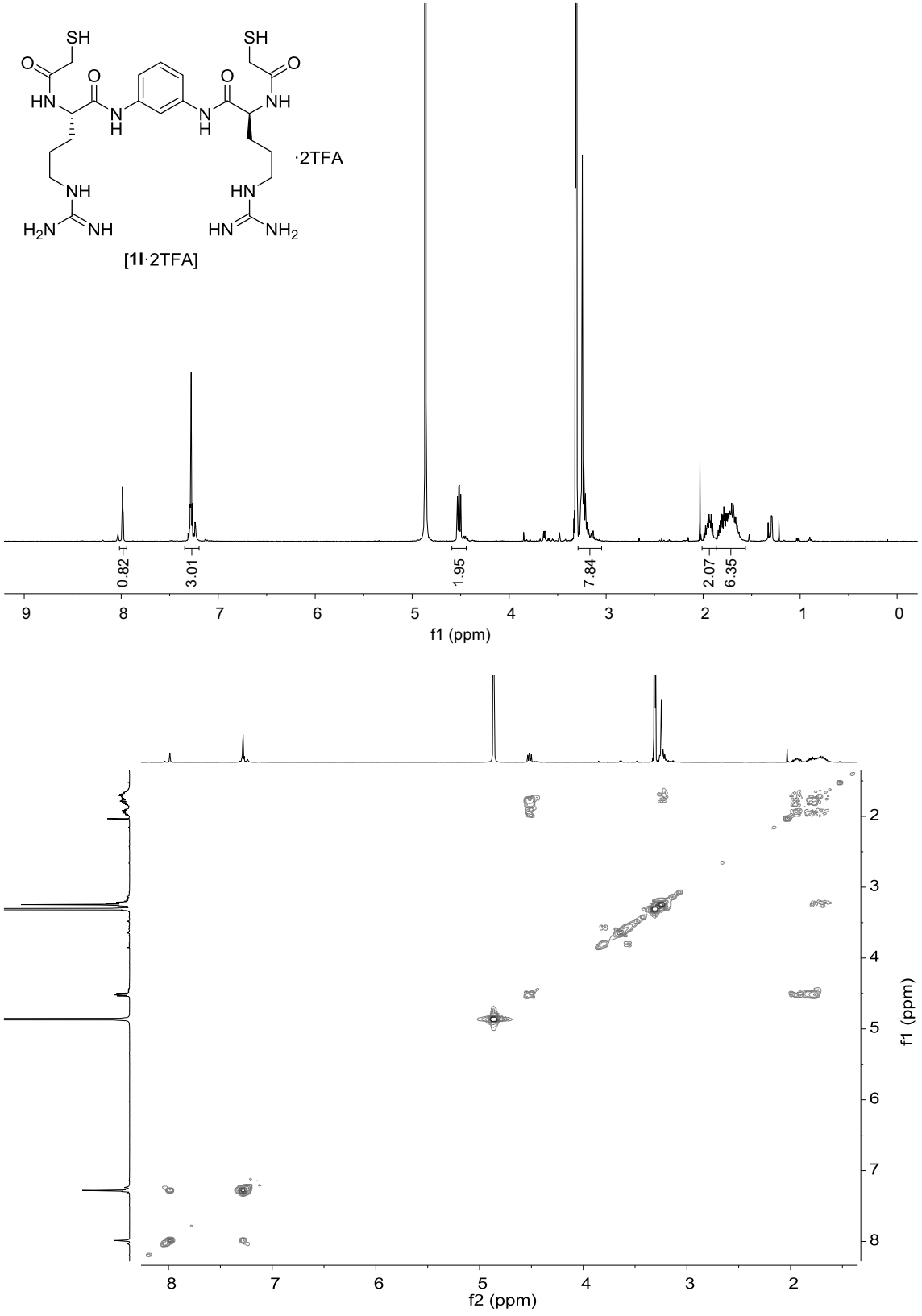

Figure A52. ^{1}H (400 MHz, 298 K in MeOD-d_4) and ^{1}H-^{1}H gCOSY (400 MHz, 298 K in MeOD-d_4) spectra of [**1l**·2TFA].

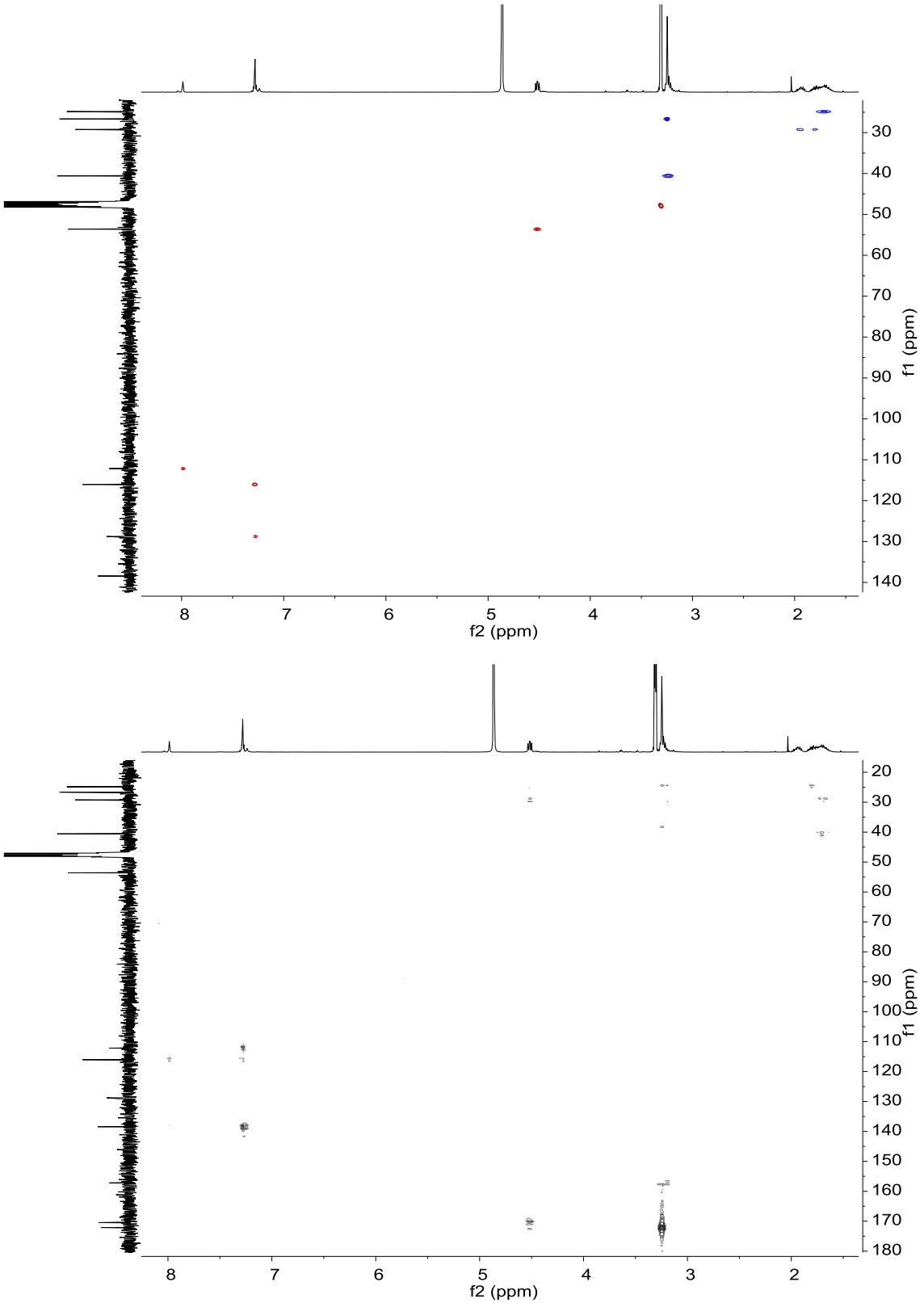

Figure A53. ^{1}H-^{13}C gHSQC (400 MHz, 298 K in MeOD-d_4) and ^{1}H-^{13}C gHMBC (400 MHz, 298 K in MeOD-d_4) spectra of [**1l**·2TFA].

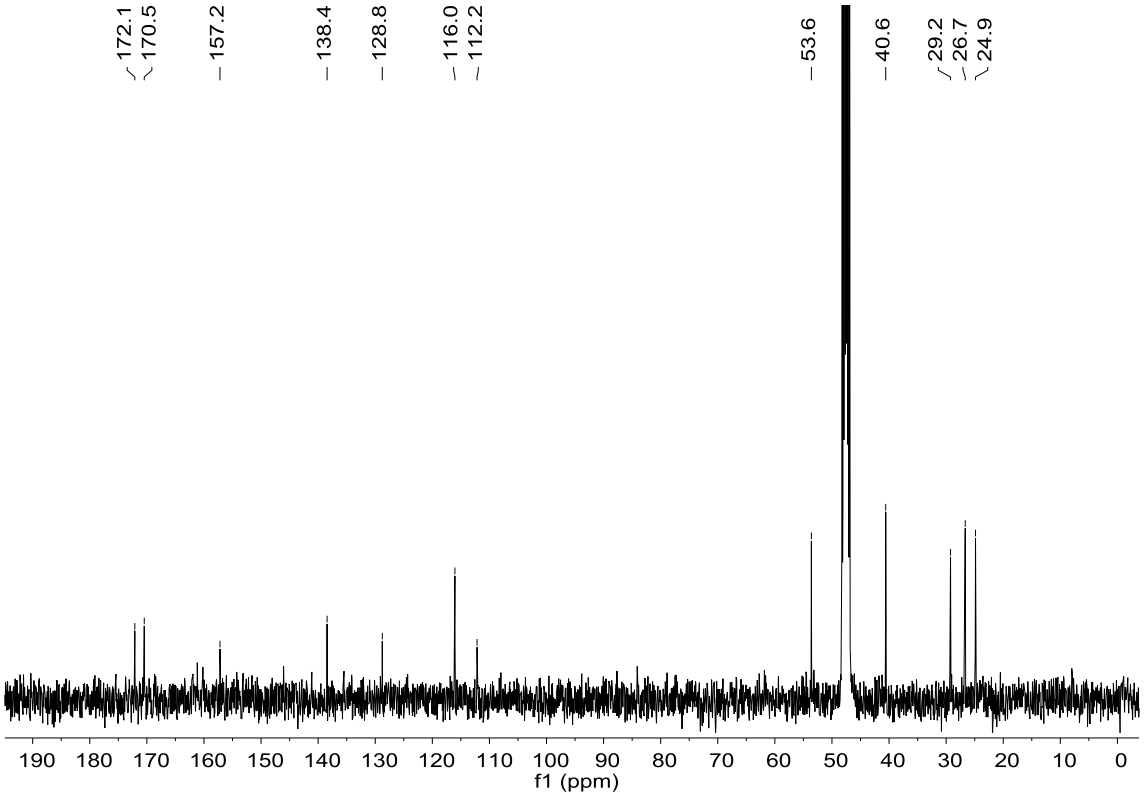

Figure A54. ^{13}C (101 MHz, 298 K in MeOD-d_4) spectrum of [**1l**·2TFA].

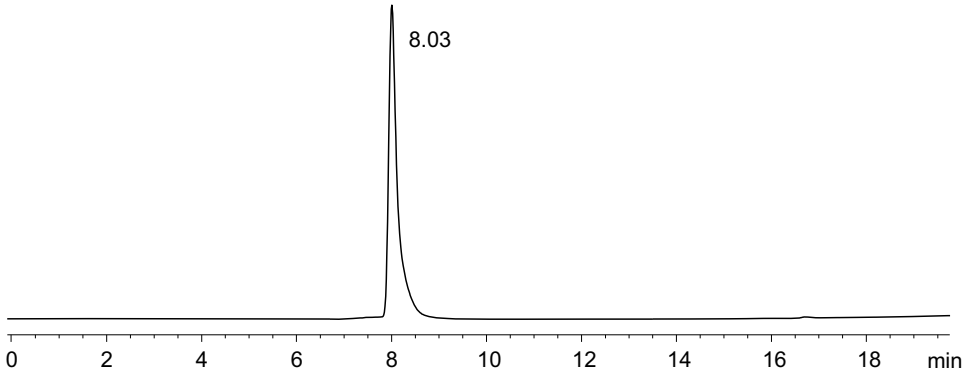

Figure A55. RP-HPLC analysis of [**1l**] (eluent: mixture of CH_3CN + 0.07% (v/v) TFA and H_2O + 0.1% (v/v) TFA; gradient: 2 min at 5% CH_3CN in H_2O, then linear gradient from 5% to 100% CH_3CN over 18 min).

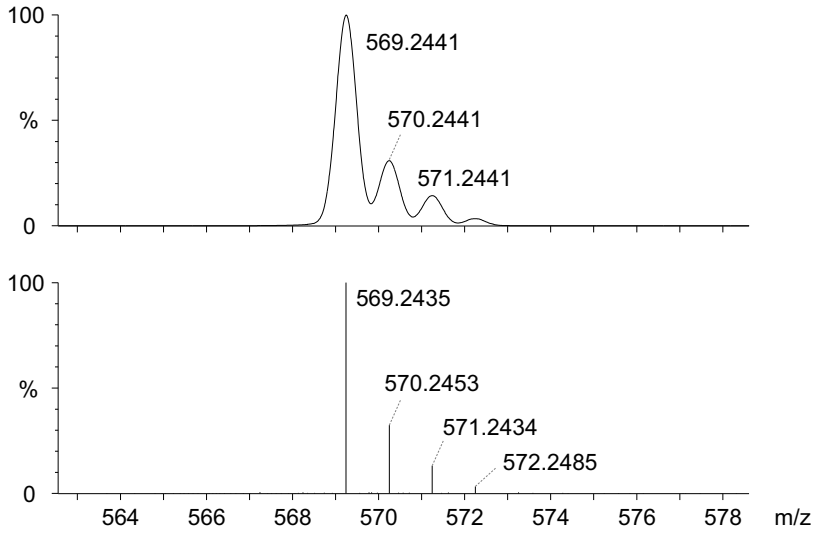

Figure A56. Experimental (lower trace) and simulated (upper trace) ESI-TOF mass spectra for $[M+H]^+$ of [**1l**].

Building block 1m

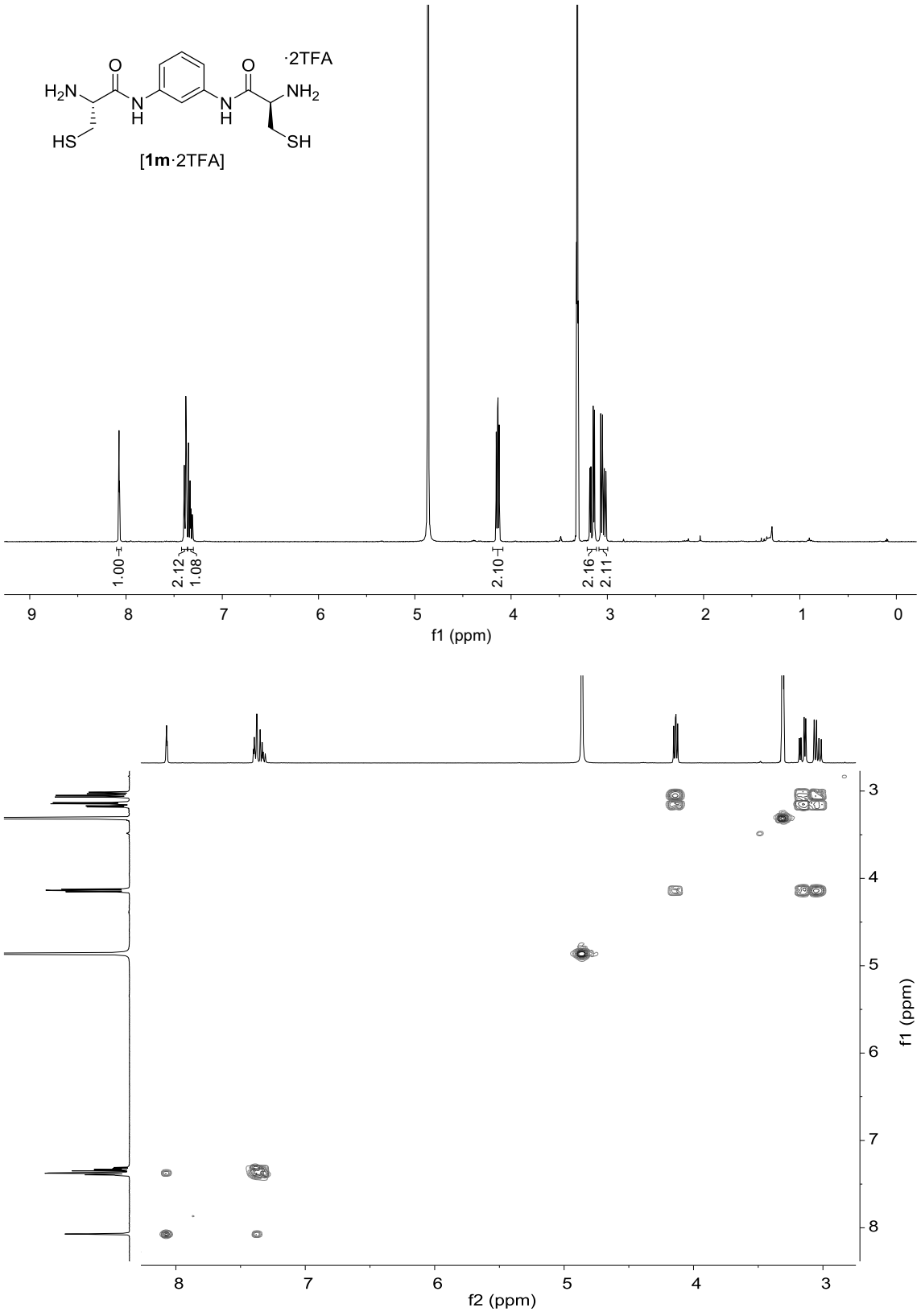

Figure A57. ^{1}H (400 MHz, 298 K in MeOD-d_4) and ^{1}H-^{1}H gCOSY (400 MHz, 298 K in MeOD-d_4) spectra of [**1m**·2TFA].

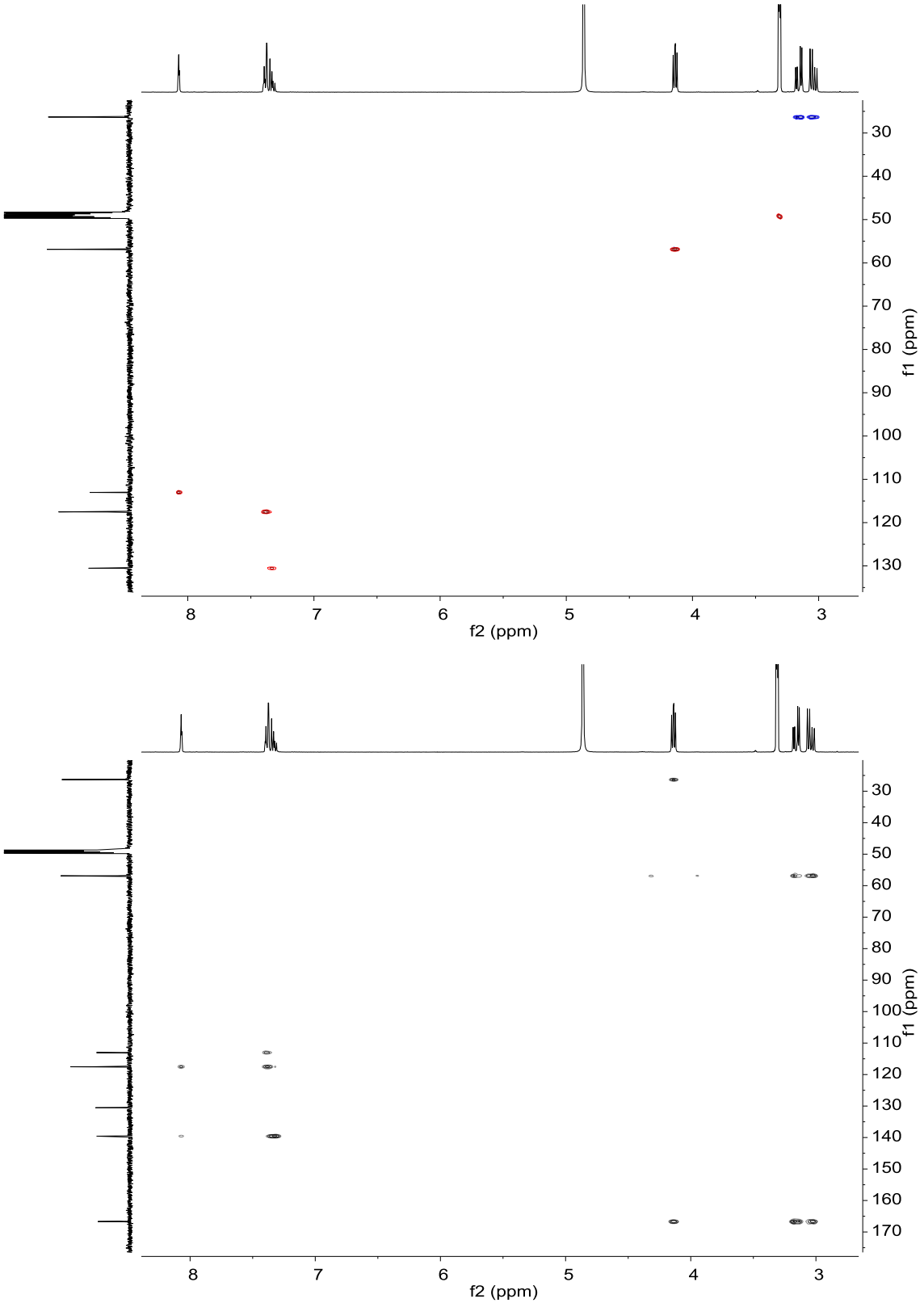

Figure A58. ^{1}H-^{13}C gHSQC (400 MHz, 298 K in MeOD-d_4) and ^{1}H-^{13}C gHMBC (400 MHz, 298 K in MeOD-d_4) spectra of [**1m**·2TFA].

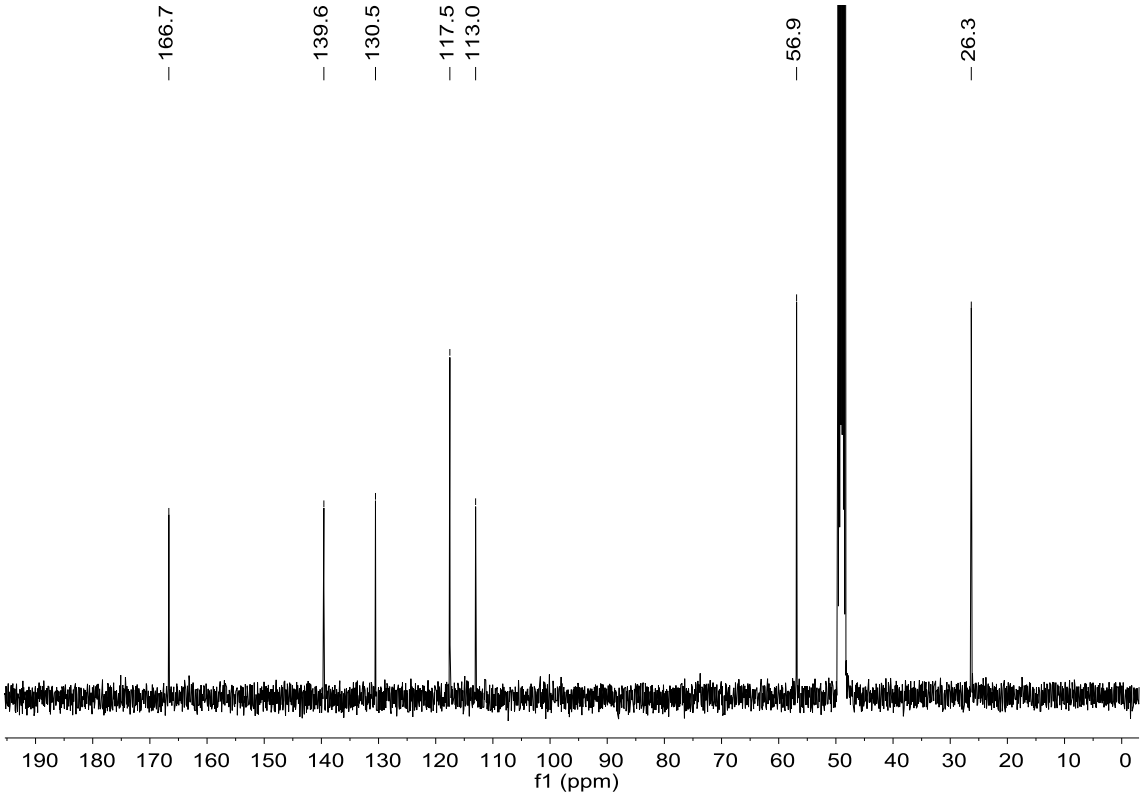

Figure A59. ^{13}C (101 MHz, 298 K in MeOD-d_4) spectrum of [**1m**·2TFA].

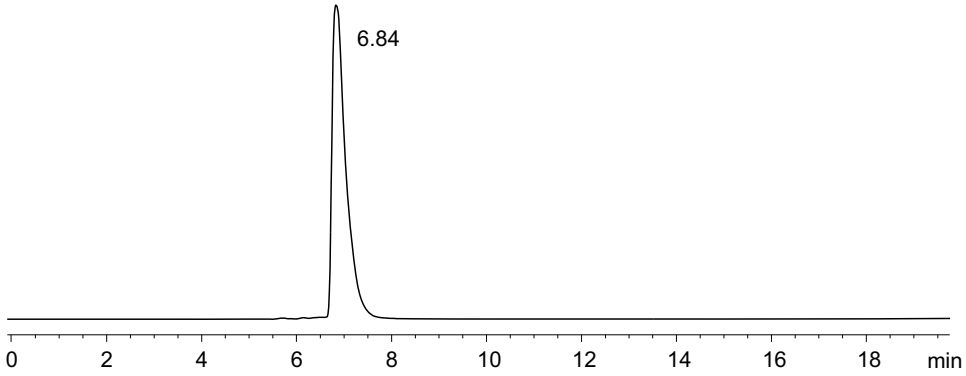

Figure A60. RP-HPLC analysis of [**1m**] (eluent: mixture of CH_3CN + 0.07% (v/v) TFA and H_2O + 0.1% (v/v) TFA; gradient: 1 min at 1% CH_3CN in H_2O, then linear gradient from 1% to 100% CH_3CN over 19 min).

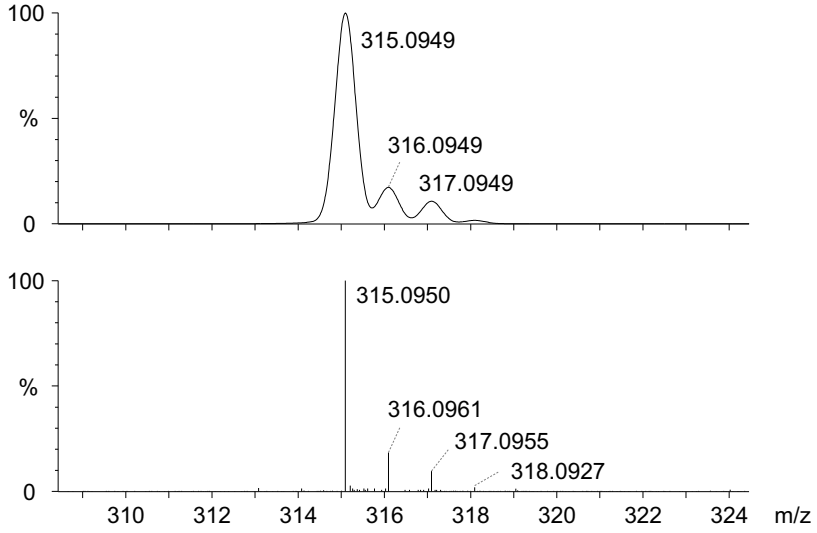

Figure A61. Experimental (lower trace) and simulated (upper trace) ESI-TOF mass spectra for $[M+H]^+$ of [**1m**].

Building block (*RR*)-1i-d_4

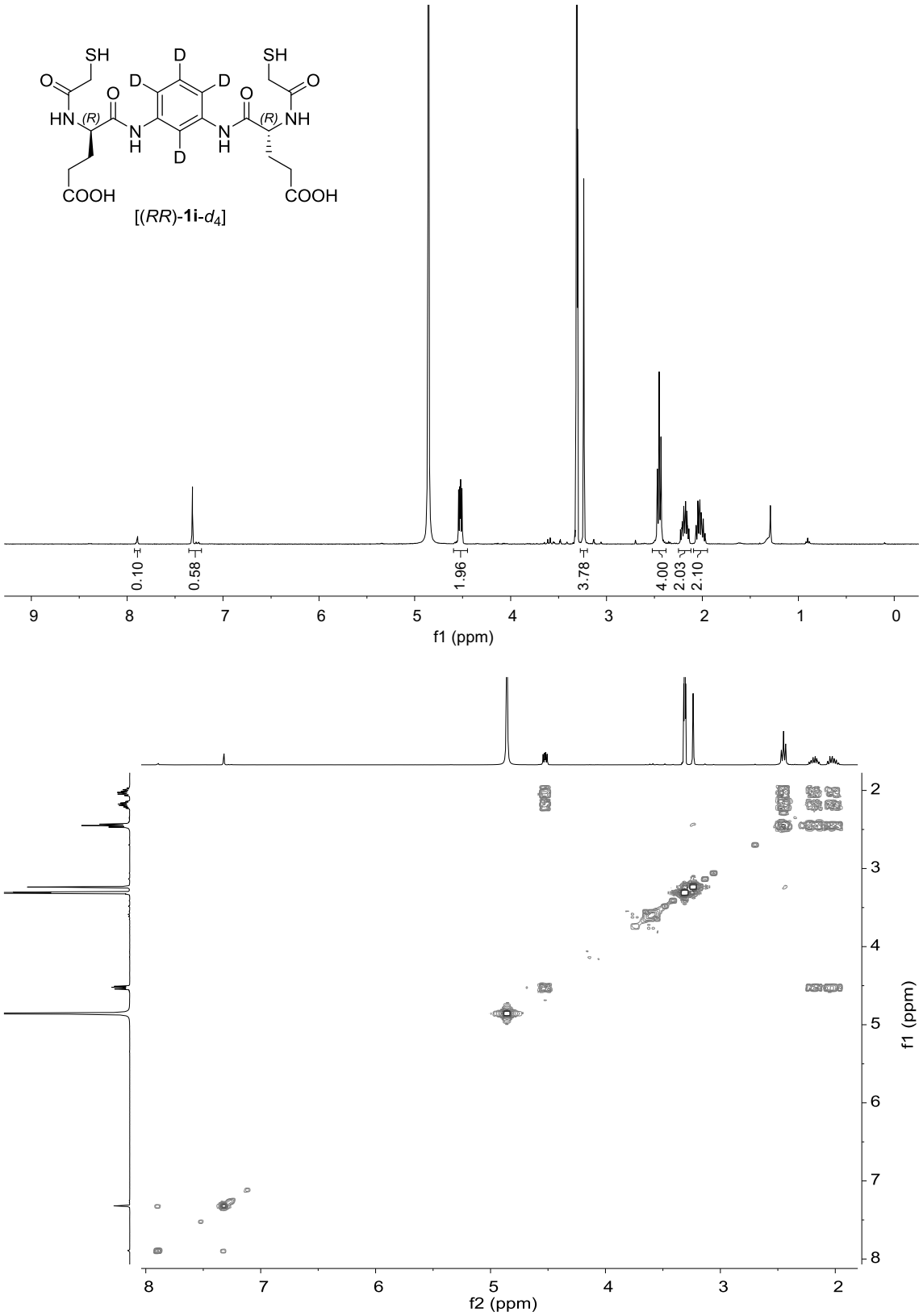

Figure A62. ^{1}H (400 MHz, 298 K in MeOD-d_4) and ^{1}H-^{1}H gCOSY (400 MHz, 298 K in MeOD-d_4) spectra of [(*RR*)-**1i**-d_4].

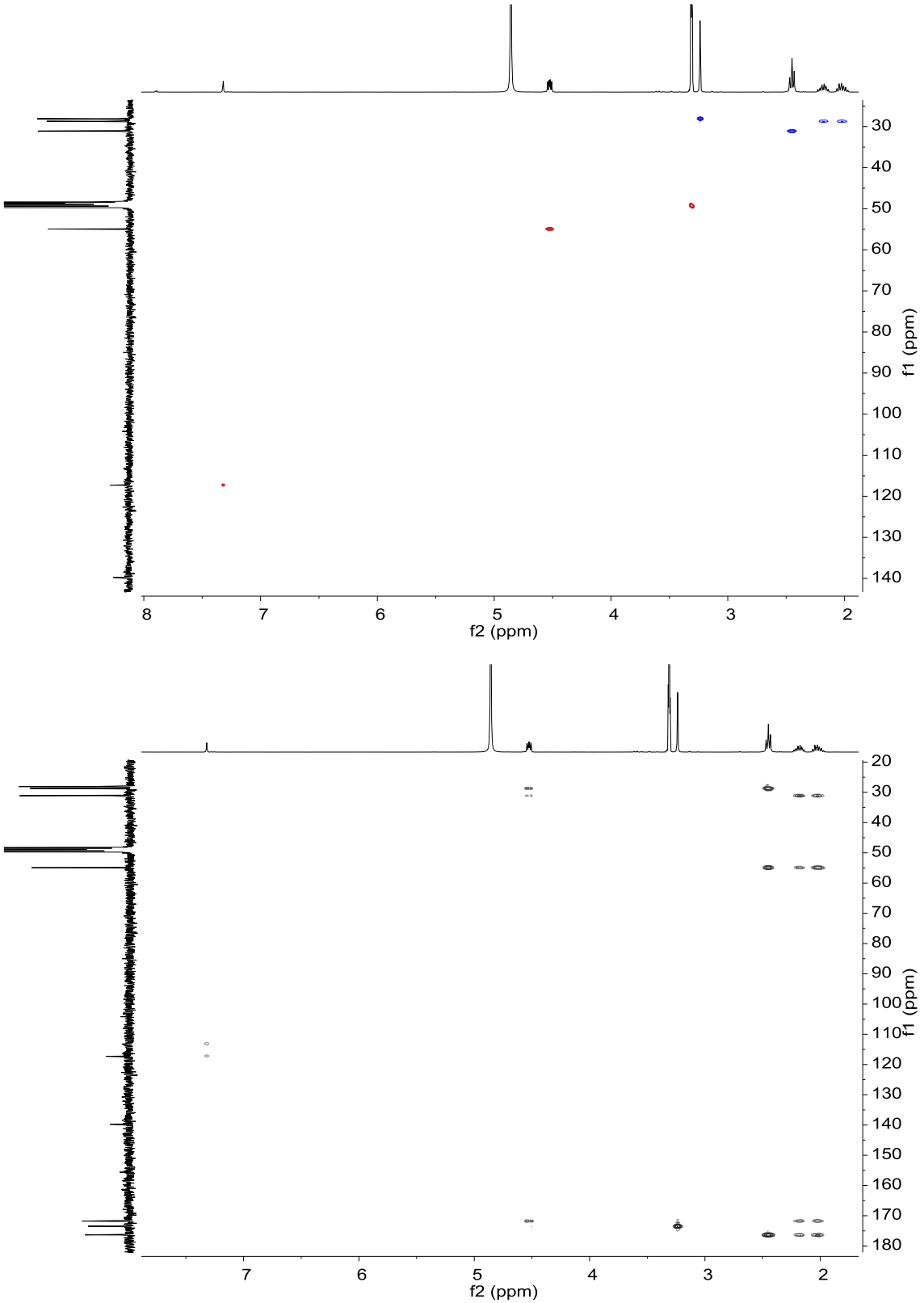

Figure A63. ^{1}H-^{13}C gHSQC (400 MHz, 298 K in MeOD-d_4) and ^{1}H-^{13}C gHMBC (400 MHz, 298 K in MeOD-d_4) spectra of [(*RR*)-**1i**-d_4].

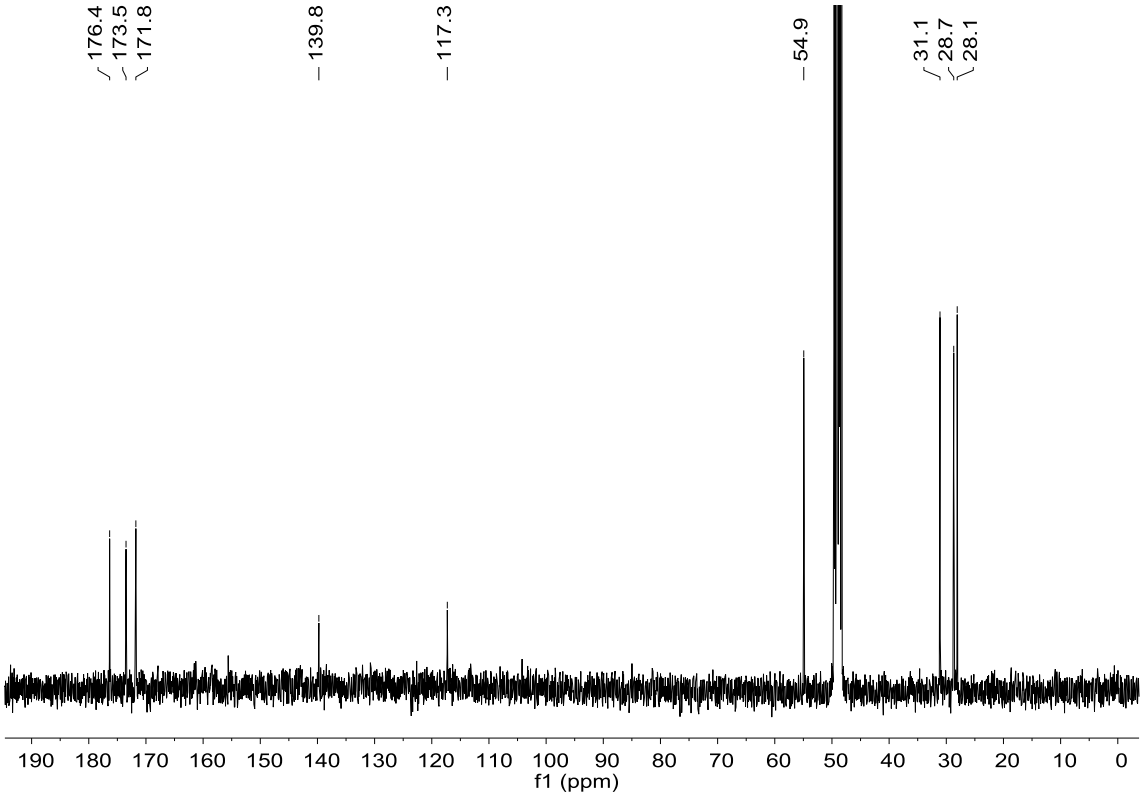

Figure A64. ^{13}C (101 MHz, 298 K in MeOD-d_4) spectrum of [(*RR*)-**1i**-d_4].

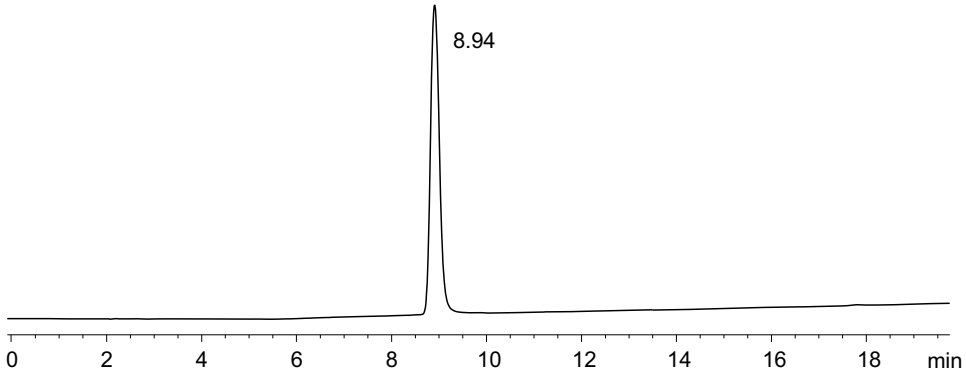

Figure A65. RP-HPLC analysis of [(*RR*)-**1i**-d_4] (eluent: mixture of CH_3CN + 0.07% (v/v) TFA and H_2O + 0.1% (v/v) TFA; gradient: 2 min at 5% CH_3CN in H_2O, then linear gradient from 5% to 100% CH_3CN over 18 min).

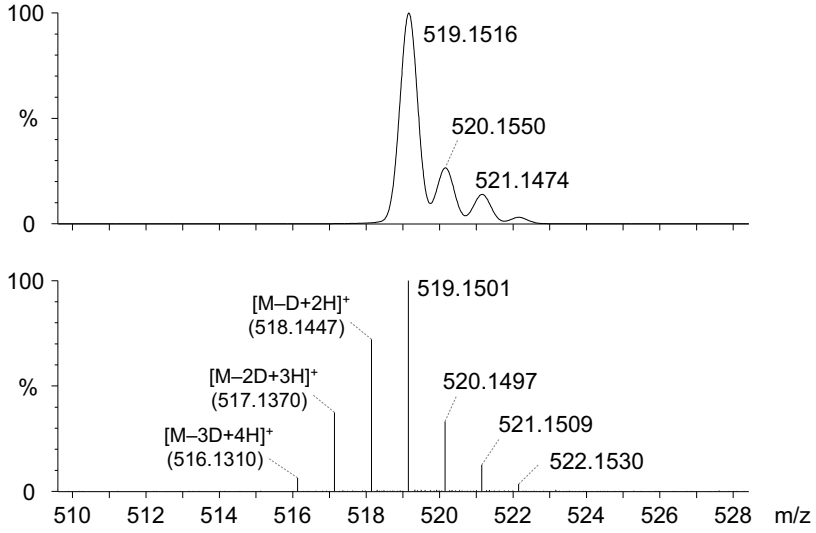

Figure A66. Experimental (lower trace) and simulated (upper trace) ESI-TOF mass spectra for $[M+H]^+$ of [(*RR*)-**1i**-d_4].

MS analysis of the dynamic combinatorial libraries

DCLs of Chapter 2

Intermediates of the oxidation of BB **1d**

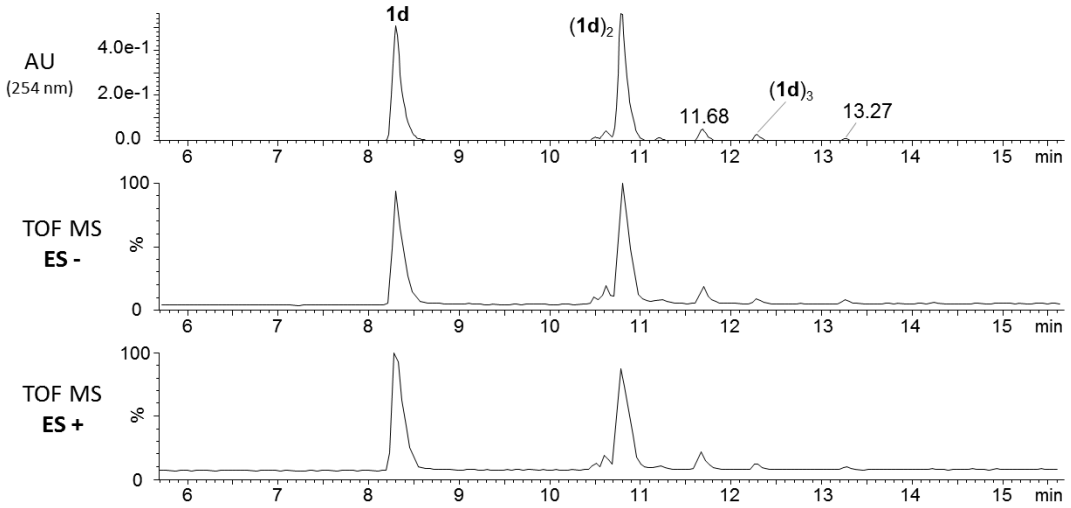

Figure A67. UPLC-UV(254 nm)-ESI-TOF traces of partialy oxidized **1d** (2 mM, reaction time = 3 hours) in aqueous phosphate-citrate buffer (pH 7.5) with 25% (v/v) DMSO.

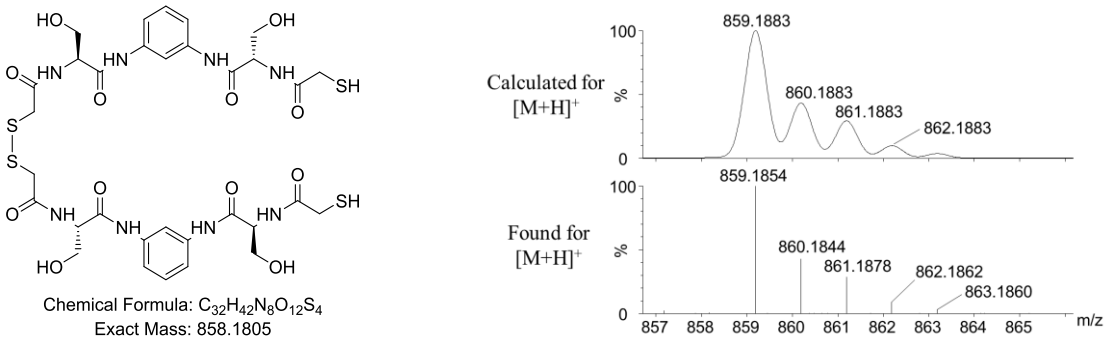

Figure A68. Structure and isotopic pattern of *o*-(**1d**)$_2$ (t_R = 11.68 min).

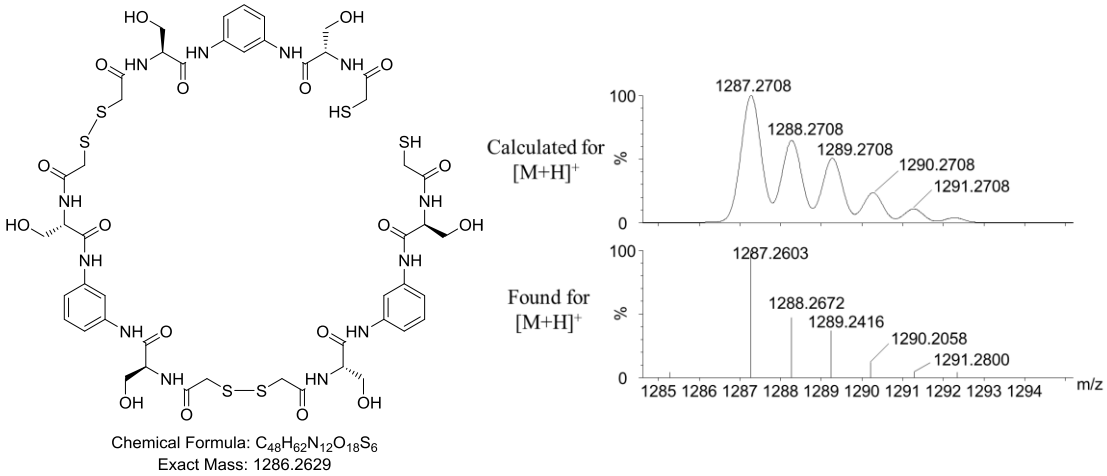

Figure A69. Structure and isotopic pattern of *o*-(**1d**)$_3$ (t_R = 13.27 min).

Mixture of BBs **1d+1h**

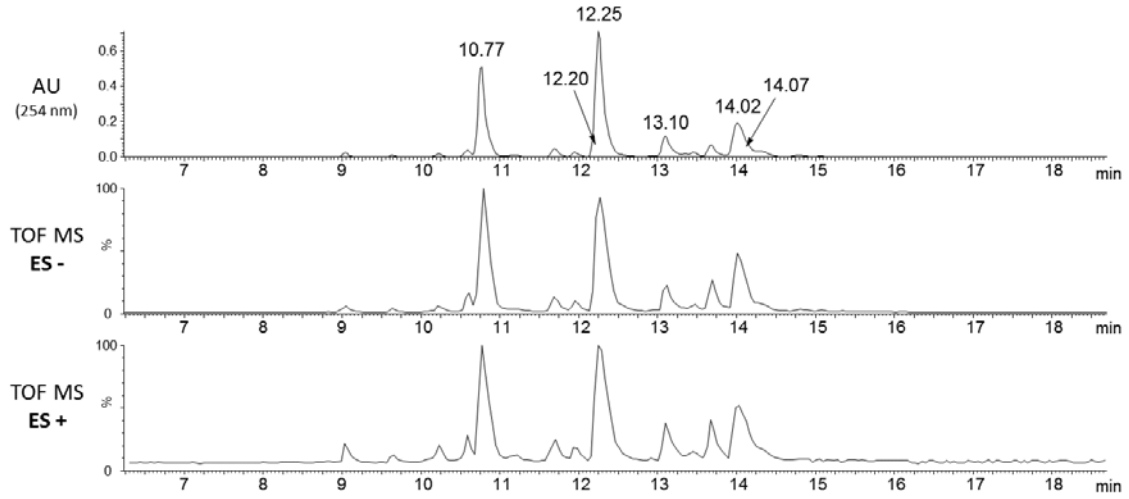

Figure A70. UPLC-UV(254 nm)-ESI-TOF traces of the equilibrated mixture of **1d**+**1h** (2 mM each) in aqueous phosphate-citrate buffer (pH 7.5) with 25% (v/v) DMSO.

Identification of the dimers:

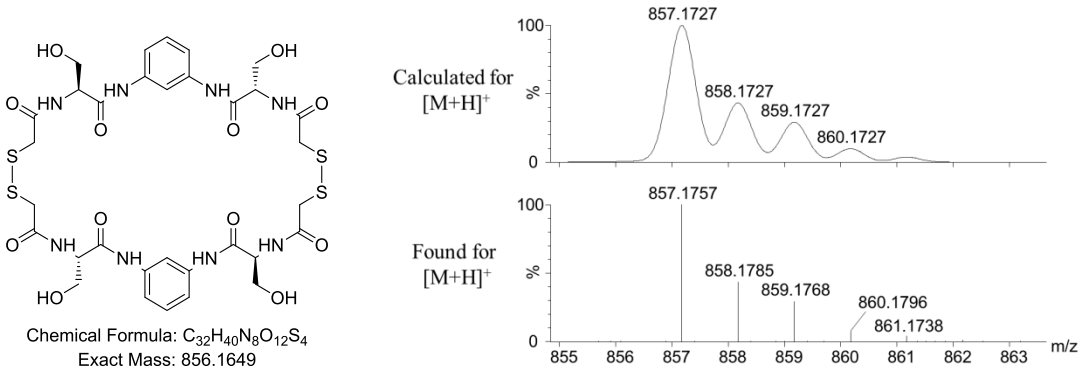

Figure A71. Structure and isotopic pattern of $(\mathbf{1d})_2$ (t_R = 10.77 min).

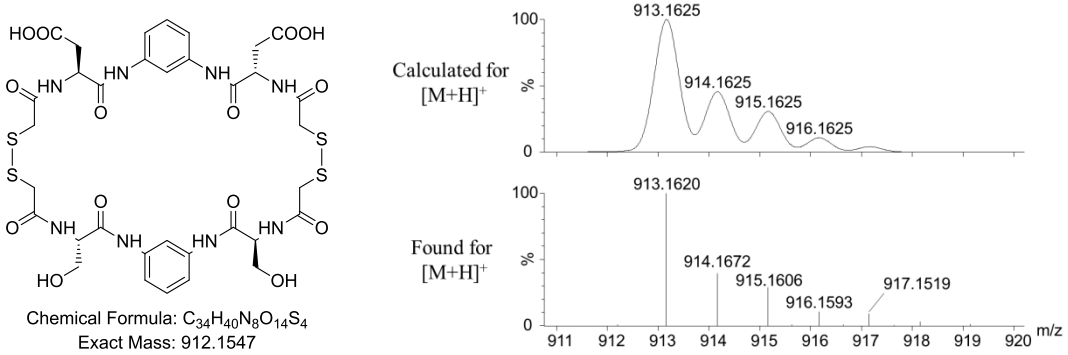

Figure A72. Structure and isotopic pattern of **1d-1h** (t_R = 12.25 min).

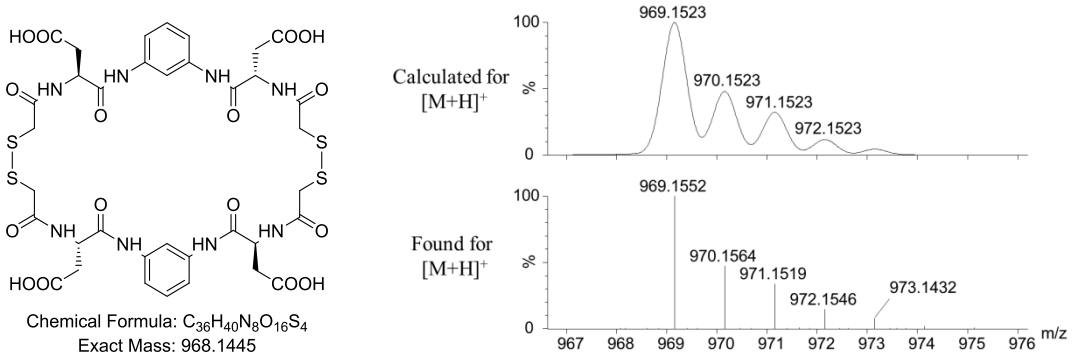

Figure A73. Structure and isotopic pattern of $(\mathbf{1h})_2$ (t_R = 14.02 min).

Identification of the trimers:

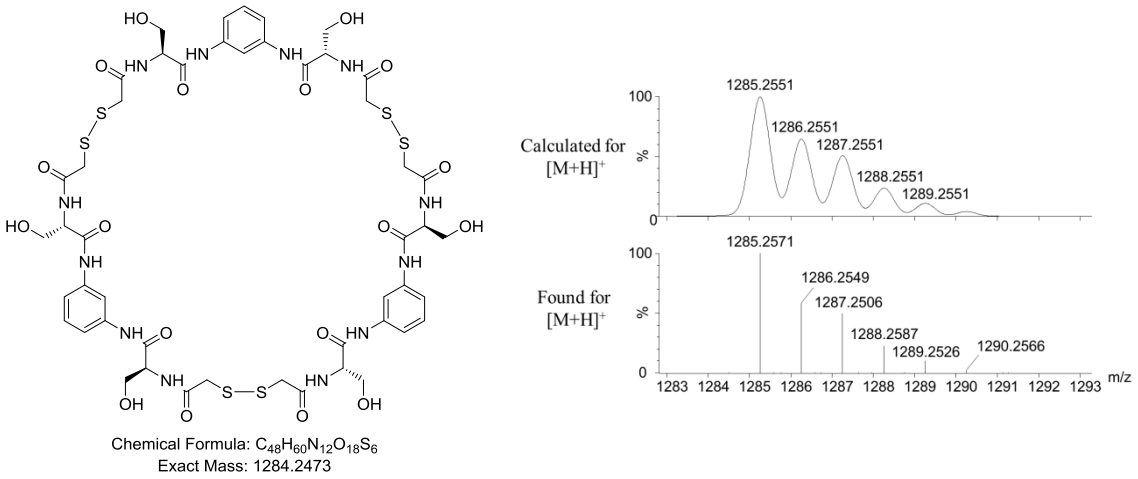

Figure A74. Structure and isotopic pattern of $(\mathbf{1d})_3$ (t_R = 12.20 min).

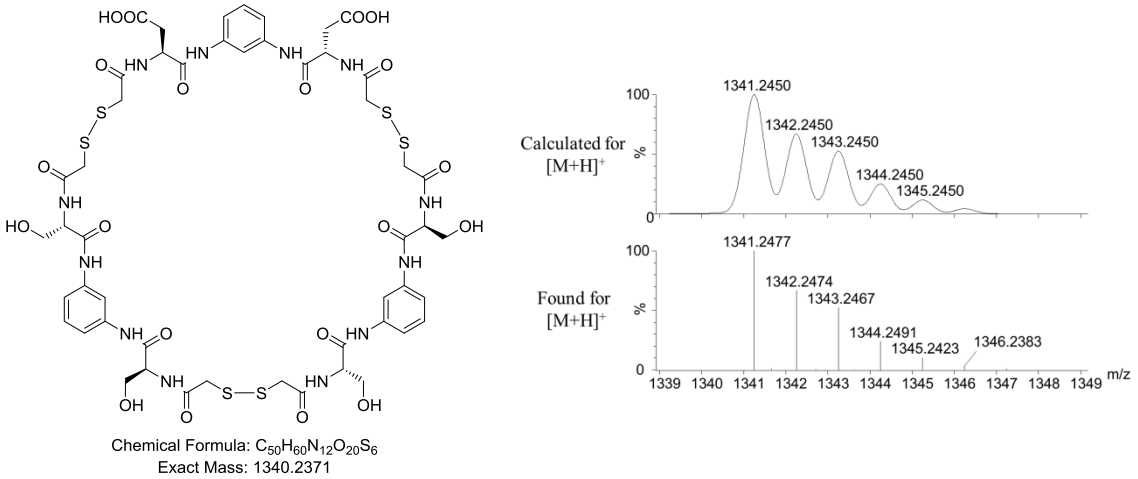

Figure A75. Structure and isotopic pattern of $(\mathbf{1d})_2$-**1h** (t_R = 13.10 min).

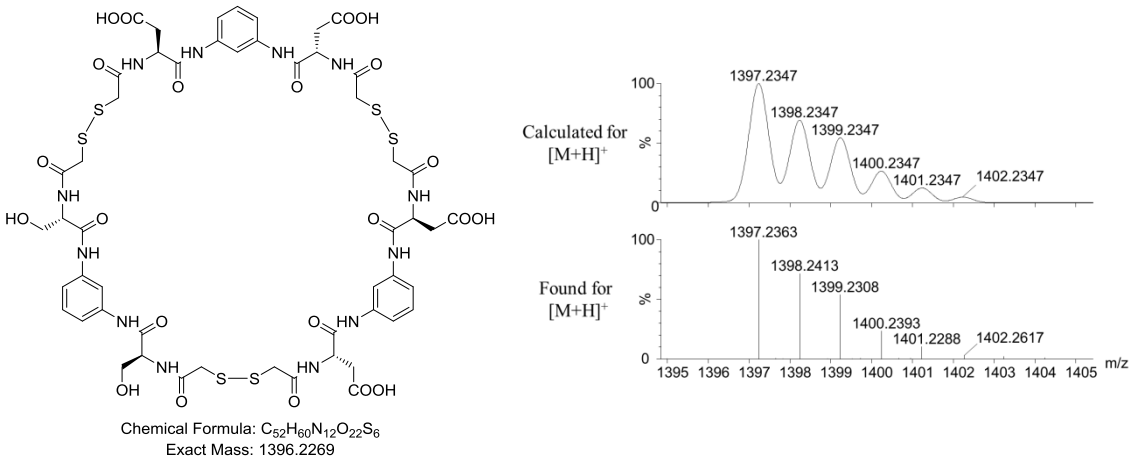

Figure A76. Structure and isotopic pattern of **1d-(1h)**$_2$ (t_R = 14.07 min).

Mixture of BBs **1d+1j**

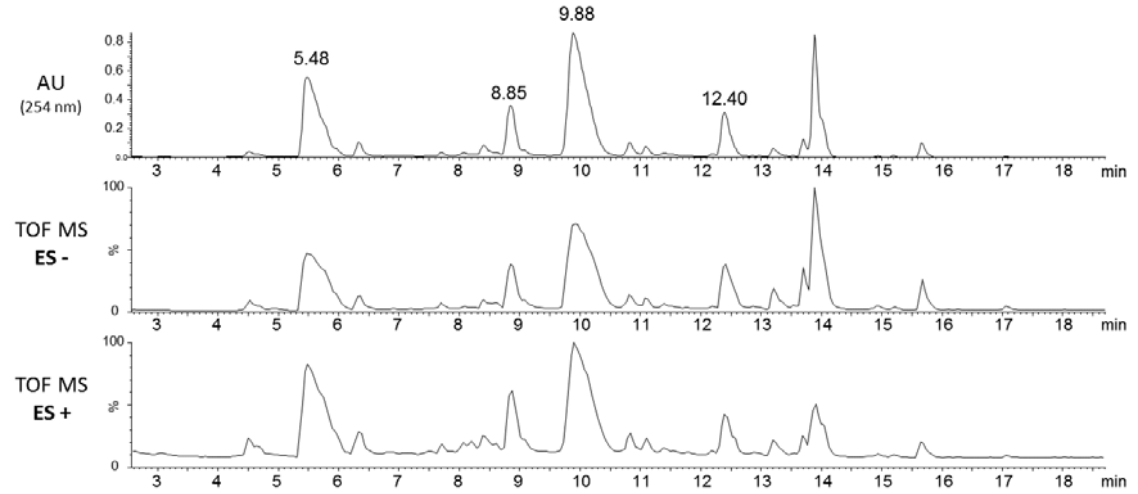

Figure A77. UPLC-UV(254 nm)-ESI-TOF traces of the equilibrated mixture of **1d**+**1j** (2 mM each) in aqueous phosphate-citrate buffer (pH 7.5) with 25% (v/v) DMSO.

Identification of the dimers (the previously identified dimers are not shown):

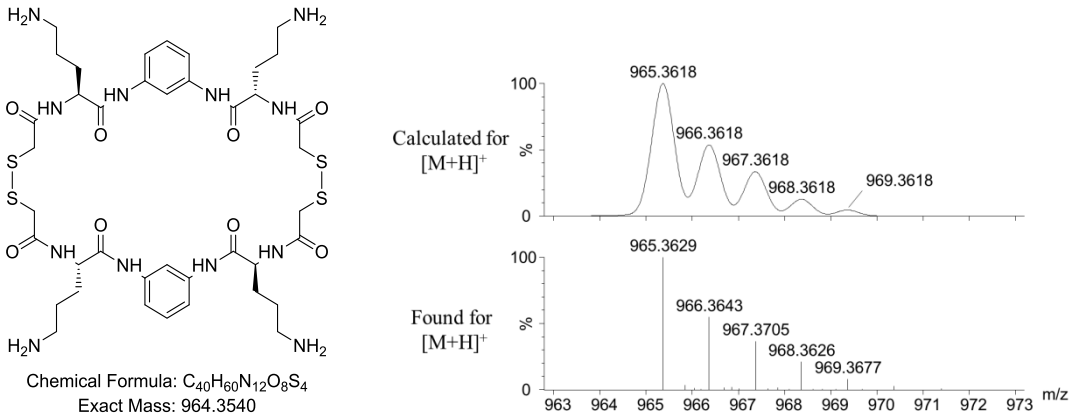

Figure A78. Structure and isotopic pattern of **(1j)**$_2$ (t_R = 5.48 min).

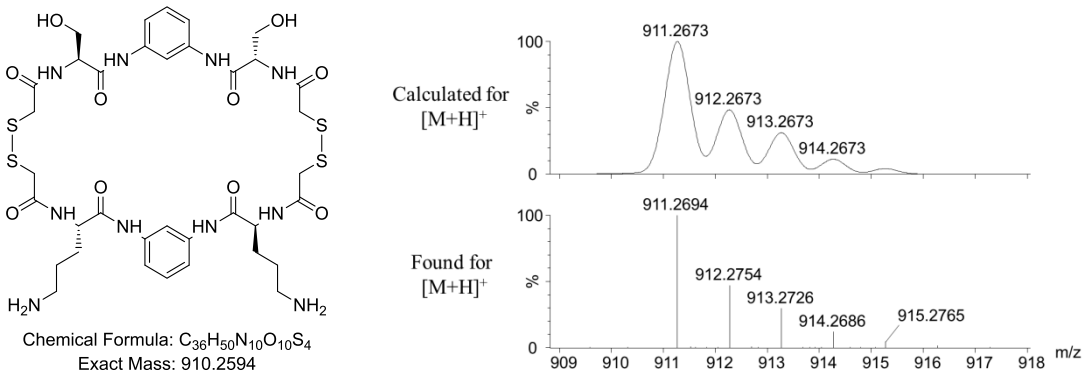

Figure A79. Structure and isotopic pattern of **1d-1j** (t_R = 9.88 min).

Identification of the trimers (the previously identified trimers are not shown):

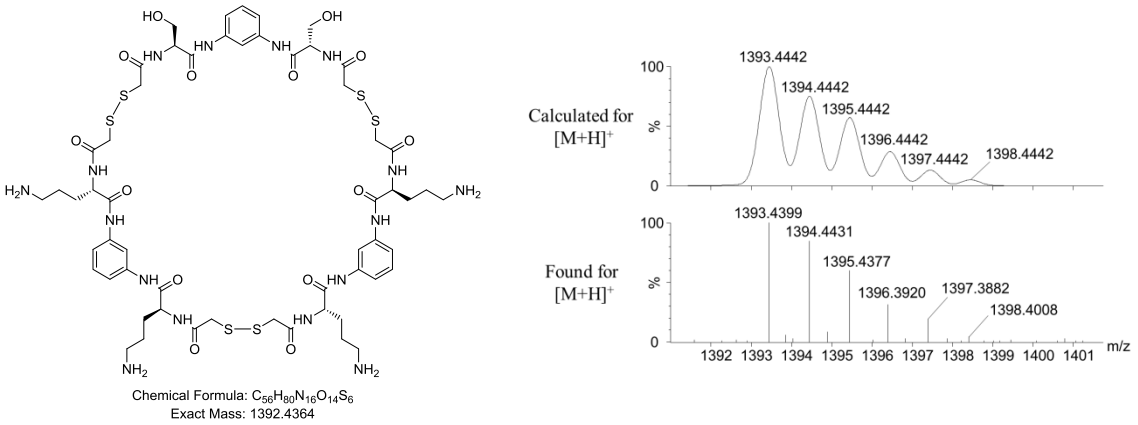

Figure A80. Structure and isotopic pattern of **1d-(1j)**$_2$ (t_R = 8.85 min).

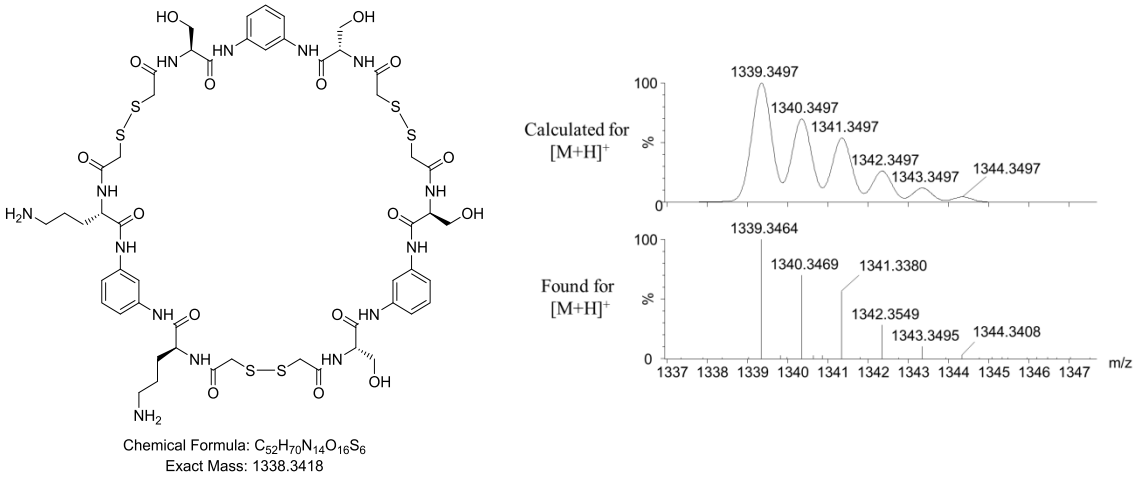

Figure A81. Structure and isotopic pattern of **(1d)**$_2$**-1j**, (t_R = 12.40 min).

Mixture of BBs **1d+1h+1j**

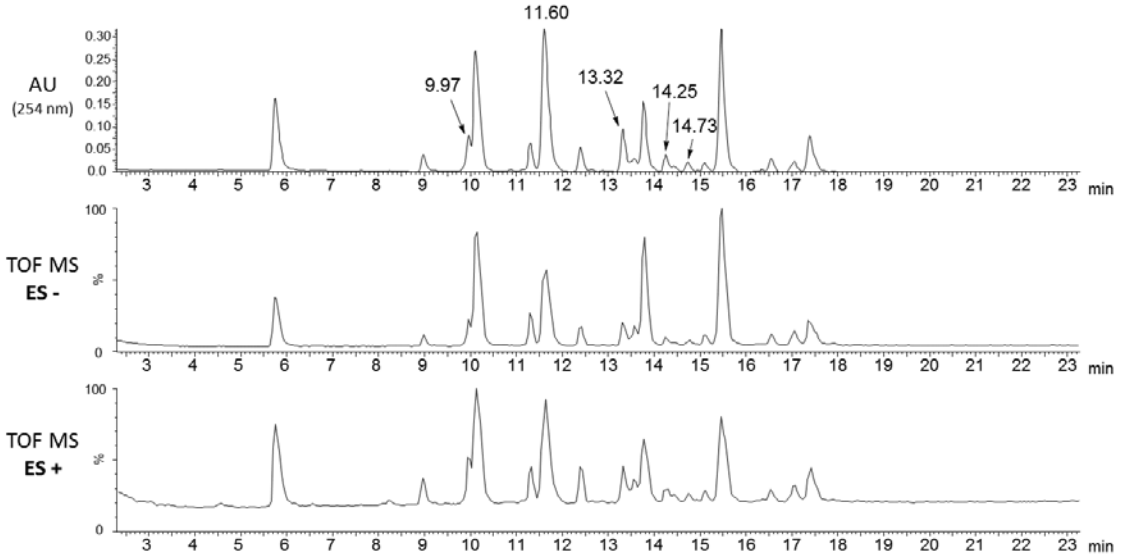

Figure A82. UPLC-UV(254 nm)-ESI-TOF traces of the equilibrated mixture of **1d**+**1h** (2 mM each) in aqueous phosphate-citrate buffer (pH 4.5) with 25% (v/v) DMSO.

Identification of the dimers (the previously identified dimers are not shown):

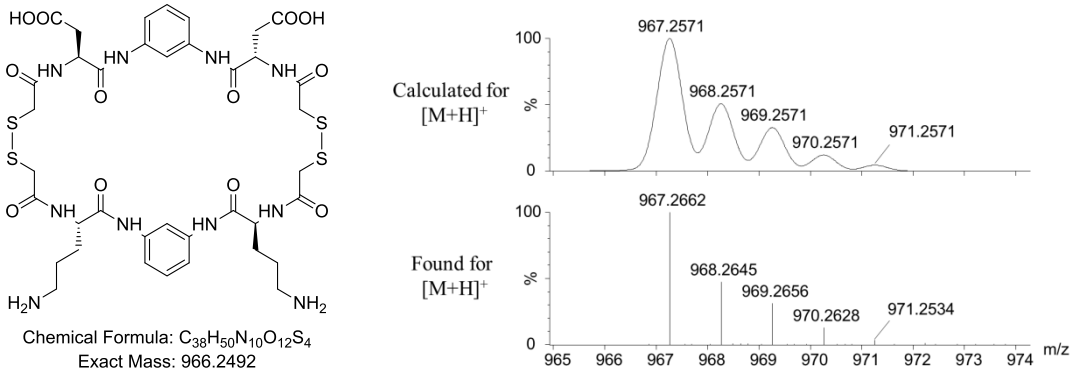

Figure A83. Structure and isotopic pattern of **1h-1j** (t_R = 11.60).

Identification of the trimers (the previously identified trimers are not shown):

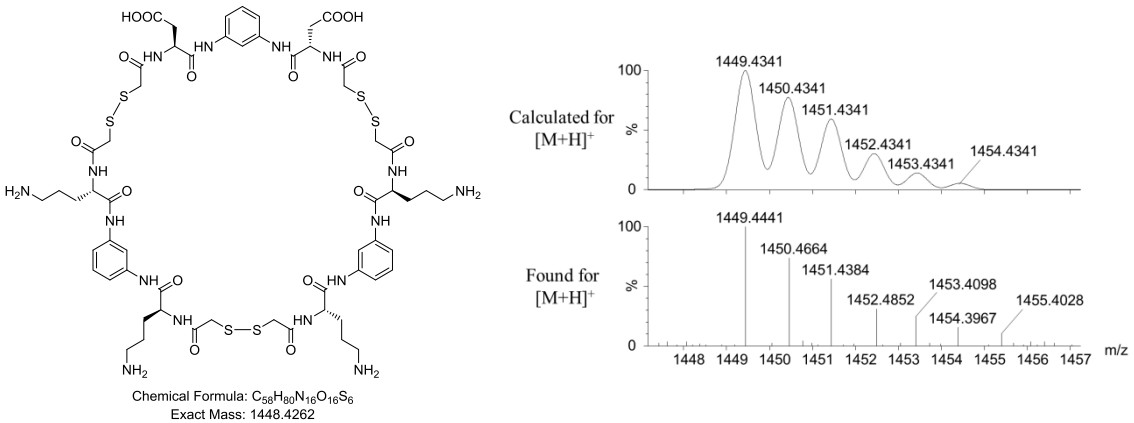

Figure A84. Structure and isotopic pattern of **1h-(1j)**$_2$ (t_R = 9.97 min).

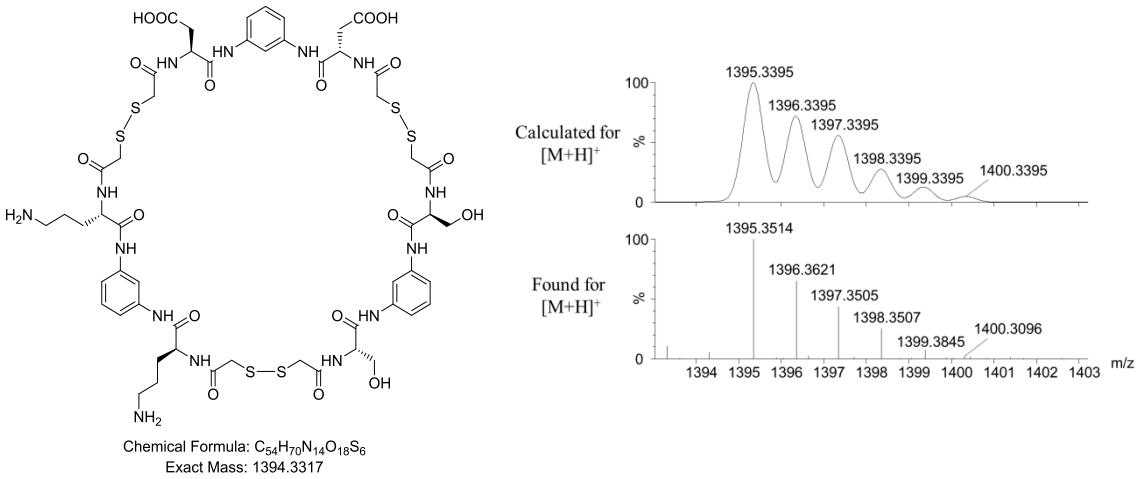

Figure A85. Structure and isotopic pattern of **1d-1h-1j**, (t_R = 13.32 min).

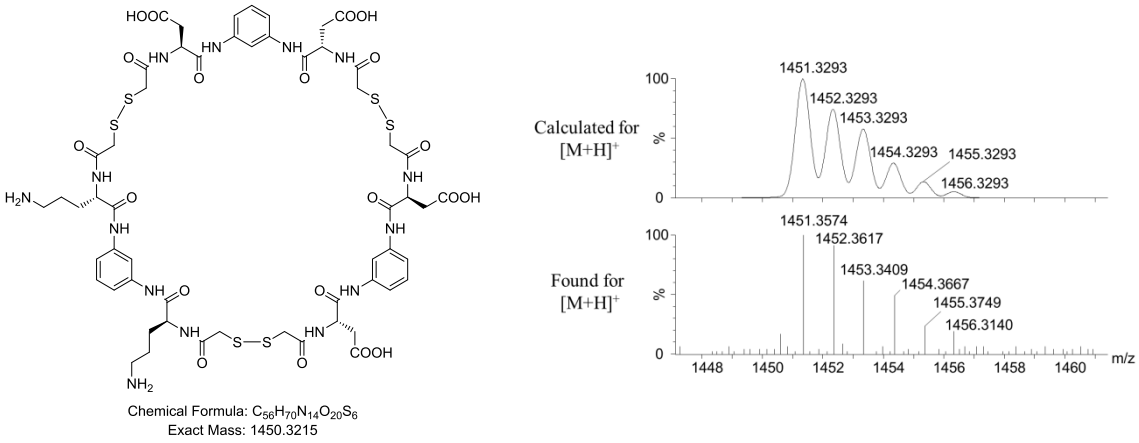

Figure A86. Structure and isotopic pattern of (**1h**)$_2$**-1j** (t_R = 14.25 min).

Identification of the tetramer **1h-(1d)$_2$-1j** (t_R = 14.73 min):

The low intensity of the corresponding peak did not allow obtaining a reliable isotopic pattern. However, the detection of the following signals allowed confirming the identity of the macrocycle:

HRMS (ESI+) calcd. for $[M+2H]^+$ (m/z): 912.2144, found: 912.2171

HRMS (ESI–) calcd. for $[M–H]^-$ (m/z): 1821.4068, found: 1821.4384

HRMS (ESI–) calcd. for $[M+Na–2H]^-$ (m/z): 1843.3888, found: 1843.3801

Identification of the dehydration products:

Chemical Formula: $C_{38}H_{48}N_{10}O_{11}S_4$
Exact Mass: 948.2387

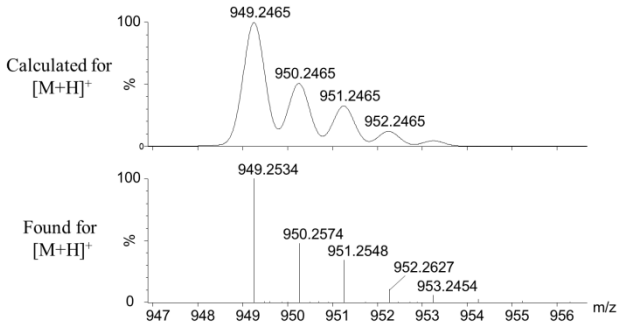

Figure A87. Chemical formula and isotopic pattern of [(**1h-1j**)–H_2O] (t_R = 11.30 min).

Chemical Formula: $C_{54}H_{68}N_{14}O_{17}S_6$
Exact Mass: 1376.3211

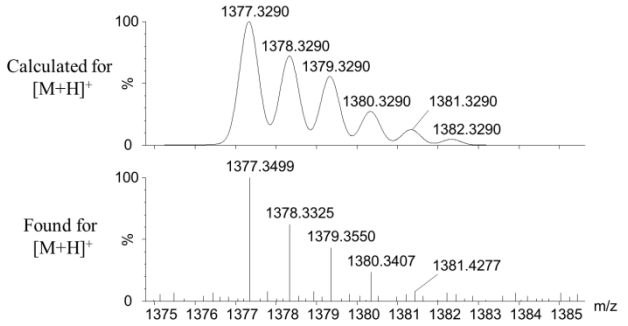

Figure A88. Chemical formula and isotopic pattern of [(**1d-1h-1j**)–H_2O], (t_R = 13.57 min).

Chemical Formula: $C_{36}H_{38}N_8O_{15}S_4$
Exact Mass: 950.1339

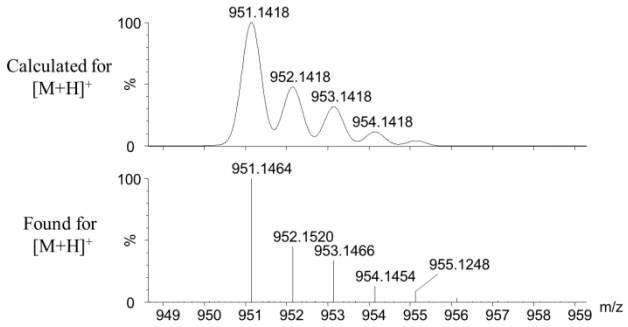

Figure A89. Chemical formula and isotopic pattern of [(**1h**)$_2$–H_2O] (t_R = 17.05 min).

DCLs of Chapter 3

Mixture of BBs **1c+1d+1i** at pH 7.5

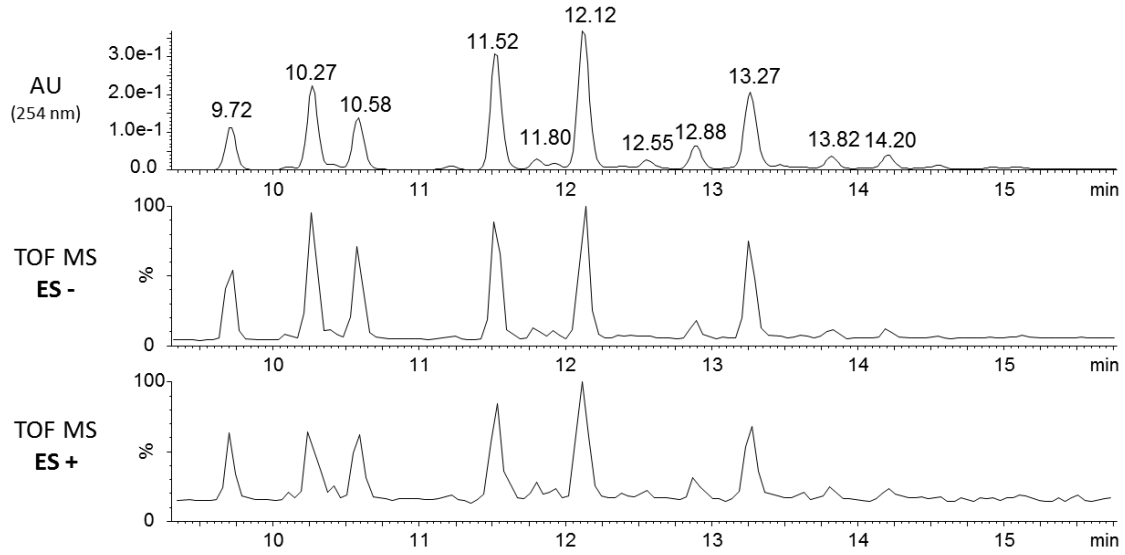

Figure A90. UPLC-UV(254 nm)-ESI-TOF traces of the equilibrated mixture of **1c**+**1d**+**1i** (2 mM each) in aqueous phosphate buffer (pH 7.5) with 25% (v/v) DMSO.

Identification of the dimers:

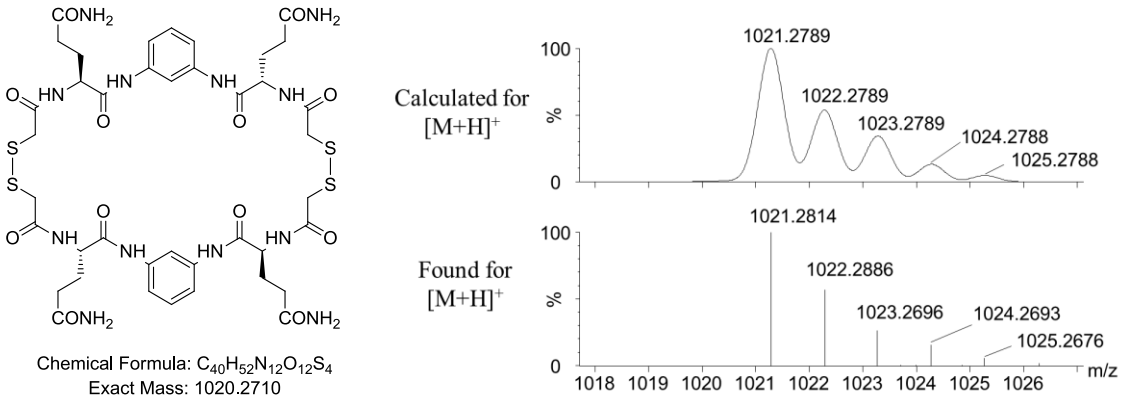

Figure A91. Structure and isotopic pattern of $(\mathbf{1c})_2$ (t_R = 9.72 min).

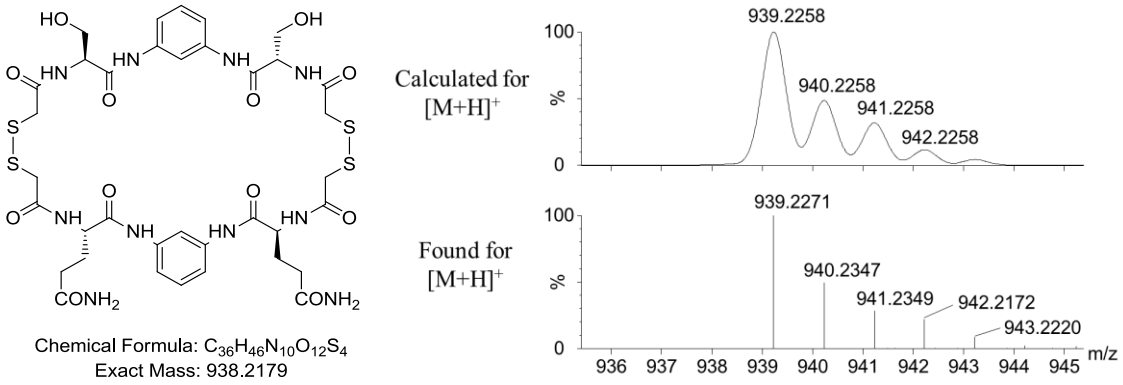

Figure A92. Structure and isotopic pattern of **1c-1d**, (t_R = 10.27 min).

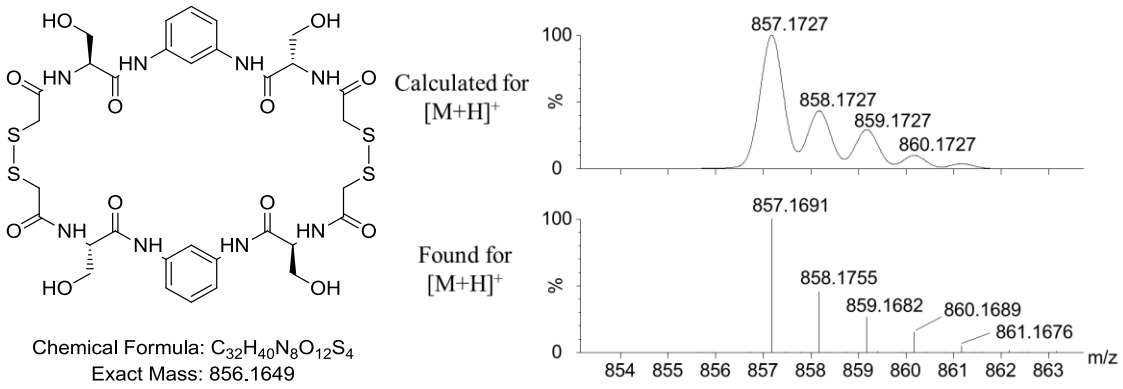

Figure A93. Structure and isotopic pattern of $(\mathbf{1d})_2$ (t_R = 10.58 min).

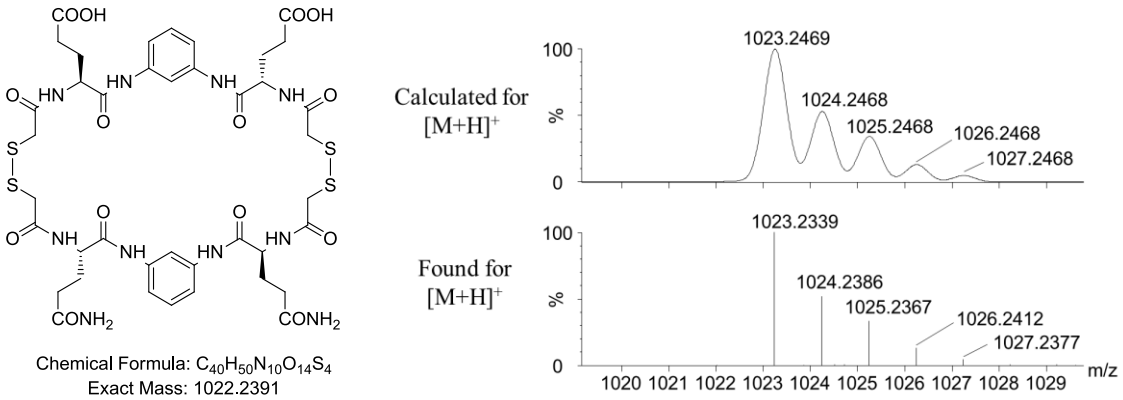

Figure A94. Structure and isotopic pattern of **1c-1i** (t_R = 11.52 min).

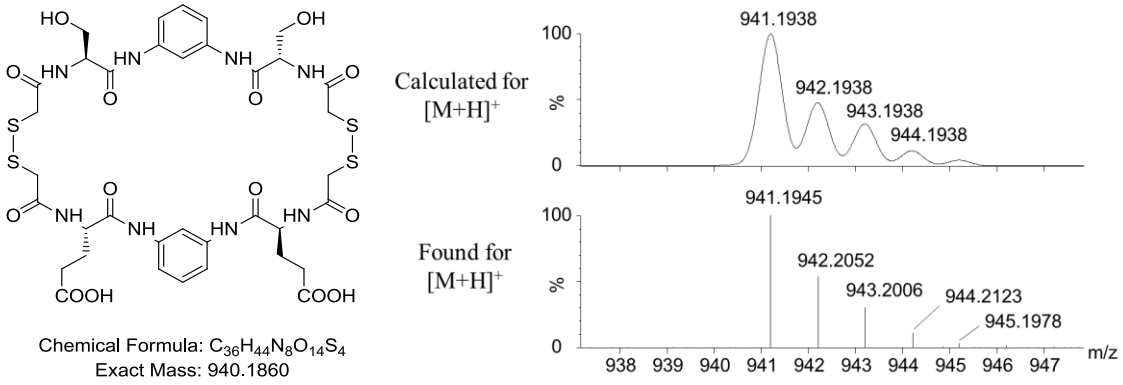

Figure A95. Structure and isotopic pattern of **1d-1i** (t_R = 12.12 min).

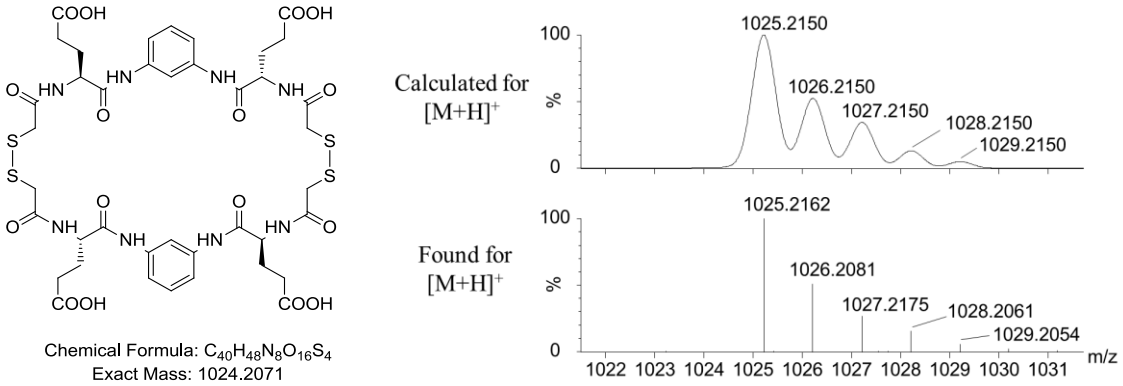

Figure A96. Structure and isotopic pattern of $(\mathbf{1i})_2$ (t_R = 13.27 min).

Identification of the trimers:

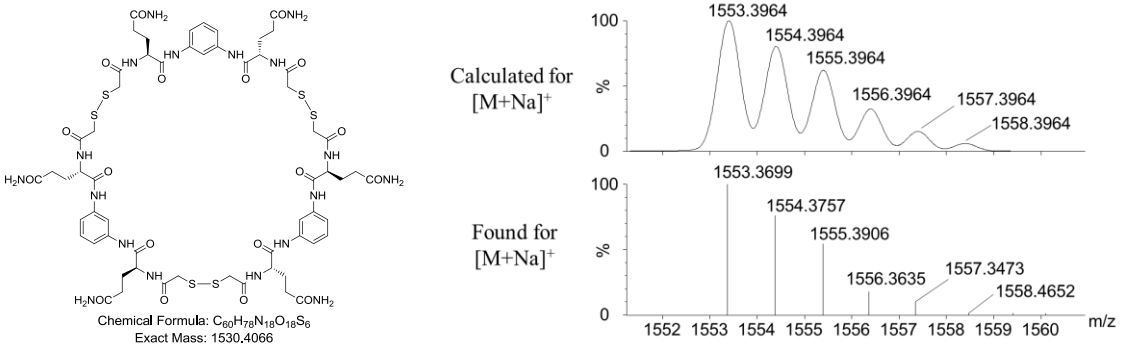

Figure A97. Structure and isotopic pattern of $(\mathbf{1c})_3$ (t_R = 11.22 min).

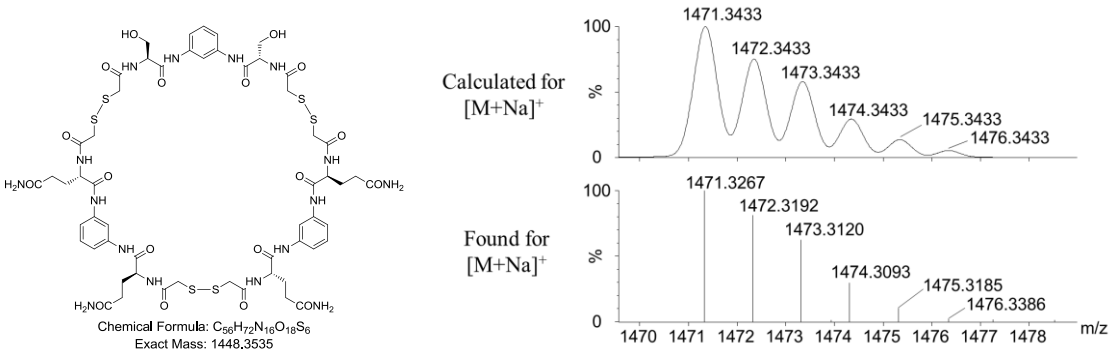

Figure A98. Structure and isotopic pattern of $(\mathbf{1c})_2$-**1d** (t_R = 11.52 min).

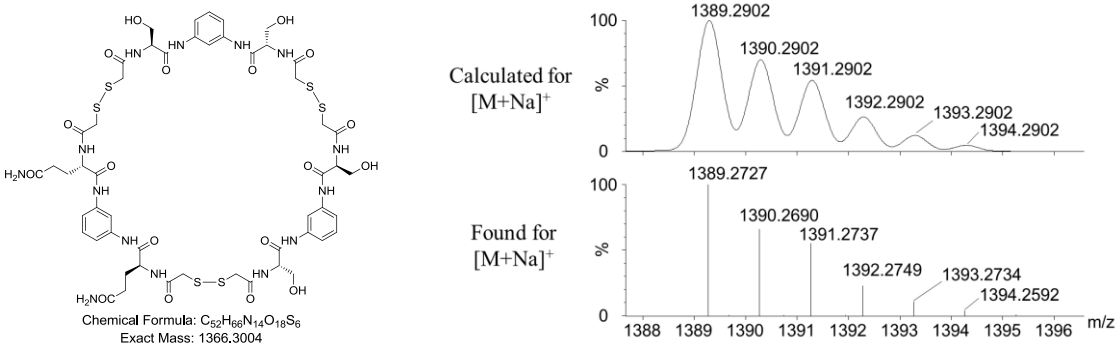

Figure A99. Structure and isotopic pattern of **1c**-$(\mathbf{1d})_2$ (t_R = 11.80 min).

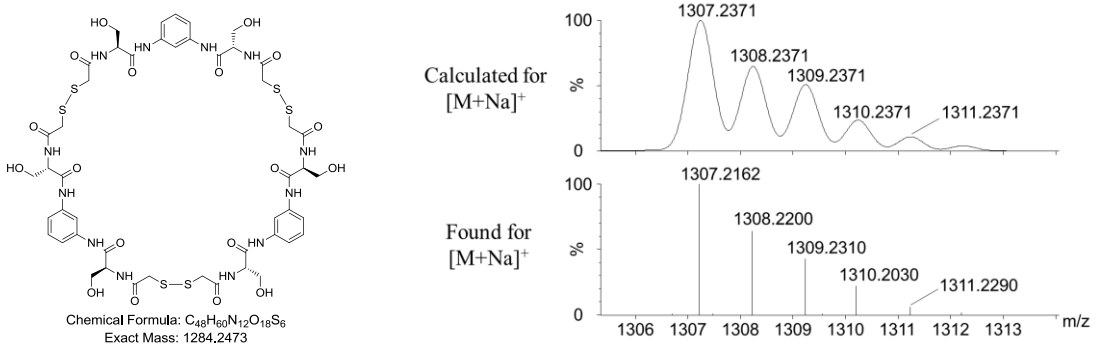

Figure A100. Structure and isotopic pattern of $(\mathbf{1d})_3$ (t_R = 12.12 min).

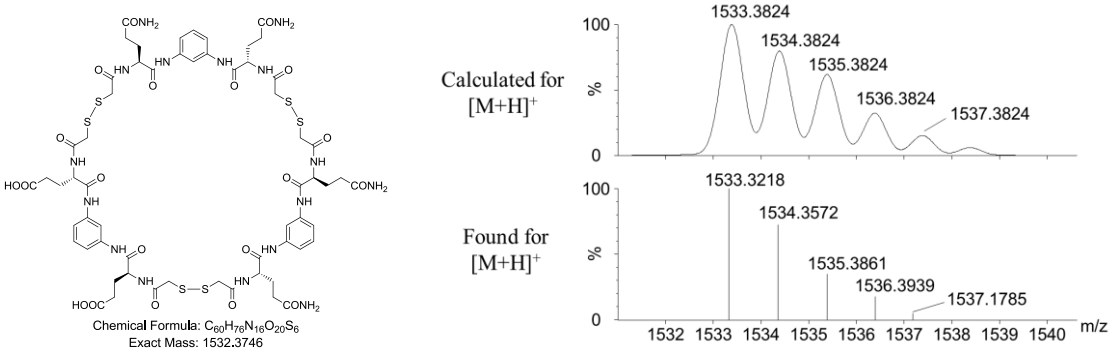

Figure A101. Structure and isotopic pattern of $(\mathbf{1c})_2$-**1i** (t_R = 12.55 min).

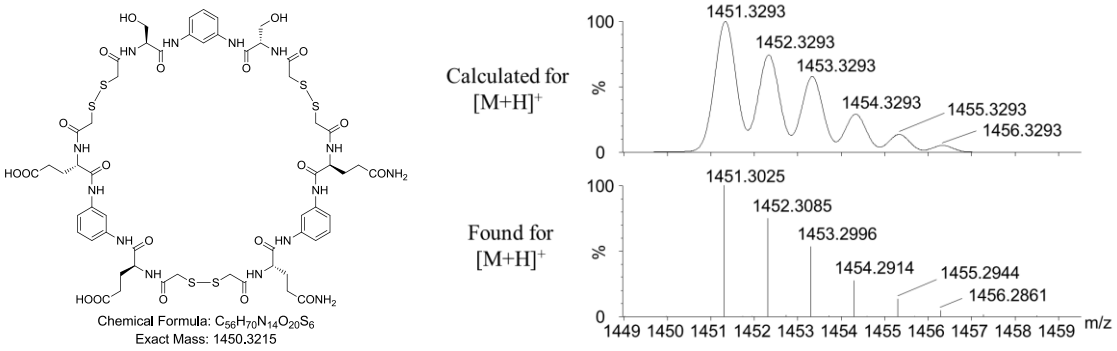

Figure A102. Structure and isotopic pattern of **1c-1d-1i** (t_R = 12.88 min).

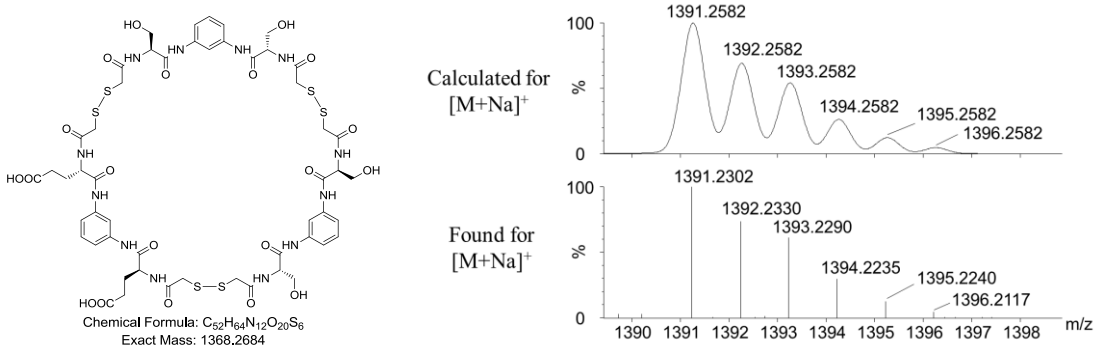

Figure A103. Structure and isotopic pattern of $(\mathbf{1d})_2$**-1i** (t_R = 13.27 min).

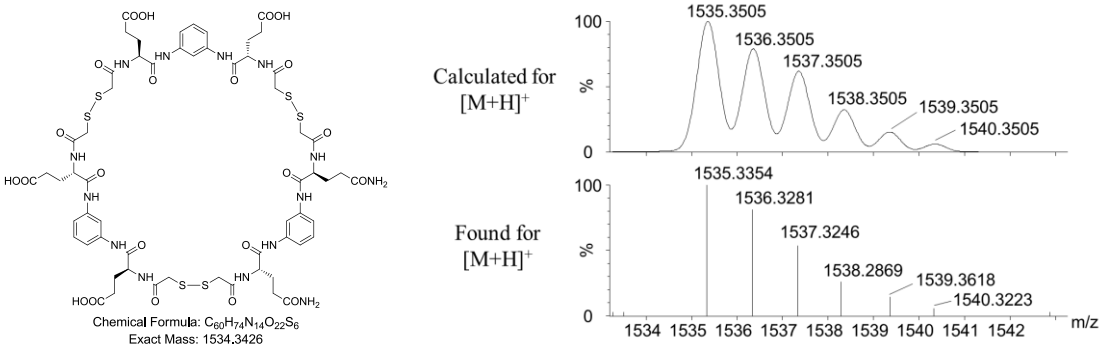

Figure A104. Structure and isotopic pattern of **1c-**$(\mathbf{1i})_2$, (t_R = 13.82 min).

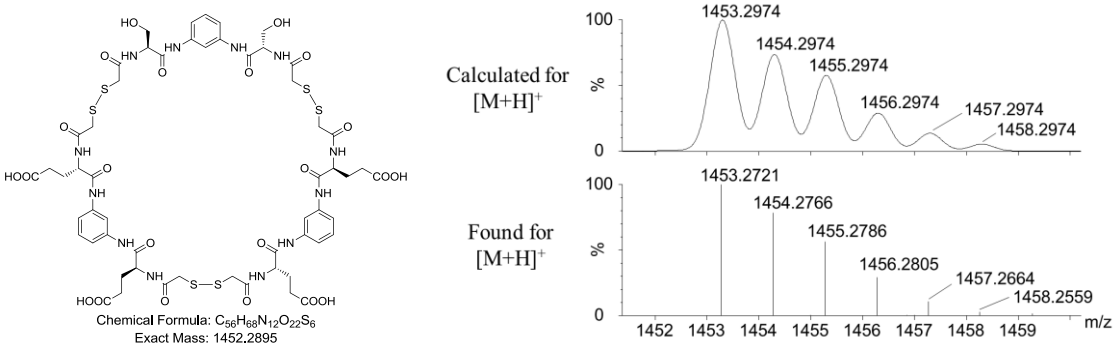

Figure A105. Structure and isotopic pattern of **1d-**$(\mathbf{1i})_2$ (t_R = 14.20 min).

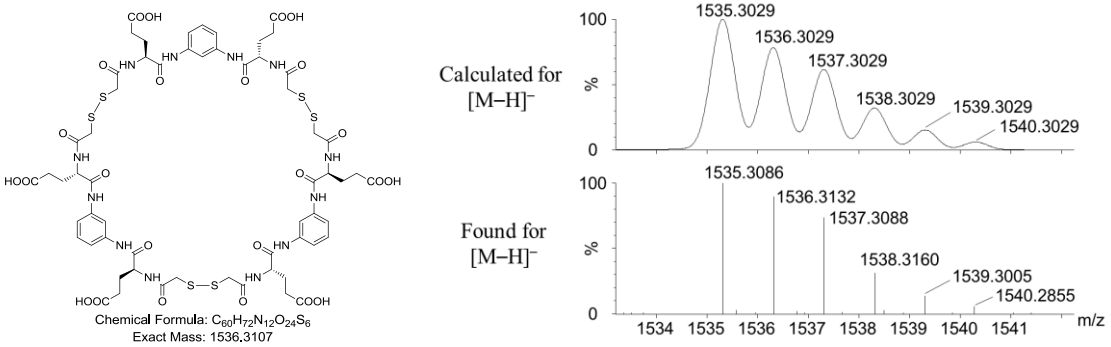

Figure A106. Structure and isotopic pattern of $(\mathbf{1i})_3$ (t_R = 15.12 min).

Mixture of BBs **1c**+**1d**+**1i** at pH 2.5

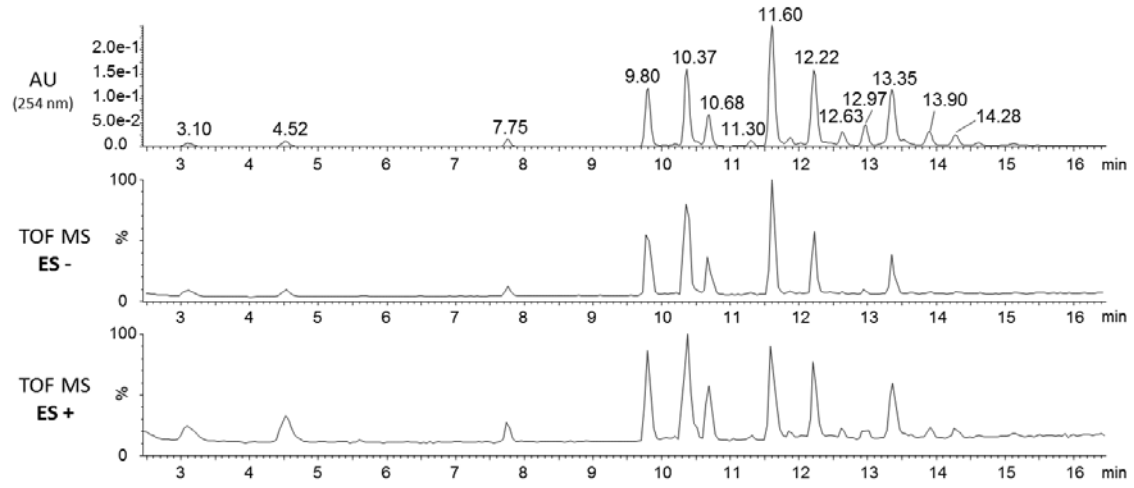

Figure A107. UPLC-UV(254 nm)-ESI-TOF traces of the equilibrated mixture of **1c**+**1d**+**1i** (2 mM each) in aqueous phosphate buffer (pH 2.5) with 25% (v/v) DMSO.

Identification of the cyclic monomers:

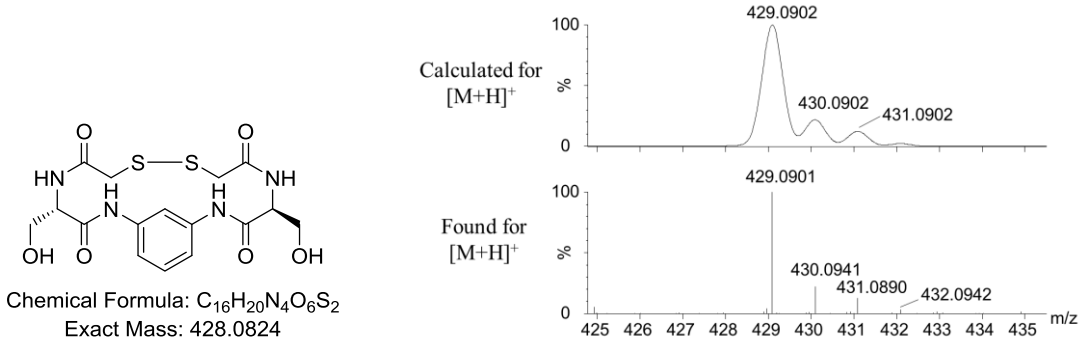

Figure A108. Structure and isotopic pattern of ***c*-1d** (t_R = 3.10 min).

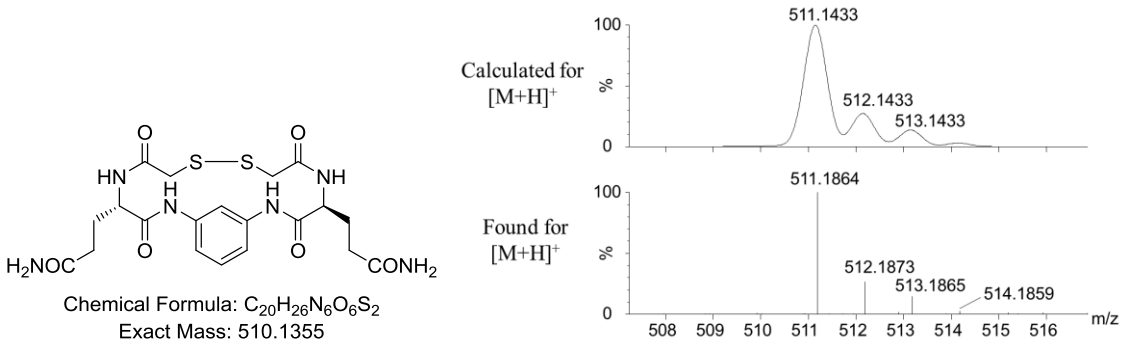

Figure A109. Structure and isotopic pattern of ***c*-1c** (t_R = 4.52 min).

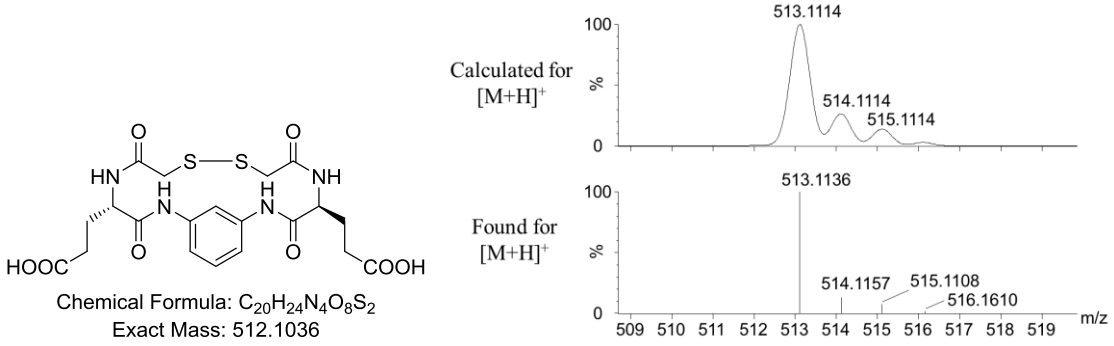

Figure A110. Structure and isotopic pattern of ***c*-1i** (t_R = 7.75 min).

Mixture of BBs **1c**+**1d**+**1h**+**1i** at pH 7.5

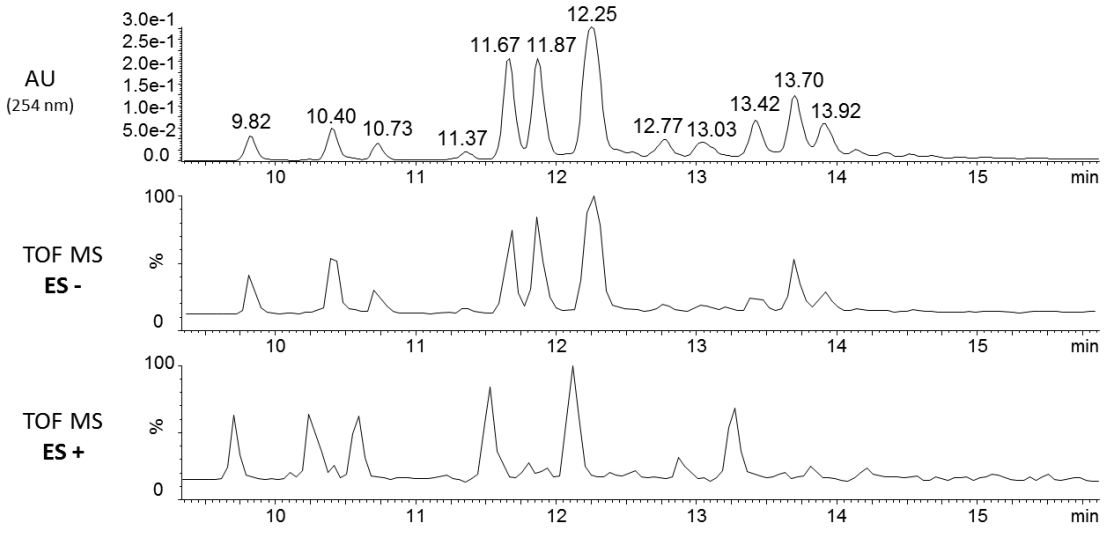

Figure A111. UPLC-UV(254 nm)-ESI-TOF traces of the equilibrated mixture of **1c**+**1d**+**1h**+**1i** (2 mM each) in aqueous phosphate buffer (pH 7.5) with 25% (v/v) DMSO.

Identification of the dimers containing **1h**:

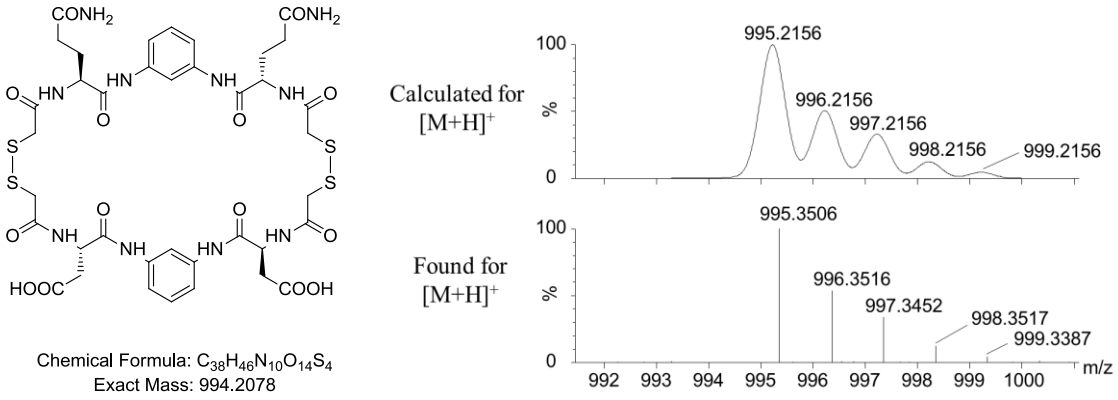

Figure A112. Structure and isotopic pattern of **1c-1h** (t_R = 11.87 min).

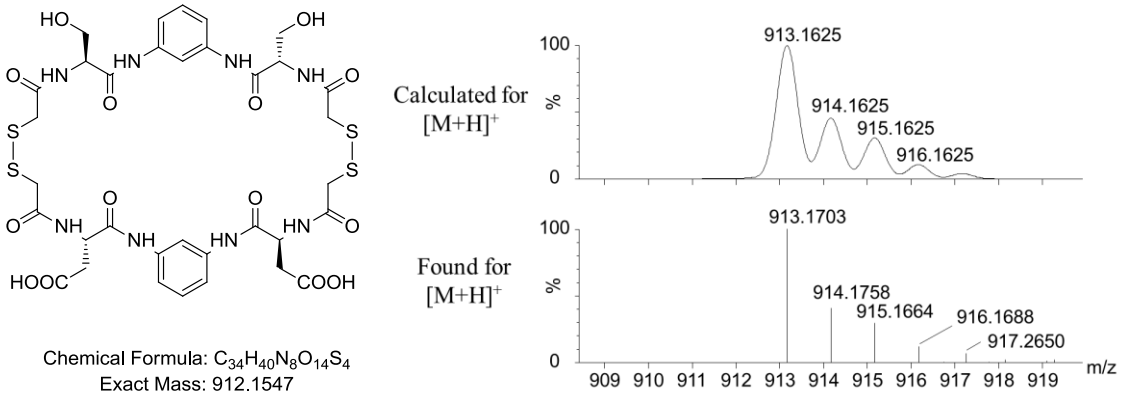

Figure A113. Structure and isotopic pattern of **1d-1h** (t_R = 12.25 min).

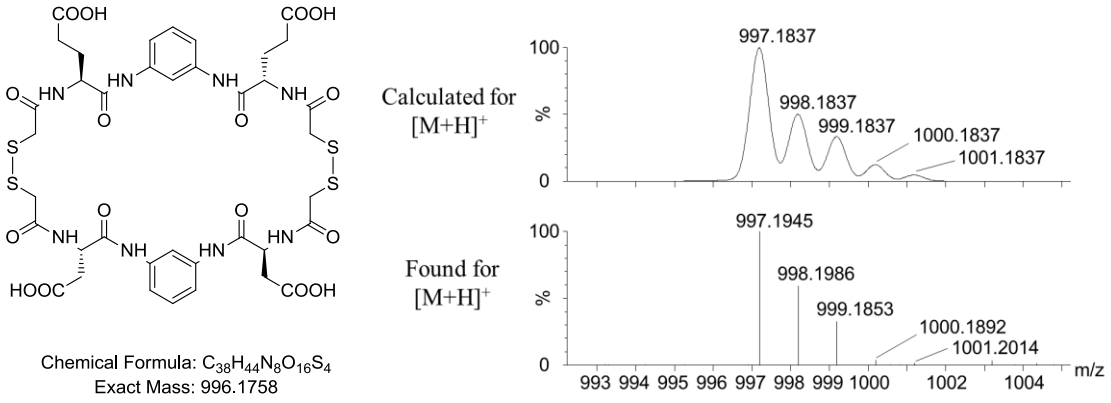

Figure A114. Structure and isotopic pattern of **1h-1i** (t_R = 13.70 min).

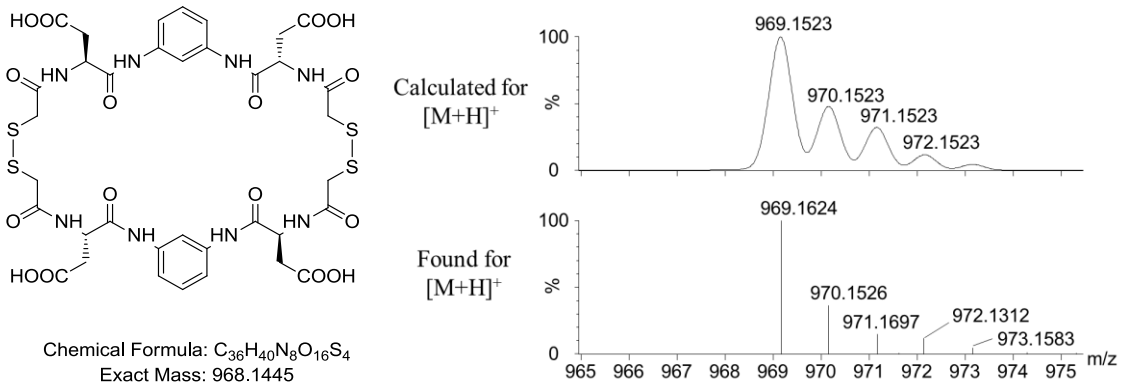

Figure A115. Structure and isotopic pattern of $(\mathbf{1h})_2$ (t_R = 13.92 min).

DCLs of Chapter 4

Mixture of BBs **1b**+**1d**+**1h**+**1i**+**1j**+**1k** with 1.0 M NaCl

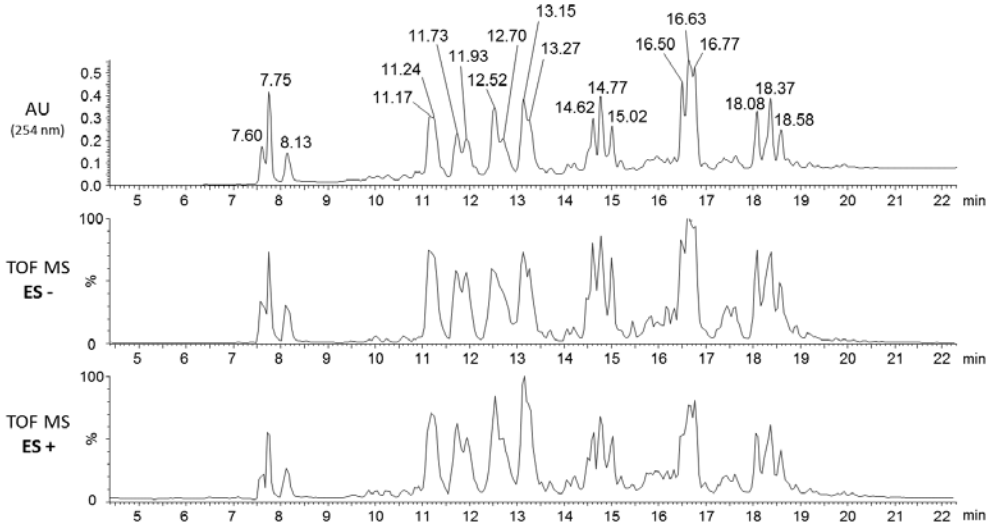

Figure A116. UPLC-UV(254 nm)-ESI-TOF traces of the equilibrated mixture of **1b**+**1d**+**1h**+**1i**+**1j**+**1k** (0.5 mM each) in 40 mM bis-Tris buffer (pH 6.5) with 25% (v/v) DMSO in the presence of 1.0 M NaCl.

Identification of the dimers of family $\mathbf{F}_{(+,+)}$:

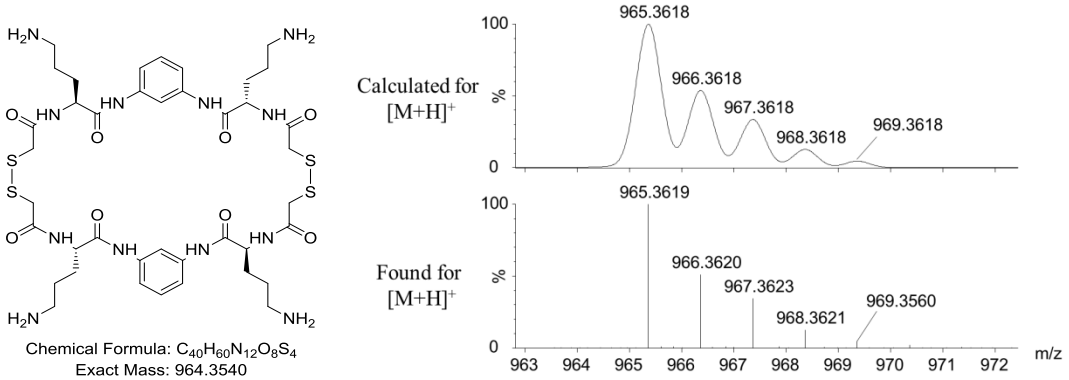

Figure A117. Structure and isotopic pattern of $(\mathbf{1j})_2$ (t_R = 7.60 min).

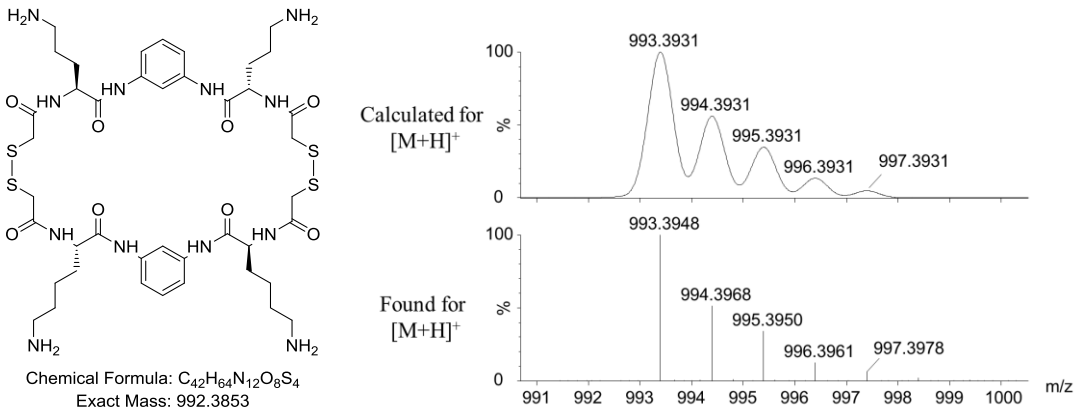

Figure A118. Structure and isotopic pattern of **1j-1k** (t_R = 7.75 min).

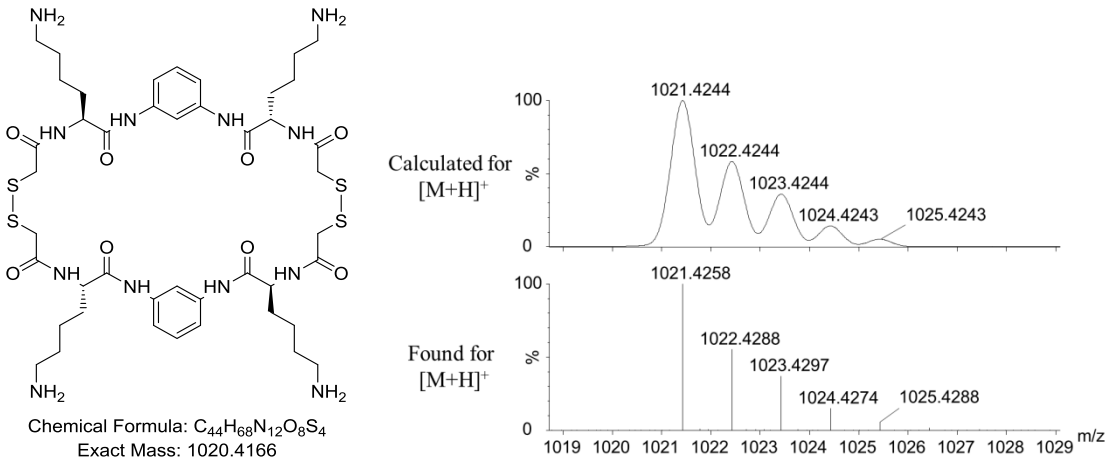

Figure A119. Structure and isotopic pattern of $(\mathbf{1k})_2$ (t_R = 8.13 min).

Identification of the dimers of family $\mathbf{F_{(0,+)}}$:

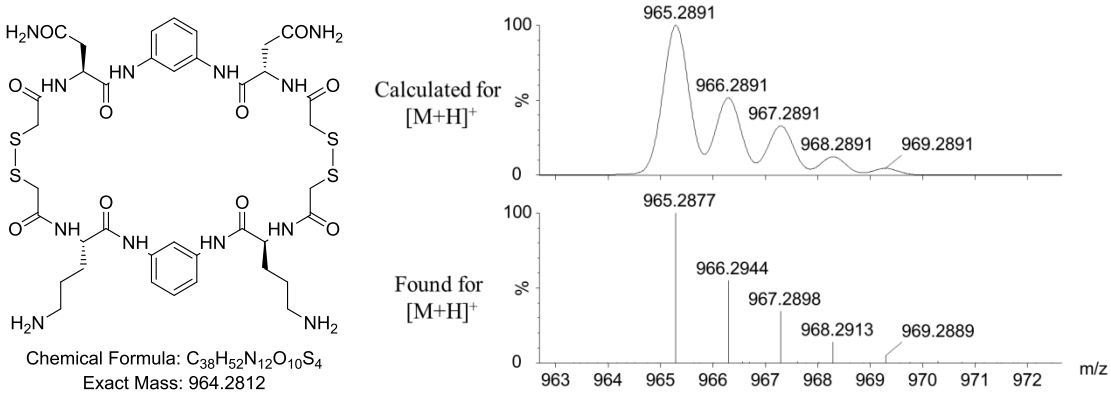

Figure A120. Structure and isotopic pattern of **1b-1j** (t_R = 11.17 min).

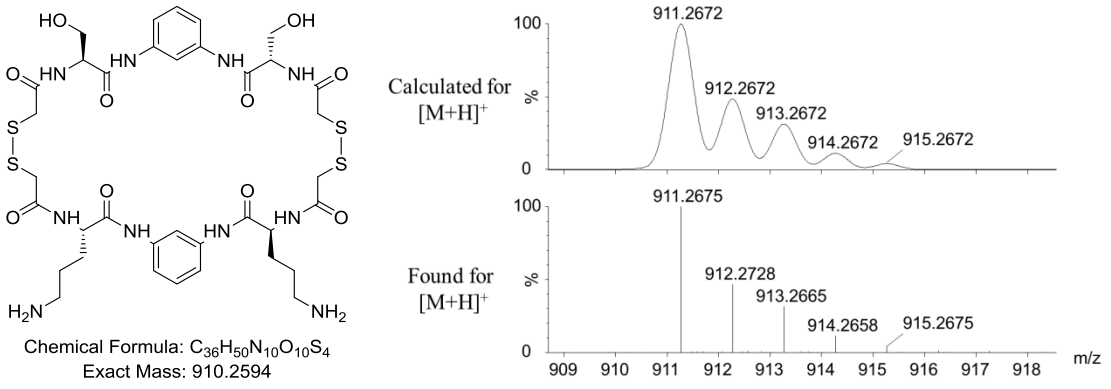

Figure A121. Structure and isotopic pattern of **1d-1j** (t_R = 11.24 min).

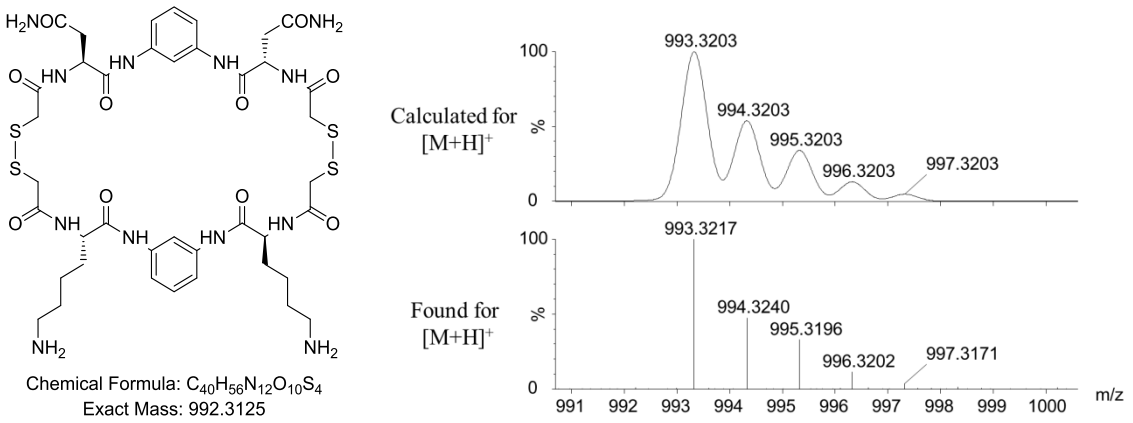

Figure A122. Structure and isotopic pattern of **1b-1k** (t_R = 11.73 min).

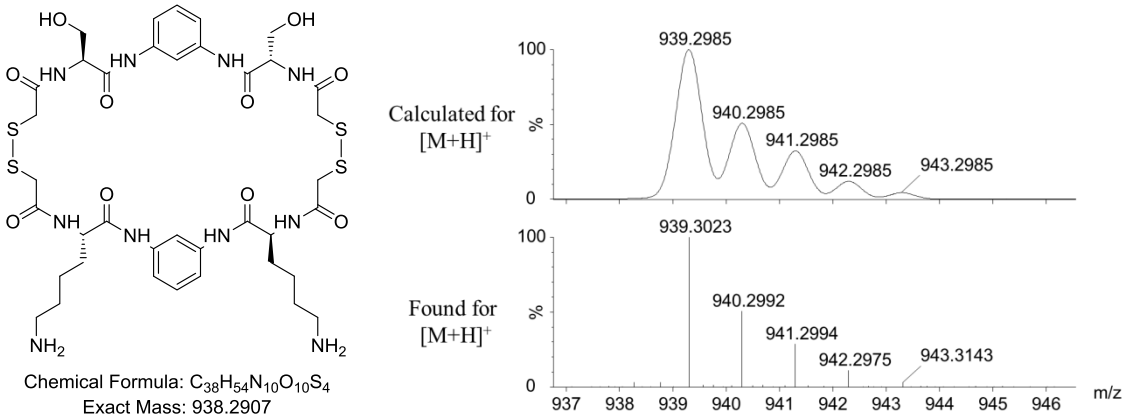

Figure A123. Structure and isotopic pattern of **1d-1k**, (t_R = 11.93 min).

Identification of the dimers of family $\mathbf{F}_{(+,-)}$:

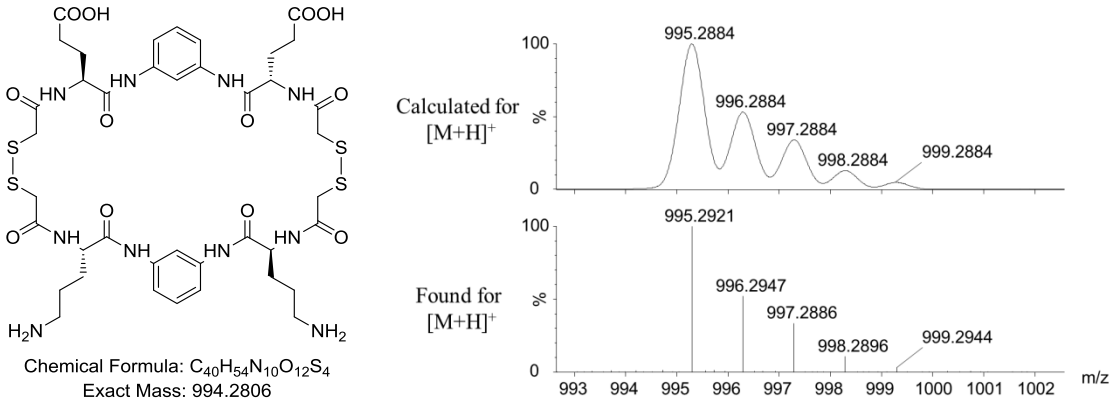

Figure A124. Structure and isotopic pattern of **1i-1j** (t_R = 12.52 min).

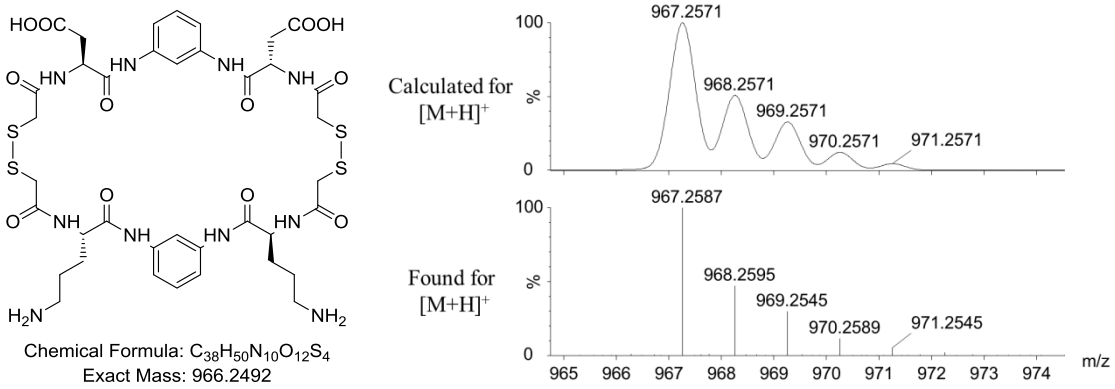

Figure A125. Structure and isotopic pattern of **1h-1j** (t_R = 12.70 min).

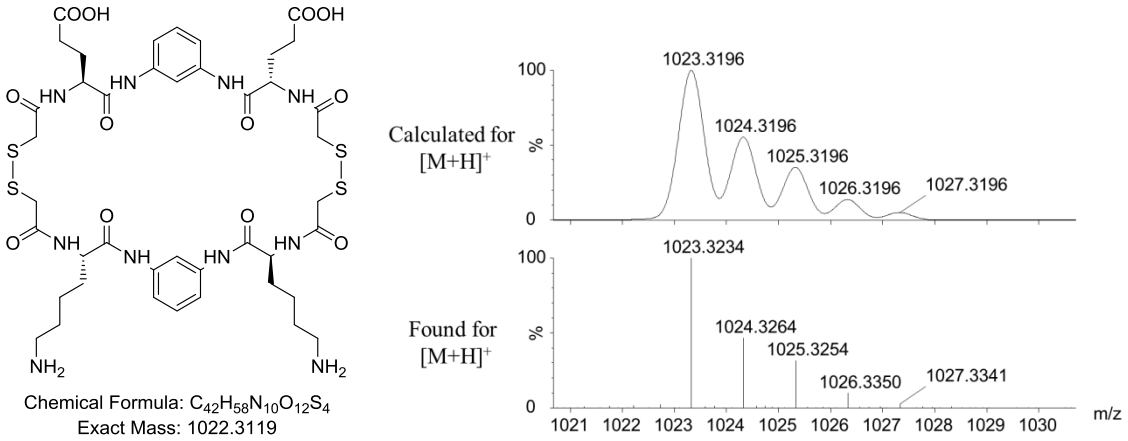

Figure A126. Structure and isotopic pattern of **1i-1k** (t_R = 13.15 min).

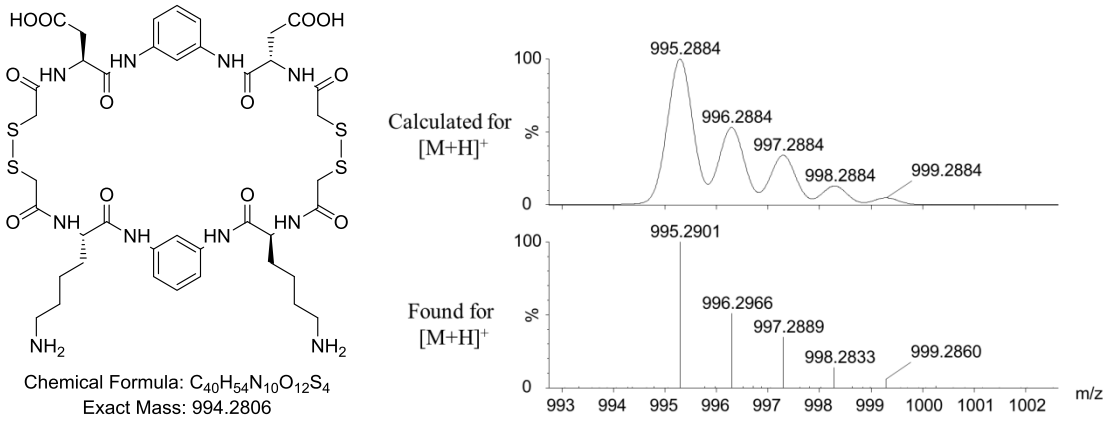

Figure A127. Structure and isotopic pattern of **1h-1k** (t_R = 13.27 min).

Identification of the dimers of family $\mathbf{F_{(0,0)}}$:

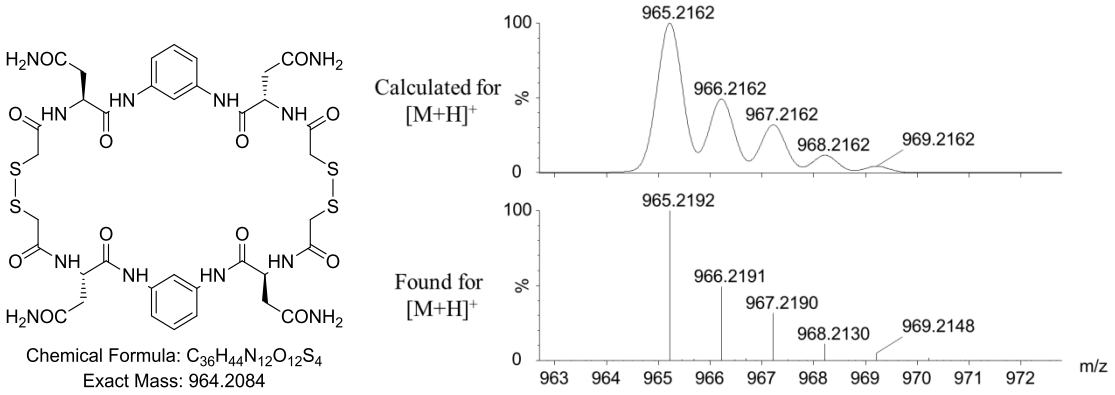

Figure A128. Structure and isotopic pattern of $(\mathbf{1b})_2$ (t_R = 14.62 min).

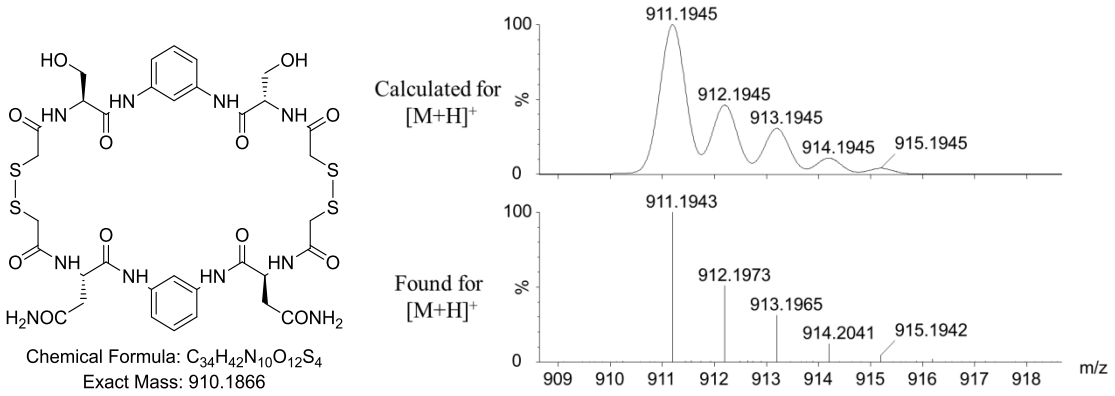

Figure A129. Structure and isotopic pattern of **1b-1d** (t_R = 14.77 min).

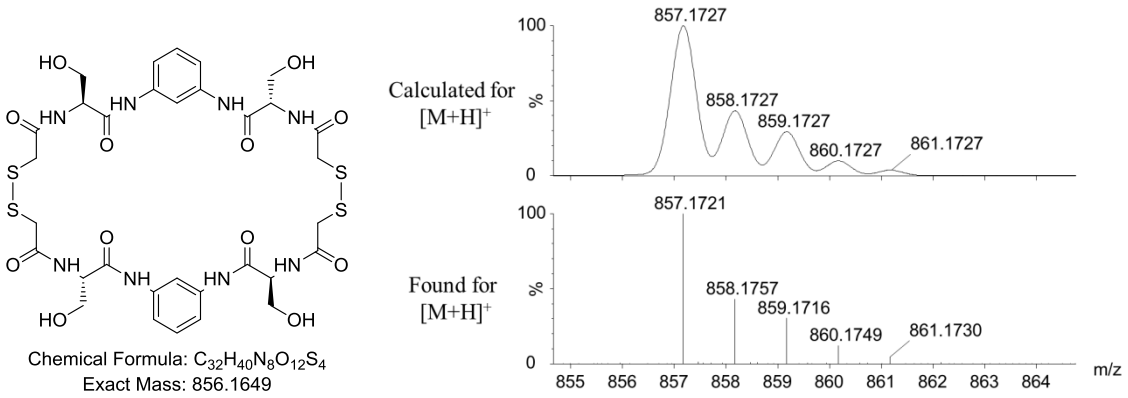

Figure A130. Structure and isotopic pattern of $(\mathbf{1d})_2$ (t_R = 15.02 min).

Identification of the dimers of family $\mathbf{F_{(0,-)}}$:

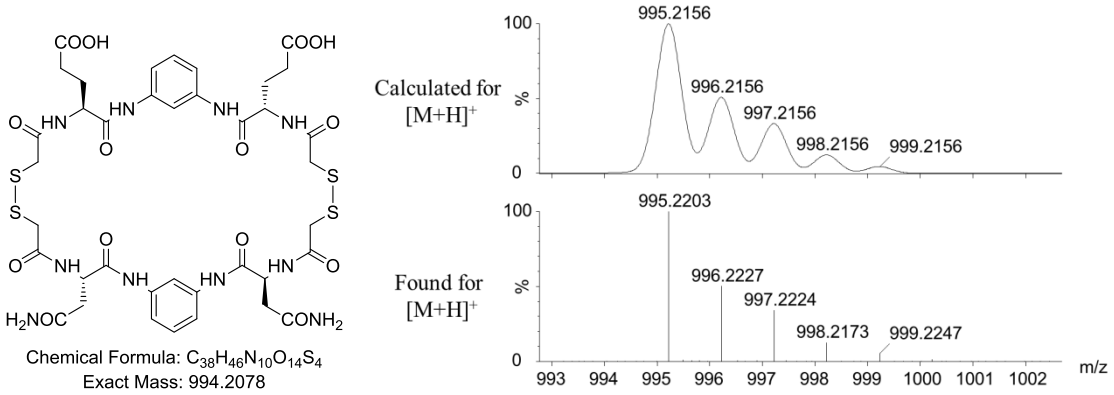

Figure A131. Structure and isotopic pattern of **1b-1i** (t_R = 16.50 min).

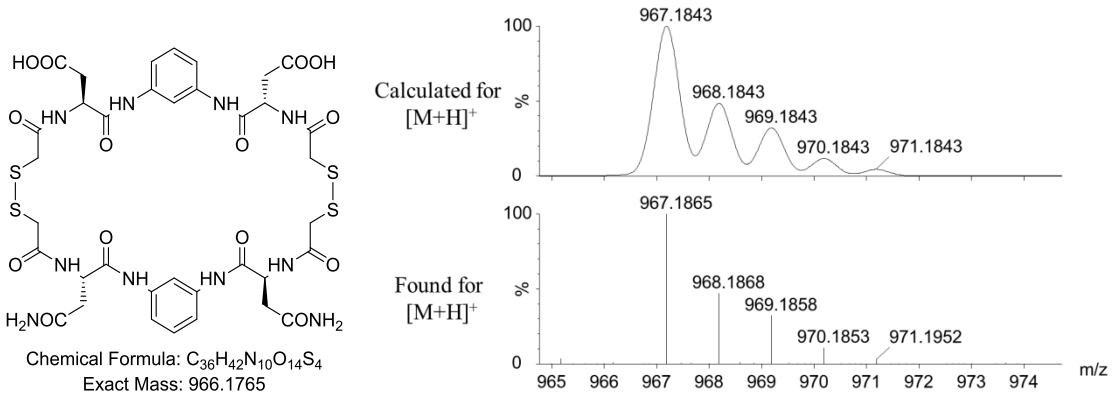

Figure A132. Structure and isotopic pattern of **1b-1h** (t_R = 16.63 min).

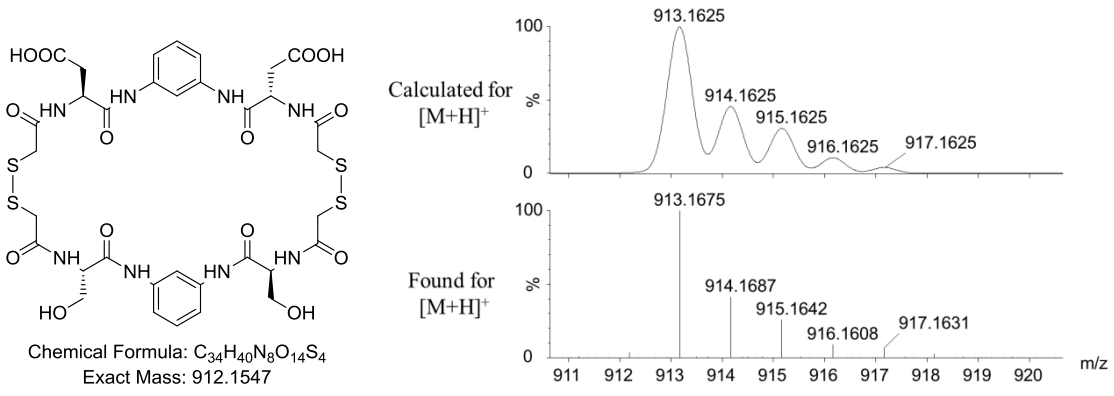

Figure A133. Structure and isotopic pattern of **1d-1h** (t_R = 16.63 min).

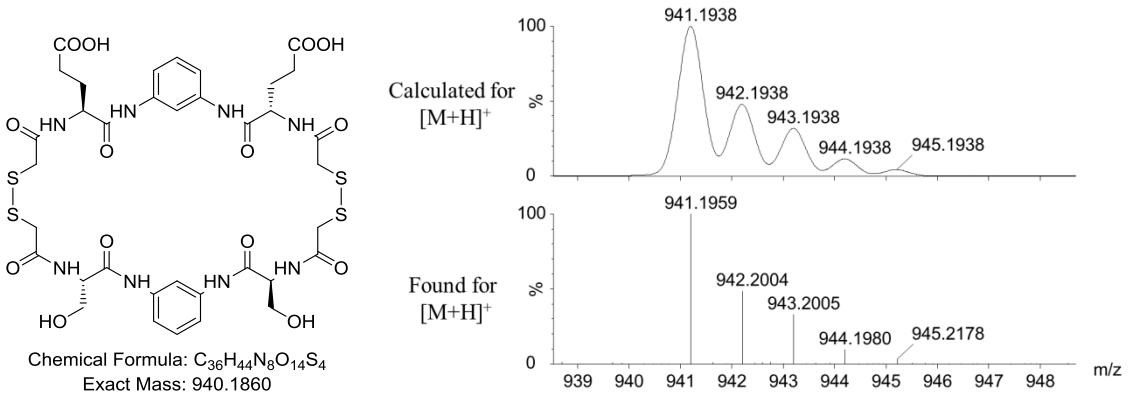

Figure A134. Structure and isotopic pattern of **1d-1i** (t_R = 16.77 min).

Identification of the dimers of family $\mathbf{F}_{(-,-)}$:

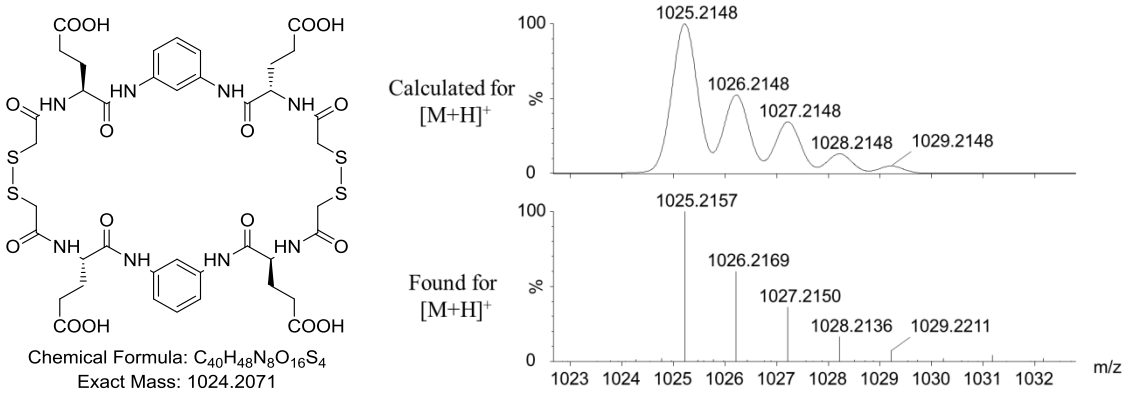

Figure A135. Structure and isotopic pattern of $(\mathbf{1b})_2$ (t_R = 18.08 min).

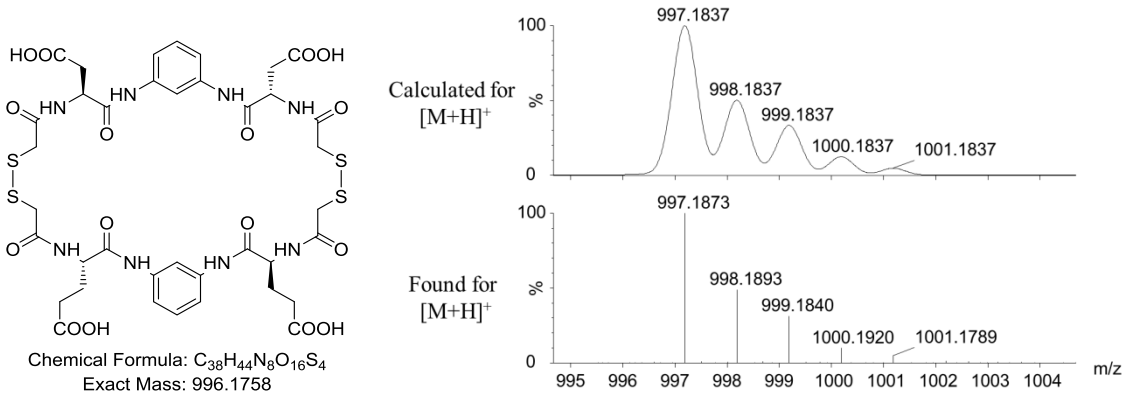

Figure A136. Structure and isotopic pattern of **1a-1b** (t_R = 18.37 min).

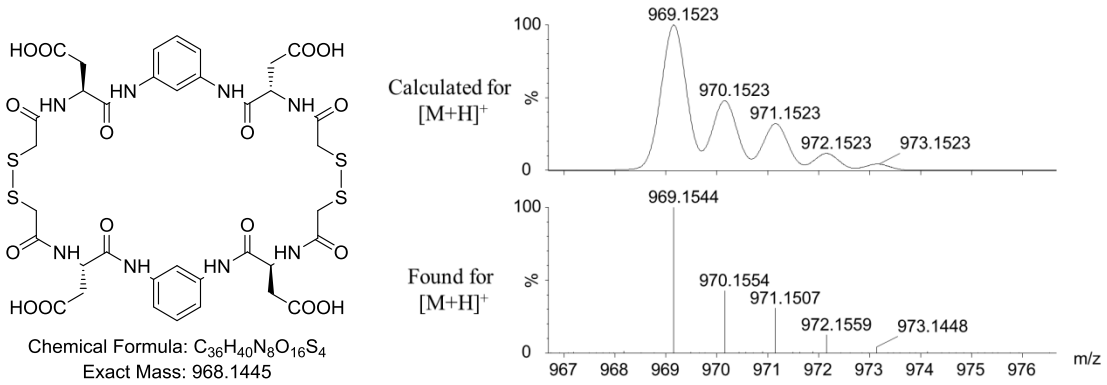

Figure A137. Structure and isotopic pattern of (**1h**)$_2$ (t_R = 18.58 min).

Conformational clusters of the MD simulations

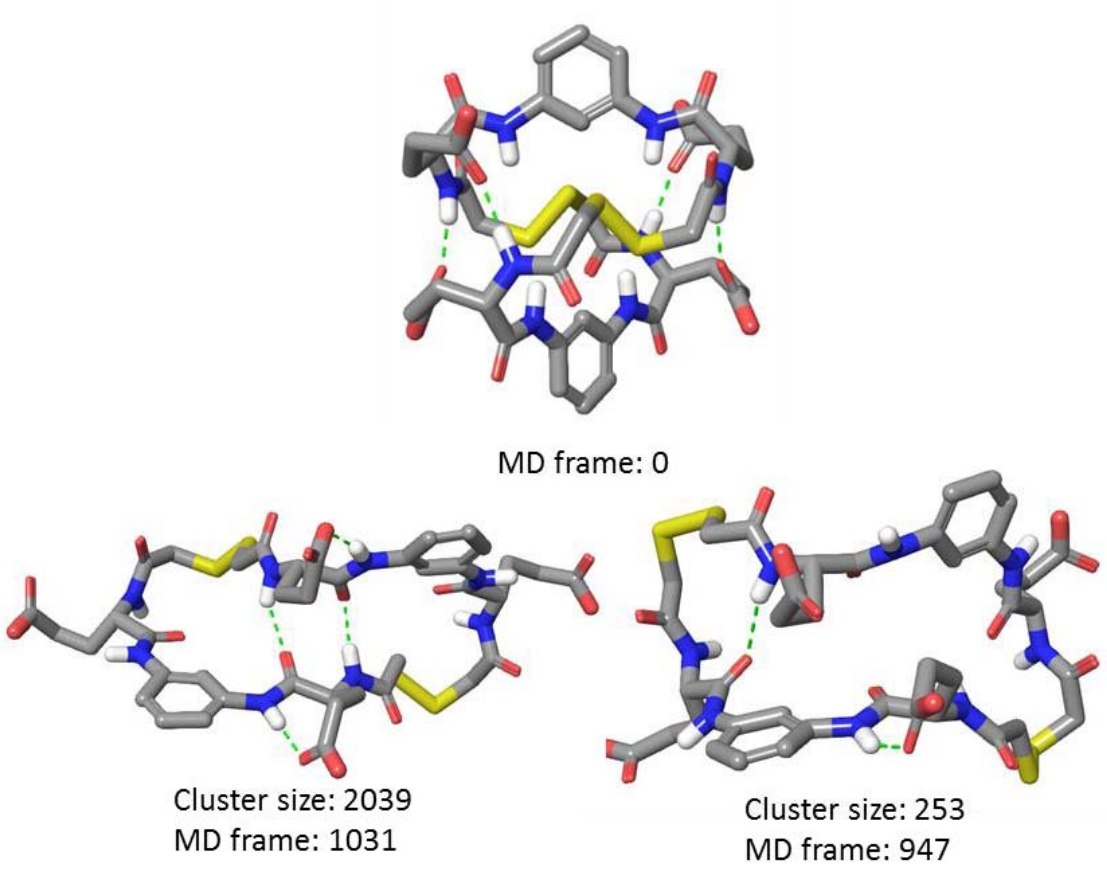

Figure A138. Initial conformation of dimer $(\mathbf{1i})_2$ used for Simulation 1 and most representative conformers of the most populated conformational clusters derived from this simulation, *i.e.* those with a population ≥5% (cluster size ≥ 125). Conformers shown represent 91.7 % of the total population of conformers (2500). Intramolecular hydrogen bonds are shown with green dashed lines.

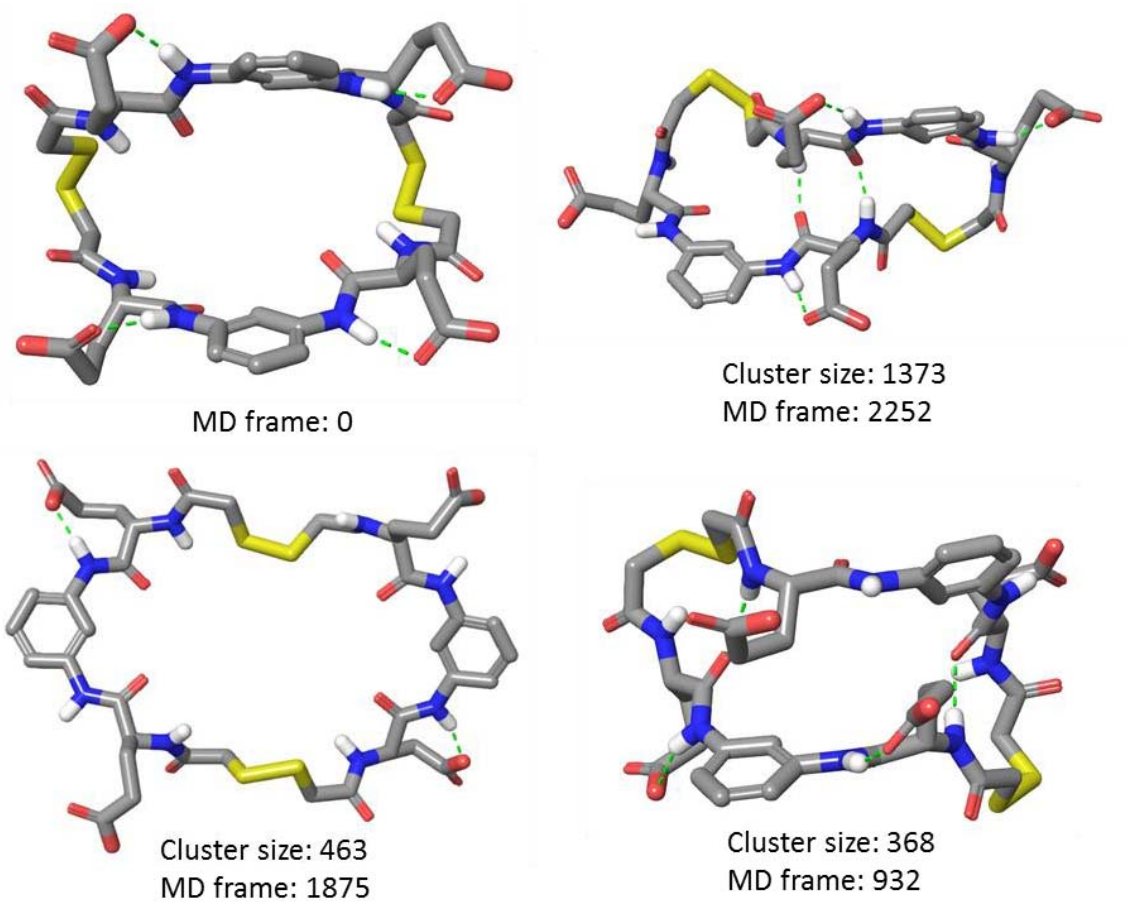

Figure A139. Initial conformation of dimer $(\mathbf{1i})_2$ used for Simulation 2 and most representative conformers of the most populated conformational clusters derived from this simulation, *i.e.* those with a population ≥5% (cluster size ≥ 125). Conformers shown represent 88.2 % of the total population of conformers (2500). Intramolecular hydrogen bonds are shown with green dashed lines.

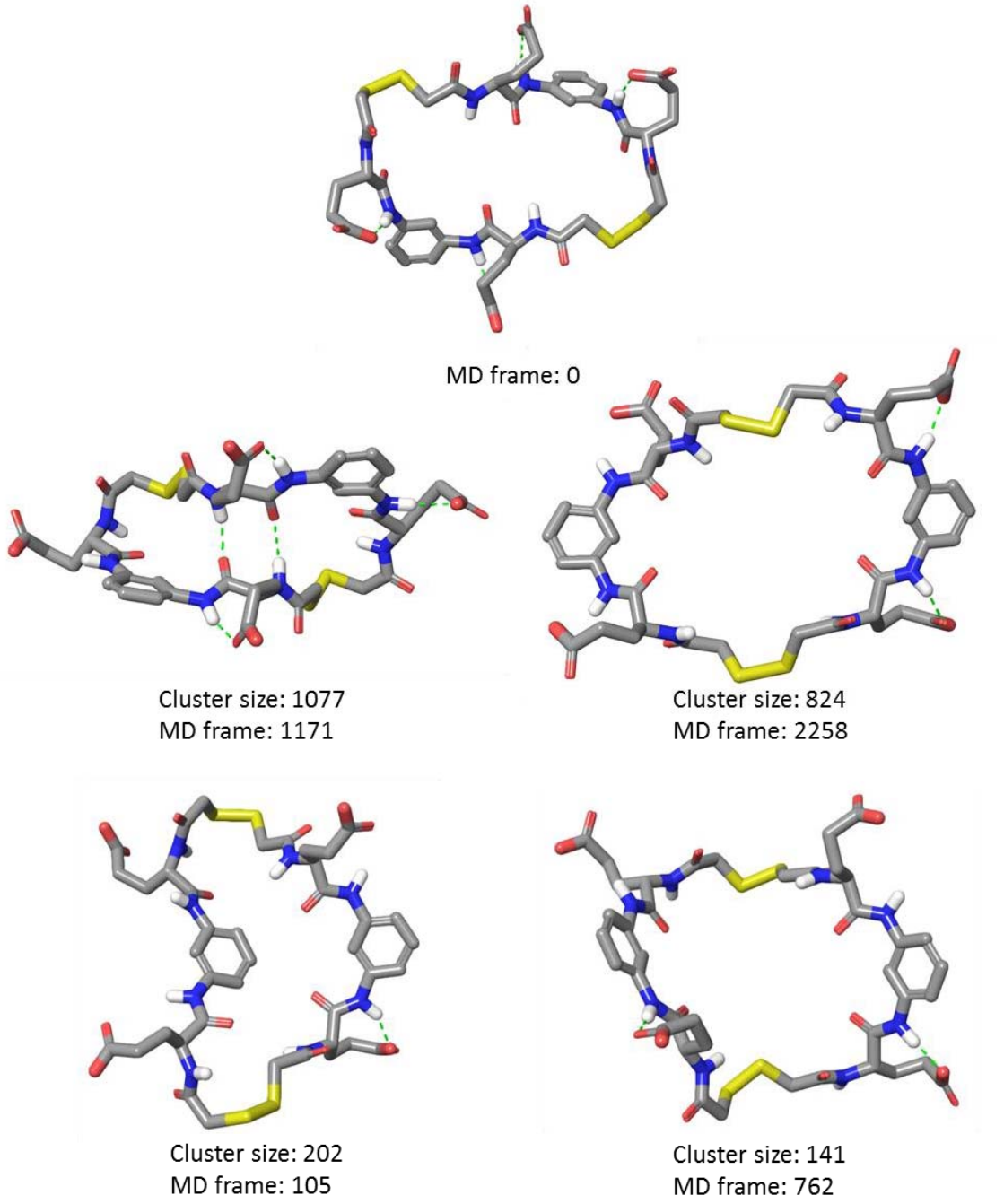

Figure A140. Initial conformation of dimer $(\mathbf{1i})_2$ used for Simulation 3 and most representative conformers of the most populated conformational clusters derived from this simulation, *i.e.* those with a population ≥5% (cluster size ≥ 125). Conformers shown represent 89.8 % of the total population of conformers (2500). Intramolecular hydrogen bonds are shown with green dashed lines.

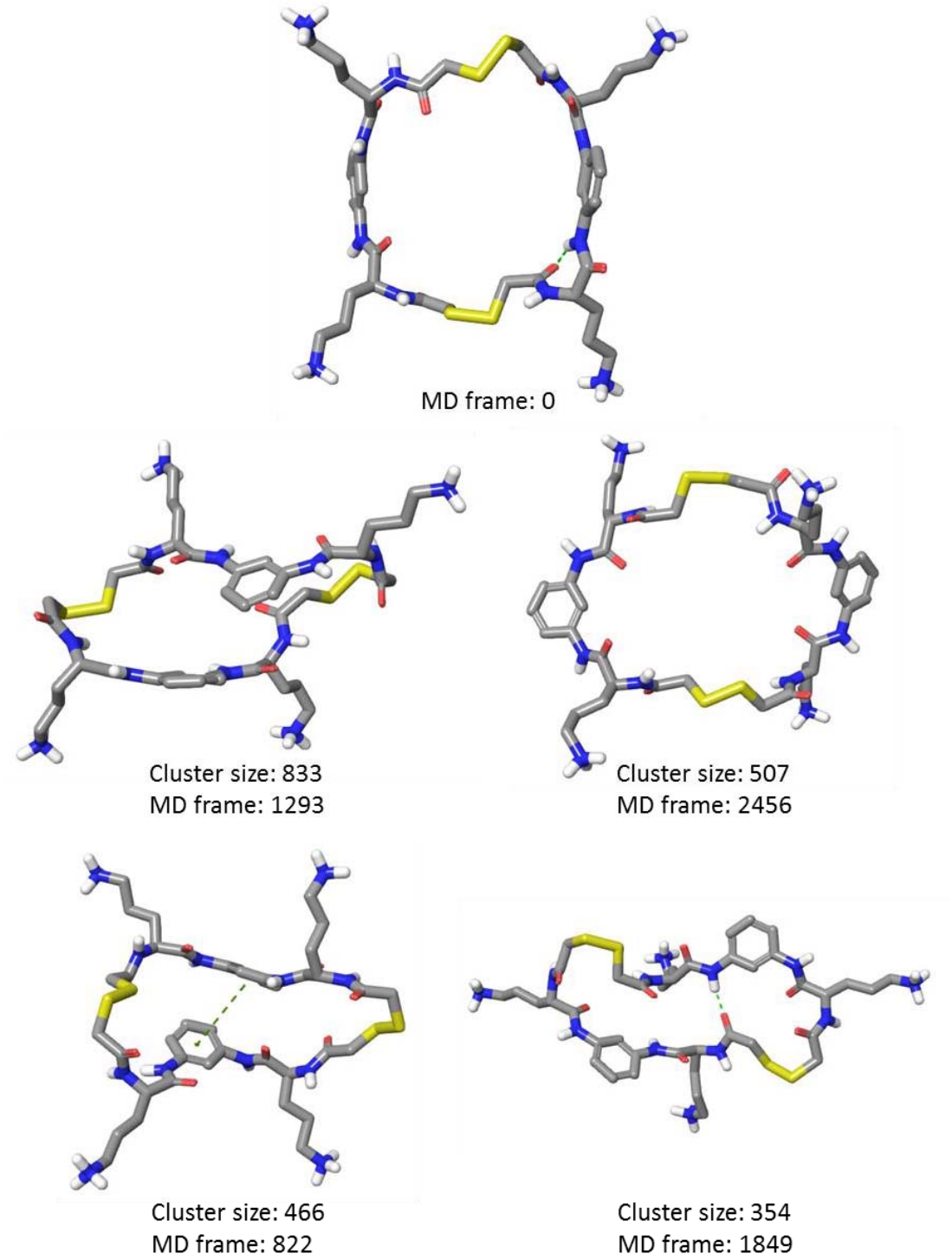

Figure A141. Initial conformation of dimer $(\mathbf{1j})_2$ used for Simulation 4 and most representative conformers of the most populated conformational clusters derived from this simulation, *i.e.* those with a population ≥5% (cluster size ≥ 125). Conformers shown represent 86.4 % of the total population of conformers (2500). Intramolecular hydrogen bonds and π-π stacking interactions between the aromatic rings are shown with green dashed lines.

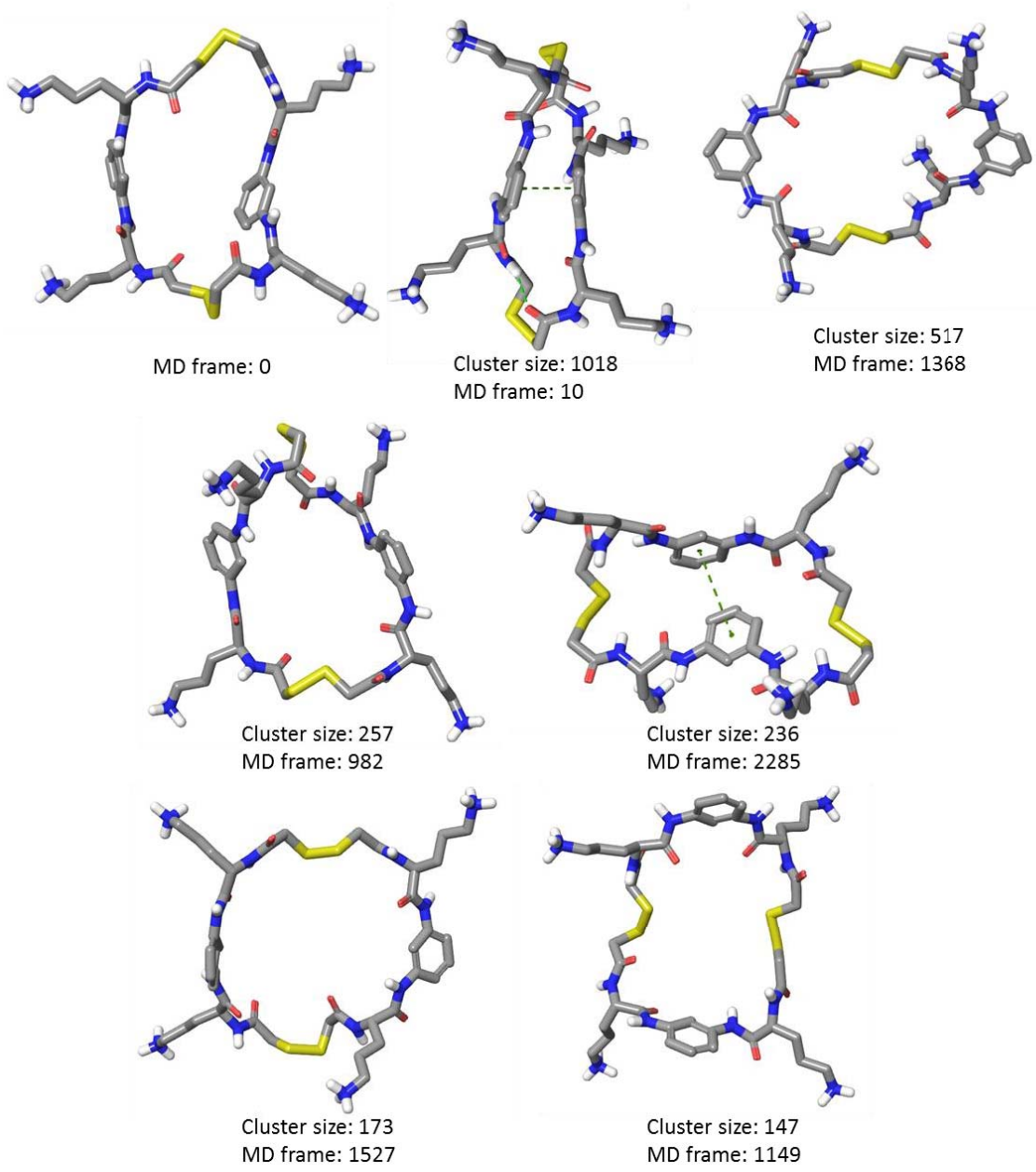

Figure A142. Initial conformation of dimer $(\mathbf{1j})_2$ used for Simulation 5 and most representative conformers of the most populated conformational clusters derived from this simulation, *i.e.* those with a population ≥5% (cluster size ≥ 125). Conformers shown represent 93.9 % of the total population of conformers (2500). Intramolecular hydrogen bonds and π-π stacking interactions between the aromatic rings are shown with green dashed lines.

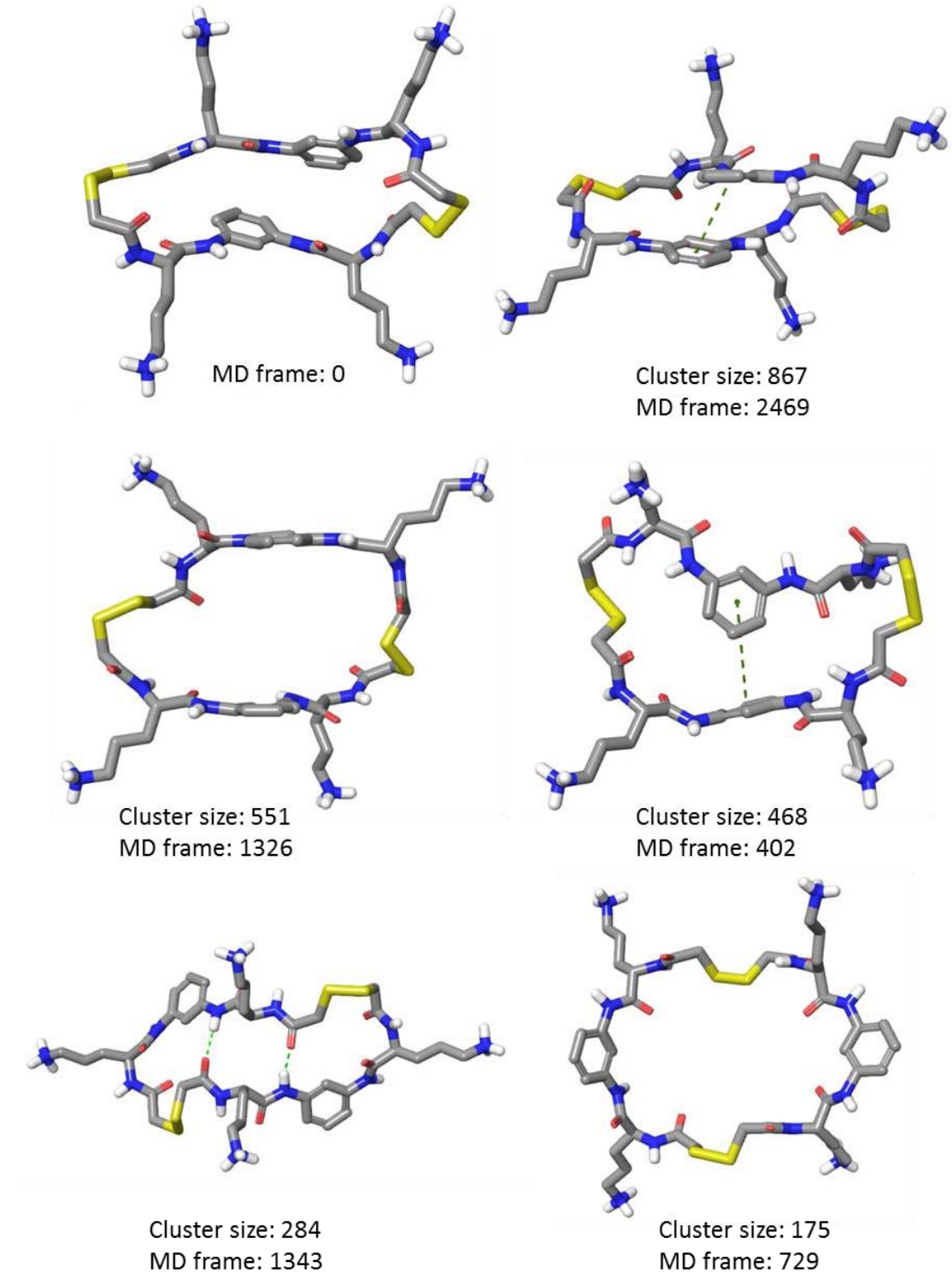

Figure A143. Initial conformation of dimer $(\mathbf{1j})_2$ used for Simulation 6 and most representative conformers of the most populated conformational clusters derived from this simulation, *i.e.* those with a population ≥5% (cluster size ≥ 125). Conformers shown represent 93.8 % of the total population of conformers (2500). Intramolecular hydrogen bonds and π-π stacking interactions between the aromatic rings are shown with green dashed lines.